# Neutron Resonance Spectroscopy. V. Nb, Ag, I, and Cs†

J. B. GARG, J. RAINWATER, AND W. W. HAVENS, JR.
*Columbia University, New York, New York*
(Received 18 September 1964)

Total neutron cross-section measurements for niobium, natural silver, iodine, and cesium have been made using a neutron velocity spectrometer with a resolution of about 0.5 nsec/m near the highest energy. The measurements were performed in the energy interval of 35 eV to 8 keV for niobium and 100 eV to about 4 keV for the other elements. The energies and neutron widths of about one thousand levels observed in these nuclei have been determined. The level-spacing distributions of these nuclei were investigated and found to be compatible with the random-matrix model of Wigner. These elements have $A$ values in the neighborhood of an expected peak in the $p$-wave strength function and relative minimum in the $s$-wave strength function. Histograms of the distribution of values for $y=\langle g\Gamma_n^0\rangle^{1/2}$ show a considerable excess of small widths over the number expected from the Porter-Thomas $\nu=1$ distribution. This excess is interpreted as being due to the observation of many $p$-wave levels. In the case of Nb, about $\frac{2}{3}$ of the observed levels are probably $p$ wave, while the percentages were much smaller for the other elements. The numerical values of the correlation coefficients between level spacings, neutron reduced widths, and local spacing have been determined for all these nuclei. The correlation coefficients, except for the spacing correlation coefficients, are found to be consistent with zero within the statistical accuracy of the measurements. The $l=0$ strength-function values averaged over spin states and isotopes of Nb, Ag, I, and Cs have been determined as $(0.36\pm0.06)\times10^{-4}$, $(0.48\pm0.04)\times10^{-4}$, $(0.69\pm0.08)\times10^{-4}$, and $(0.70\pm0.10)\times10^{-4}$, respectively.

## I. INTRODUCTION

THIS is the fifth in a series[1–4] of papers reporting results using the Columbia University Synchrocyclotron for time-of-flight neutron spectroscopy.[5] It is the third paper reporting the results of total neutron cross-section measurements using a 200-m flight path having 0.5 nsec/m resolution for $E>1$ keV. This recent substantial improvement in resolution has made possible a considerable increase in the energy range over which resonance levels may be resolved and level parameters obtained for elements having mean level spacings from a few eV to about 1000 eV.

The present paper presents results for niobium ($Z=41$, $A=93$), silver ($Z=47$, $A=107$, 109), iodine ($Z=53$, $A=127$), and cesium ($Z=55$, $A=133$) to about 8 keV for Nb and 4 keV for the other elements. Level parameters have been obtained for about 150 levels for Cs, to over 300 levels for Ag which represents a considerable increase in the number of levels studied compared with earlier published results for these elements.[2,6–9] We therefore have been able to obtain more precise values of the mean level spacing, the strength function, and other statistical properties of levels for which it is essential to have a large statistical sample for analysis.

The elements studied extend the $A$ values beyond the values of 75–81 for As and Br of the previous paper[4] into the region of the $p$-wave maximum ($A=90$ to 110) and towards the next $s$-wave maximum ($A=140$ to 190). The observed excess of small $\langle g\Gamma_n^0\rangle$ values, relative to that expected for the $l=0$ Porter-Thomas distribution, offers some estimate of the number of the observed levels which correspond to $l=1$. The fraction of such levels is greatest for niobium and smallest for iodine.

## II. EXPERIMENTAL DETAILS AND LEVEL-PARAMETER ANALYSIS

### A. Niobium ($Z=41$, $A=93$, $I=\frac{9}{2}$)

The neutron-transmission measurements for niobium were made in three different energy intervals: (1) 30–200 eV, (2) 200–1800 eV, (3) 1800–8000 eV. Detection channel widths of 0.4, 0.2, and 0.1 μsec, respectively, were used for the three intervals to give energy resolutions of about 1 eV at 1000 eV, and 5 eV at 5000 eV. The corresponding Doppler widths for Nb are $\Delta=1$ eV at 1000 eV and 2.4 eV at 5000 eV.

The transmission samples were niobium metal sheets. Four thicknesses, having $1/n=10.6$, 28.8, 117, and 470 b/atom, were used above 200 eV. Since the region from 30 to 200 eV has been thoroughly investigated previously,[9] only the thick sample, $(1/n)=10.6$ b/atom,

† Work supported in part by the U. S. Atomic Energy Commission.

[1] J. L. Rosen, J. S. Desjardins, J. Rainwater, and W. W. Havens, Jr., Phys. Rev. **118**, 687 (1960).

[2] J. S. Desjardins, J. L. Rosen, W. W. Havens, Jr., and J. Rainwater, Phys. Rev. **120**, 2214 (1960). This paper presents results for Ag using self-indication and a 35-m flight path. Similar results for Nb and I were presented only at meetings. Cf. S. Desjardins, J. L. Rosen, J. Rainwater, and W. W. Havens, Jr., Bull. Am. Phys. Soc. **5**, 32 and 289 (1960).

[3] J. B. Garg, J. Rainwater, J. S. Petersen, and W. W. Havens, Jr., Phys. Rev. **134**, B985 (1964).

[4] J. B. Garg, W. W. Havens, Jr., and J. Rainwater, Phys. Rev. **136**, B177 (1964).

[5] J. Rainwater, W. W. Havens, Jr., and J. B. Garg, Rev. Sci. Instr. **35**, 263 (1964).

[6] D. J. Hughes, B. A. Magurno, and M. K. Brussel, Brookhaven National Laboratory Report BNL-325 Suppl. 1, 1960 (unpublished).

[7] F. G. P. Seidl, D. J. Hughes, H. Palevsky, J. S. Levin, W. Y. Kato, and N. G. Sjöstrand, Phys. Rev. **95**, 467 (1954).

[8] J. A. Harvey, D. J. Hughes, R. S. Carter, and V. E. Pilcher, Phys. Rev. **99**, 10 (1955).

[9] A. Saplakoglu, L. M. Bollinger, and R. E. Coté, Phys. Rev. **109**, 1258 (1958).

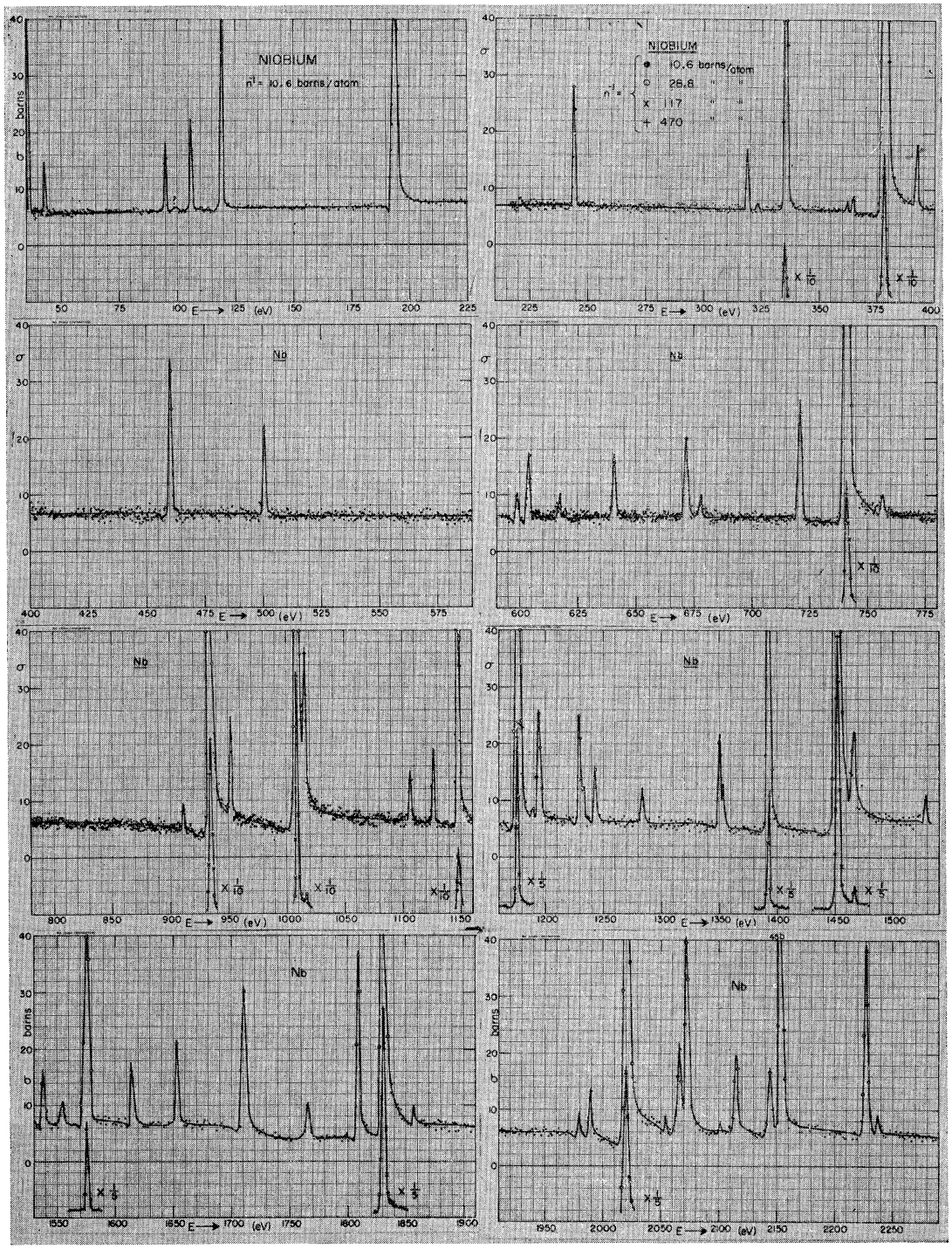


FIG. 1. The "measured" total neutron cross section of $Nb^{93}$ versus energy from 35 to 7250 eV. The measurements used four sample thicknesses as indicated, with the cross section between resonances mainly determined from the thick-sample data. At resonance the data for progressively thinner samples was used. When the resonance cross section exceeds full-scale value an insert scale is shown having its zero start at the bottom of the page with a factor of 5, 10, or 20, as indicated reduction in the height of the curve. In the region of resonance the peak cross-section values are distorted by Doppler level broadening, the instrumental energy resolution, and by the $(1/n)$ value for the thinnest sample. The cross-section values are in barns.

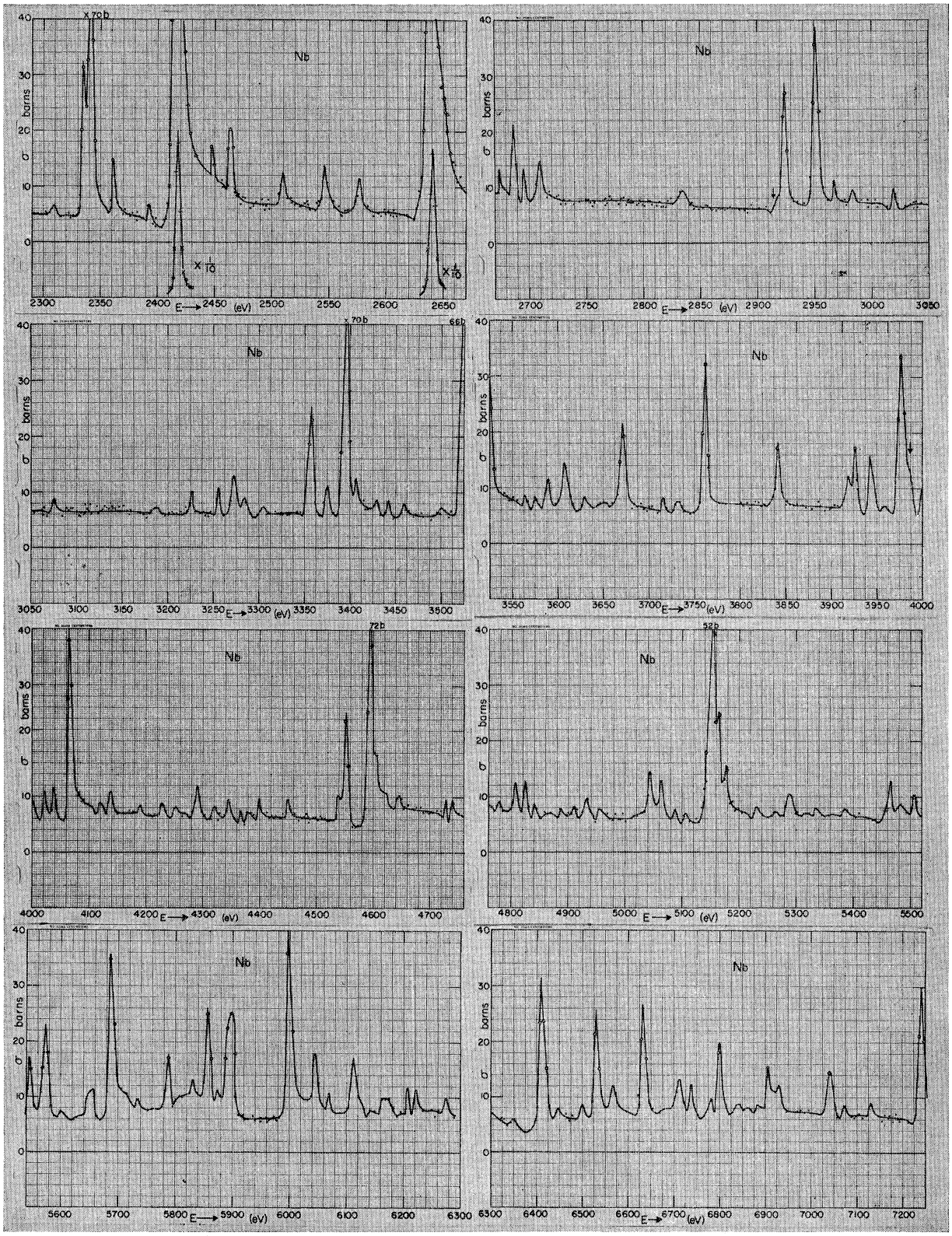


FIG. 1. *Continued.*

TABLE I. Resonance parameters for the levels in niobium. $g=9/20$ and $11/20$ for $J=4$ and 5, respectively. The corresponding values of $\langle g\Gamma_n^1\rangle$ are given in column 6. Resonance parameters for levels below 200 eV are from Ref. 2.

| $E_0$ (eV) | $\Delta E_0$ (eV) | $\Delta$ (eV) | $\langle 2g\Gamma_n^0\rangle$ (meV) | $\Delta\langle 2g\Gamma_n^0\rangle$ (meV) | $\langle g\Gamma_n^1\rangle$ (meV) |
|---|---|---|---|---|---|
| 35.50 | 0.06 | 0.21 | 0.024 | 0.004 | |
| 42.50 | 0.06 | 0.22 | 0.02 | 0.004 | 127 |
| 95.00 | 0.08 | 0.33 | 0.038 | 0.016 | 108 |
| 105.80 | 0.10 | 0.35 | 0.05 | 0.022 | 126 |
| 119.20 | 0.15 | 0.38 | 0.42 | 0.28 | |
| 193.80 | 0.20 | 0.48 | 2.60 | 0.20 | |
| 243.70 | 0.11 | 0.54 | 0.14 | 0.01 | |
| 319.00 | 0.16 | 0.61 | 0.11 | 0.01 | 92 |
| 335.50 | 0.17 | 0.63 | 0.80 | 0.10 | |
| 362.40 | 0.19 | 0.65 | 0.01 | 0.00 | 10 |
| 365.00 | 0.19 | 0.66 | 0.02 | 0.00 | 15 |
| 378.50 | 0.20 | 0.67 | 5.50 | 0.60 | |
| 392.40 | 0.22 | 0.68 | 0.14 | 0.02 | 96 |
| 460.30 | 0.27 | 0.74 | 0.36 | 0.02 | |
| 500.30 | 0.31 | 0.77 | 0.20 | 0.02 | 107 |
| 599.30 | 0.41 | 0.84 | 0.08 | 0.04 | 36 |
| 603.70 | 0.41 | 0.88 | 0.14 | 0.02 | 62 |
| 617.80 | 0.43 | 0.86 | 0.06 | 0.06 | 26 |
| 640.70 | 0.45 | 0.87 | 0.20 | 0.02 | 84 |
| 671.90 | 0.48 | 0.89 | 0.36 | 0.04 | 143 |
| 678.20 | 0.49 | 0.90 | 0.08 | 0.02 | 32 |
| 721.20 | 0.54 | 0.92 | 0.50 | 0.06 | 186 |
| 741.20 | 0.56 | 0.94 | 7.40 | 1.00 | |
| 757.00 | 0.58 | 0.95 | 0.06 | 0.02 | 21 |
| 911.80 | 0.76 | 1.04 | 0.08 | 0.02 | 24 |
| 934.10 | 0.79 | 1.05 | 15.00 | 1.00 | |
| 952.00 | 0.82 | 1.06 | 0.50 | 0.10 | 141 |
| 1008.50 | 0.89 | 1.09 | 18.00 | 2.00 | |
| 1016.00 | 0.90 | 1.10 | 0.30 | 0.10 | 79 |
| 1107.00 | 1.02 | 1.14 | 0.28 | 0.02 | 68 |
| 1126.50 | 1.05 | 1.15 | 0.36 | 0.02 | 86 |
| 1147.50 | 1.08 | 1.17 | 5.40 | 0.40 | |
| 1175.00 | 1.12 | 1.18 | 8.00 | 0.80 | |
| 1193.00 | 1.14 | 1.19 | 1.40 | 0.10 | |
| 1228.00 | 1.20 | 1.21 | 1.20 | 0.10 | |
| 1233.00 | 1.20 | 1.21 | 0.10 | 0.10 | 22 |
| 1242.50 | 1.22 | 1.21 | 0.40 | 0.04 | 86 |
| 1283.50 | 1.28 | 1.23 | 0.30 | 0.04 | 63 |
| 1349.50 | 1.38 | 1.26 | 0.96 | 0.04 | |
| 1352.50 | 1.38 | 1.27 | 0.20 | 0.10 | 40 |
| 1393.00 | 1.44 | 1.28 | 5.00 | 1.00 | |
| 1451.50 | 1.54 | 1.31 | 22.00 | 2.00 | |
| 1466.00 | 1.56 | 1.32 | 0.60 | 0.20 | 110 |
| 1528.50 | 1.66 | 1.35 | 0.28 | 0.08 | 49 |
| 1538.50 | 1.68 | 1.35 | 0.60 | 0.20 | 105 |
| 1555.00 | 1.70 | 1.36 | 0.30 | 0.08 | 52 |
| 1575.50 | 1.74 | 1.37 | 5.40 | 0.60 | |
| 1615.00 | 1.80 | 1.38 | 0.60 | 0.20 | 100 |
| 1653.00 | 1.87 | 1.40 | 0.80 | 0.20 | 130 |
| 1710.50 | 1.97 | 1.42 | 1.56 | 0.20 | |
| 1765.50 | 2.06 | 1.45 | 0.32 | 0.10 | 49 |
| 1809.0 | 1.1 | 1.5 | 1.84 | 0.10 | |
| 1831.0 | 1.1 | 1.5 | 17.00 | 2.00 | |
| 1857.0 | 1.1 | 1.5 | 0.06 | 0.06 | 9 |
| 1980.0 | 1.2 | 1.5 | 0.10 | 0.06 | 14 |
| 1989.1 | 1.2 | 1.5 | 0.42 | 0.04 | 57 |
| 2020.0 | 1.3 | 1.5 | 15.00 | 2.00 | |
| 2053.0 | 1.3 | 1.6 | 0.04 | 0.04 | 5 |
| 2066.0 | 1.3 | 1.6 | 1.00 | 0.40 | 130 |
| 2072.0 | 1.3 | 1.6 | 3.00 | 0.60 | |
| 2099.0 | 1.3 | 1.6 | 0.04 | 0.04 | 5 |
| 2115.0 | 1.4 | 1.6 | 0.82 | 0.10 | 104 |
| 2144.0 | 1.4 | 1.6 | 0.70 | 0.10 | 88 |
| 2152.5 | 1.4 | 1.6 | 4.60 | 1.00 | |
| 2227.5 | 1.5 | 1.6 | 3.40 | 0.60 | |
| 2237.0 | 1.5 | 1.6 | 0.06 | 0.06 | 7 |
| 2310.0 | 1.5 | 1.7 | 0.06 | 0.06 | 7 |
| 2335.0 | 1.6 | 1.7 | 1.00 | 0.00 | 115 |
| 2341.0 | 1.6 | 1.7 | 9.60 | 1.00 | |
| 2361.0 | 1.6 | 1.7 | 0.80 | 0.10 | 91 |
| 2392.5 | 1.6 | 1.7 | 0.12 | 0.04 | 14 |
| 2418.0 | 1.7 | 1.7 | 40.00 | 4.00 | |
| 2448.0 | 1.7 | 1.7 | 0.40 | 0.40 | 44 |
| 2464.0 | 1.7 | 1.7 | 1.60 | 0.40 | |
| 2510.0 | 1.7 | 1.7 | 0.70 | 0.20 | 75 |
| 2546.0 | 1.8 | 1.7 | 1.00 | 0.20 | 106 |
| 2577.0 | 1.8 | 1.7 | 0.70 | 0.20 | 73 |
| 2641.0 | 1.9 | 1.8 | 44.00 | 6.00 | |
| 2674.0 | 1.9 | 1.8 | 0.20 | 0.08 | 20 |
| 2687.0 | 1.9 | 1.8 | 0.80 | 0.20 | 80 |
| 2696.0 | 1.9 | 1.8 | 0.30 | 0.10 | 30 |
| 2710.0 | 2.0 | 1.8 | 0.60 | 0.08 | 60 |
| 2832.0 | 2.1 | 1.8 | 0.30 | 0.10 | 29 |
| 2925.0 | 2.2 | 1.9 | 3.20 | 0.40 | |
| 2951.0 | 2.2 | 1.9 | 6.00 | 1.00 | |
| 2967.5 | 2.2 | 1.9 | 0.12 | 0.04 | 11 |
| 2984.0 | 2.3 | 1.9 | 0.08 | 0.04 | 7 |
| 3020.0 | 2.3 | 1.9 | 0.12 | 0.04 | 11 |
| 3075.0 | 2.4 | 1.9 | 0.08 | 0.08 | 7 |
| 3187.0 | 2.5 | 1.9 | 0.06 | 0.06 | 5 |
| 3226.5 | 2.5 | 2.0 | 0.30 | 0.10 | 25 |
| 3256.8 | 2.6 | 2.0 | 0.30 | 0.10 | 25 |
| 3274.0 | 2.6 | 2.0 | 0.60 | 0.20 | 49 |
| 3284.0 | 2.6 | 2.0 | 0.12 | 0.06 | 10 |
| 3305.0 | 2.6 | 2.0 | 0.10 | 0.06 | 8 |
| 3358.0 | 2.7 | 2.0 | 3.00 | 0.60 | |
| 3375.0 | 2.7 | 2.0 | 0.40 | 0.20 | 32 |
| 3393.2 | 2.7 | 2.0 | 18.00 | 2.00 | |
| 3406.8 | 2.8 | 2.0 | 0.10 | 0.10 | 8 |
| 3429.0 | 2.8 | 2.0 | 0.08 | 0.08 | 6 |
| 3442.0 | 2.8 | 2.0 | 0.08 | 0.08 | 6 |
| 3459.0 | 2.8 | 2.0 | 0.08 | 0.04 | 6 |
| 3500.0 | 2.9 | 2.0 | 0.06 | 0.06 | 5 |
| 3524.0 | 2.9 | 2.0 | 16.00 | 2.00 | |
| 3564.4 | 3.0 | 2.1 | 0.10 | 0.10 | 8 |
| 3575.0 | 3.0 | 2.1 | 0.10 | 0.10 | 8 |
| 3590.8 | 3.0 | 2.1 | 0.40 | 0.10 | 30 |
| 3608.0 | 3.0 | 2.1 | 1.10 | 0.20 | 82 |
| 3628.0 | 3.0 | 2.1 | 0.12 | 0.08 | 9 |
| 3650.0 | 3.1 | 2.1 | 0.06 | 0.06 | 4 |
| 3671.7 | 3.1 | 2.1 | 2.80 | 0.40 | |
| 3716.0 | 3.1 | 2.1 | 0.10 | 0.10 | 7 |
| 3732.0 | 3.2 | 2.1 | 0.10 | 0.10 | 7 |
| 3761.5 | 3.2 | 2.1 | 6.60 | 0.60 | |
| 3841.7 | 3.3 | 2.1 | 1.70 | 0.20 | 119 |
| 3918.0 | 3.4 | 2.2 | 0.20 | 0.10 | 14 |
| 3925.0 | 3.4 | 2.2 | 1.30 | 0.20 | 89 |
| 3942.0 | 3.4 | 2.2 | 1.00 | 0.20 | 68 |
| 3958.0 | 3.5 | 2.2 | 0.04 | 0.04 | 3 |
| 3975.0 | 3.5 | 2.2 | 8.00 | 1.00 | |
| 3985.0 | 3.5 | 2.2 | 0.20 | 0.20 | 14 |
| 4000.0 | 3.5 | 2.2 | 0.40 | 0.20 | 27 |
| 4024.0 | 4.0 | 2.0 | 0.50 | 0.20 | 34 |
| 4038.0 | 4.0 | 2.0 | 0.50 | 0.20 | 34 |
| 4066.0 | 4.0 | 2.0 | 12.80 | 0.80 | |
| 4120.0 | 4.0 | 2.0 | 0.26 | 0.06 | 17 |
| 4138.0 | 4.0 | 2.0 | 0.40 | 0.20 | 26 |
| 4190.0 | 4.0 | 2.0 | 0.10 | 0.10 | 6 |
| 4228.0 | 4.0 | 2.0 | 0.20 | 0.10 | 13 |
| 4252.0 | 4.0 | 2.0 | 0.20 | 0.10 | 13 |
| 4291.0 | 4.0 | 2.0 | 0.60 | 0.20 | 38 |
| 4320.0 | 4.0 | 2.0 | 0.16 | 0.10 | 10 |
| 4346.0 | 4.0 | 2.0 | 0.40 | 0.20 | 25 |
| 4365.0 | 4.0 | 2.0 | 0.10 | 0.10 | 6 |
| 4380.0 | 4.0 | 2.0 | 0.10 | 0.10 | 6 |
| 4401.0 | 4.0 | 2.0 | 0.20 | 0.10 | 12 |
| 4449.0 | 4.0 | 2.0 | 0.30 | 0.20 | 18 |
| 4480.0 | 4.0 | 2.0 | 0.04 | 0.04 | 2 |
| 4539.0 | 4.0 | 2.0 | 0.20 | 0.20 | 12 |
| 4553.0 | 4.0 | 2.0 | 4.60 | 1.00 | |
| 4595.0 | 4.0 | 2.0 | 32.00 | 6.00 | |
| 4606.0 | 4.0 | 2.0 | 0.20 | 0.20 | 12 |

TABLE I (*continued*)

| $E_0$ (eV) | $\Delta E_0$ (eV) | $\Delta$ (eV) | $\langle 2g\Gamma_n^0\rangle$ (meV) | $\Delta\langle 2g\Gamma_n^0\rangle$ (meV) | $\langle g\Gamma_n^1\rangle$ (meV) |
|---|---|---|---|---|---|
| 4647.0 | 4.0 | 2.0 | 0.20 | 0.10 | 12 |
| 4728.0 | 5.0 | 2.0 | 0.20 | 0.10 | 11 |
| 4740.0 | 5.0 | 2.0 | 0.30 | 0.20 | 17 |
| 4780.0 | 5.0 | 2.0 | 0.10 | 0.10 | 6 |
| 4807.0 | 5.0 | 2.0 | 1.08 | 0.10 | 61 |
| 4825.0 | 5.0 | 2.0 | 1.08 | 0.20 | 60 |
| 4840.0 | 5.0 | 2.0 | 0.10 | 0.10 | 6 |
| 4868.0 | 5.0 | 2.0 | 0.10 | 0.10 | 6 |
| 4885.0 | 5.0 | 2.0 | 0.06 | 0.06 | 3 |
| 4910.0 | 5.0 | 2.0 | 0.10 | 0.10 | 6 |
| 4932.0 | 5.0 | 2.0 | 0.30 | 0.10 | 16 |
| 4955.0 | 5.0 | 2.0 | 0.10 | 0.10 | 5 |
| 5043.0 | 5.0 | 2.0 | 2.40 | 0.60 | |
| 5063.0 | 5.0 | 2.0 | 1.60 | 0.40 | |
| 5085.0 | 5.0 | 2.0 | 0.30 | 0.10 | |
| 5105.0 | 5.0 | 2.0 | 0.20 | 0.10 | |
| 5150.0 | 5.0 | 2.0 | 46.00 | 10.00 | |
| 5165.0 | 5.0 | 2.0 | 0.40 | 0.40 | |
| 5178.0 | 5.0 | 2.0 | 0.20 | 0.20 | |
| 5229.0 | 5.0 | 2.0 | 0.40 | 0.20 | |
| 5265.0 | 5.0 | 2.0 | 0.10 | 0.10 | |
| 5292.0 | 5.0 | 3.0 | 1.40 | 0.20 | |
| 5335.0 | 5.0 | 3.0 | 0.20 | 0.20 | |
| 5387.0 | 5.0 | 3.0 | 0.20 | 0.20 | |
| 5465.0 | 6.0 | 3.0 | 1.50 | 0.40 | |
| 5480.0 | 6.0 | 3.0 | 0.20 | 0.20 | |
| 5509.0 | 6.0 | 3.0 | 1.00 | 0.20 | |
| 5543.0 | 6.0 | 3.0 | 3.80 | 0.80 | |
| 5571.0 | 6.0 | 3.0 | 7.00 | 1.40 | |
| 5600.0 | 6.0 | 3.0 | 0.20 | 0.10 | |
| 5652.0 | 6.0 | 3.0 | 4.00 | 1.00 | |
| 5687.0 | 6.0 | 3.0 | 24.00 | 6.00 | |
| 5716.0 | 6.0 | 3.0 | 0.20 | 0.20 | |
| 5735.0 | 6.0 | 3.0 | 0.40 | 0.20 | |
| 5788.0 | 6.0 | 3.0 | 4.60 | 1.00 | |
| 5830.0 | 6.0 | 3.0 | 1.00 | 0.40 | |
| 5855.0 | 6.0 | 3.0 | 10.00 | 3.00 | |
| 5874.0 | 6.0 | 3.0 | 0.24 | 0.00 | |
| 5898.0 | 6.0 | 3.0 | 12.00 | 4.00 | |
| 5936.0 | 6.0 | 3.0 | 0.10 | 0.10 | |
| 5999.0 | 6.0 | 3.0 | 44.00 | 10.00 | |
| 6044.0 | 7.0 | 3.0 | 8.00 | 2.00 | |
| 6069.0 | 7.0 | 3.0 | 0.60 | 0.20 | |
| 6108.0 | 7.0 | 3.0 | 10.00 | 1.60 | |
| 6145.0 | 7.0 | 3.0 | 0.20 | 0.20 | |
| 6168.0 | 7.0 | 3.0 | 2.80 | 0.60 | |
| 6208.0 | 7.0 | 3.0 | 1.60 | 0.40 | |
| 6221.0 | 7.0 | 3.0 | 1.80 | 0.40 | |
| 6275.0 | 7.0 | 3.0 | 0.70 | 0.20 | |
| 6350.0 | 7.0 | 3.0 | 0.30 | 0.10 | |
| 6406.0 | 7.0 | 3.0 | 30.00 | 6.00 | |
| 6445.0 | 7.0 | 3.0 | 0.60 | 0.20 | |
| 6498.0 | 7.0 | 3.0 | 1.30 | 0.40 | |
| 6535.0 | 7.0 | 3.0 | 11.00 | 2.00 | |
| 6565.0 | 7.0 | 3.0 | 3.00 | 0.60 | |
| 6630.0 | 7.0 | 3.0 | 12.00 | 2.00 | |
| 6711.0 | 8.0 | 3.0 | 3.00 | 0.60 | |
| 6734.0 | 8.0 | 3.0 | 2.80 | 0.60 | |
| 6780.0 | 8.0 | 3.0 | 0.90 | 0.30 | |
| 6795.0 | 8.0 | 3.0 | 9.00 | 2.00 | |
| 6841.0 | 8.0 | 3.0 | 0.60 | 0.20 | |
| 6860.0 | 8.0 | 3.0 | 0.20 | 0.20 | |
| 6880.0 | 8.0 | 3.0 | 0.40 | 0.20 | |
| 6904.0 | 8.0 | 3.0 | 7.00 | 2.00 | |
| 6927.0 | 8.0 | 3.0 | 3.00 | 1.00 | |
| 7039.0 | 8.0 | 3.0 | 8.00 | 1.60 | |
| 7071.0 | 8.0 | 3.0 | 0.50 | 0.20 | |
| 7129.0 | 8.0 | 3.0 | 0.70 | 0.20 | |
| 7237.0 | 9.0 | 3.0 | 24.00 | 6.00 | |
| 7322.0 | 9.0 | 3.0 | 2.20 | 0.60 | |

was used in this region to see if any weak levels had been missed in earlier measurements.

The "measured" curves of total cross section versus energy for Nb are shown in Fig. 1. The measured resonance parameters $E_0$ and $\langle 2g\Gamma_n^0\rangle$ and their uncertainties, and the calculated Doppler widths for the levels are given in Table I. The parameters $\langle 2g\Gamma_n^0\rangle$ are given for the weaker levels for which $\langle 2g\Gamma_n^1\rangle \leqslant 300$ meV. These values, which are discussed in more detail in a later section, are based on an analysis that treats them as possible $l=1$ levels. Two examples of area analysis for resonance parameters are shown in Figs. 5(a) and 5(b). A detailed discussion of the area analysis method used for the determination of neutron widths has been given previously.[3,4] In Fig. 5(b), curves of $g\Gamma_n^0$ versus $\Gamma$ have been shown for three different choices of transmission between resonances ($T_r$) in order to give some idea of the uncertainty in the values of $\Gamma$ and $\Gamma_n^0$ for possible choices of $T_r$. It is evident from the figure that the relative uncertainty in the values of $g\Gamma_n^0$ is much smaller than the uncertainty in the value of $\Gamma$. Moreover, the value of $g\Gamma_n^0$ is not greatly affected by the choice of $\Gamma$. We have given the values of $g\Gamma_n^0$ and not $\Gamma$, since the latter are not determined very precisely by this method. For economy of space we have not quoted the values of $\Gamma_n$, since these can be determined by using the expression $\Gamma_n = 2g\Gamma_n^0(E)^{1/2}$.

The parameters in Table I for the Nb levels below 200 eV are from earlier 35-meter flight path self-indication measurements[2] using our spectrometer system. The listing of $\langle 2g\Gamma_n^0\rangle$ values ends at 7300 eV because the analysis for higher energy levels did not seem to be sufficiently reliable to be included.

### B. Silver ($Z=47$, $\sim 50\%$ Each $A=107$ and 109, $I=\frac{1}{2}$ for Each)

The total-cross-section measurements for natural silver used foils of the metal. The energy intervals 90–300 eV, 300–1200 eV, and 1200–4000 eV were studied using detection channel widths of 0.4, 0.2, and 0.1 $\mu$sec, respectively. The energy resolution and Doppler broadening values were nearly the same as for Nb.

Transmission samples having $(1/n)=7.4$, 34.4, 103.3, and 360 b/atom were used for the lowest energy interval. The three thickest samples were used for the intermediate energy region. Samples having $(1/n)=18$ and 50 b/atom were used for the highest energy region.

Figure 2 shows curves of the "measured" cross

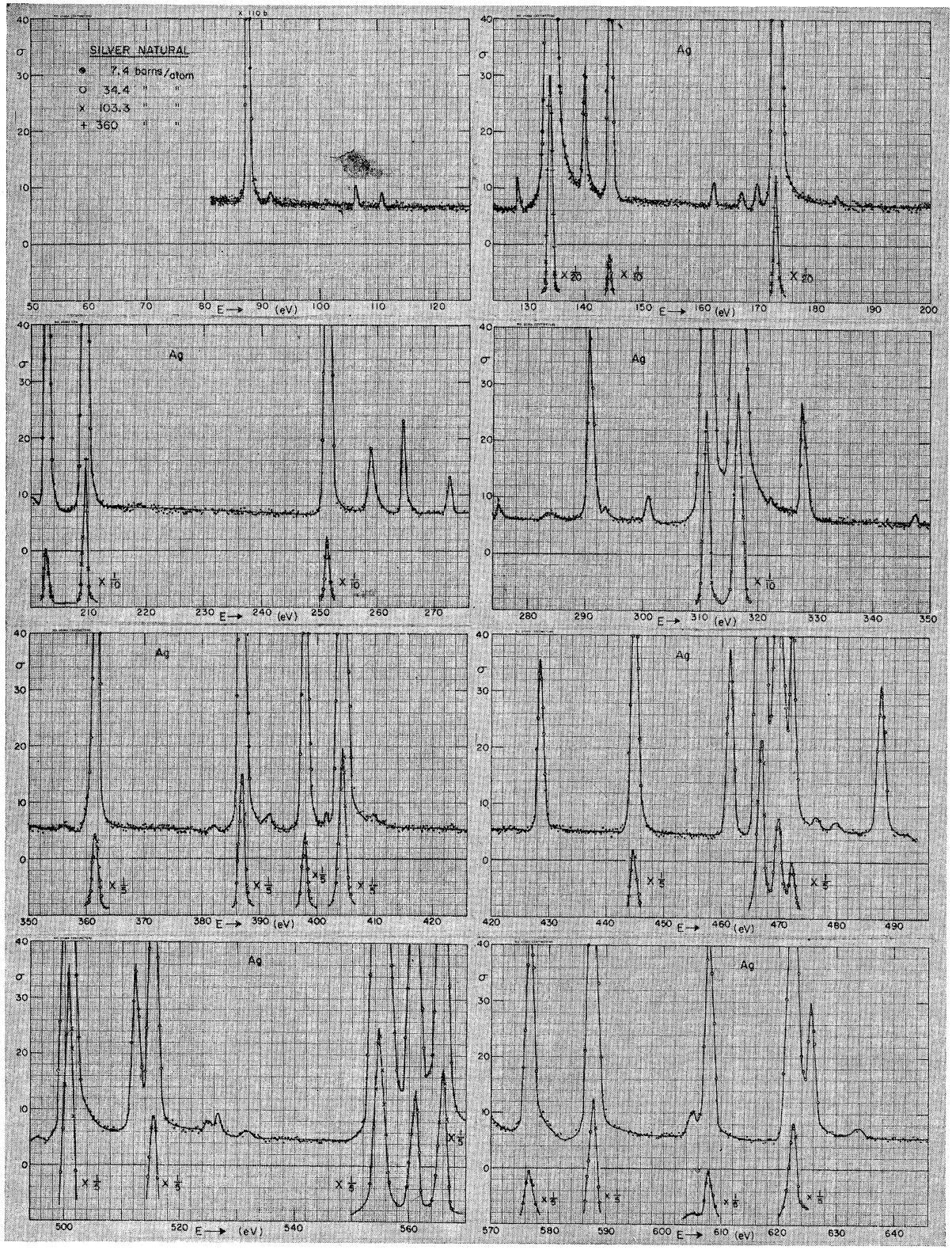


FIG. 2. The "measured" total neutron cross section for natural silver versus energy from 80 to 4000 eV. The considerations for the curves are similar to those described in the caption of Fig. 1.

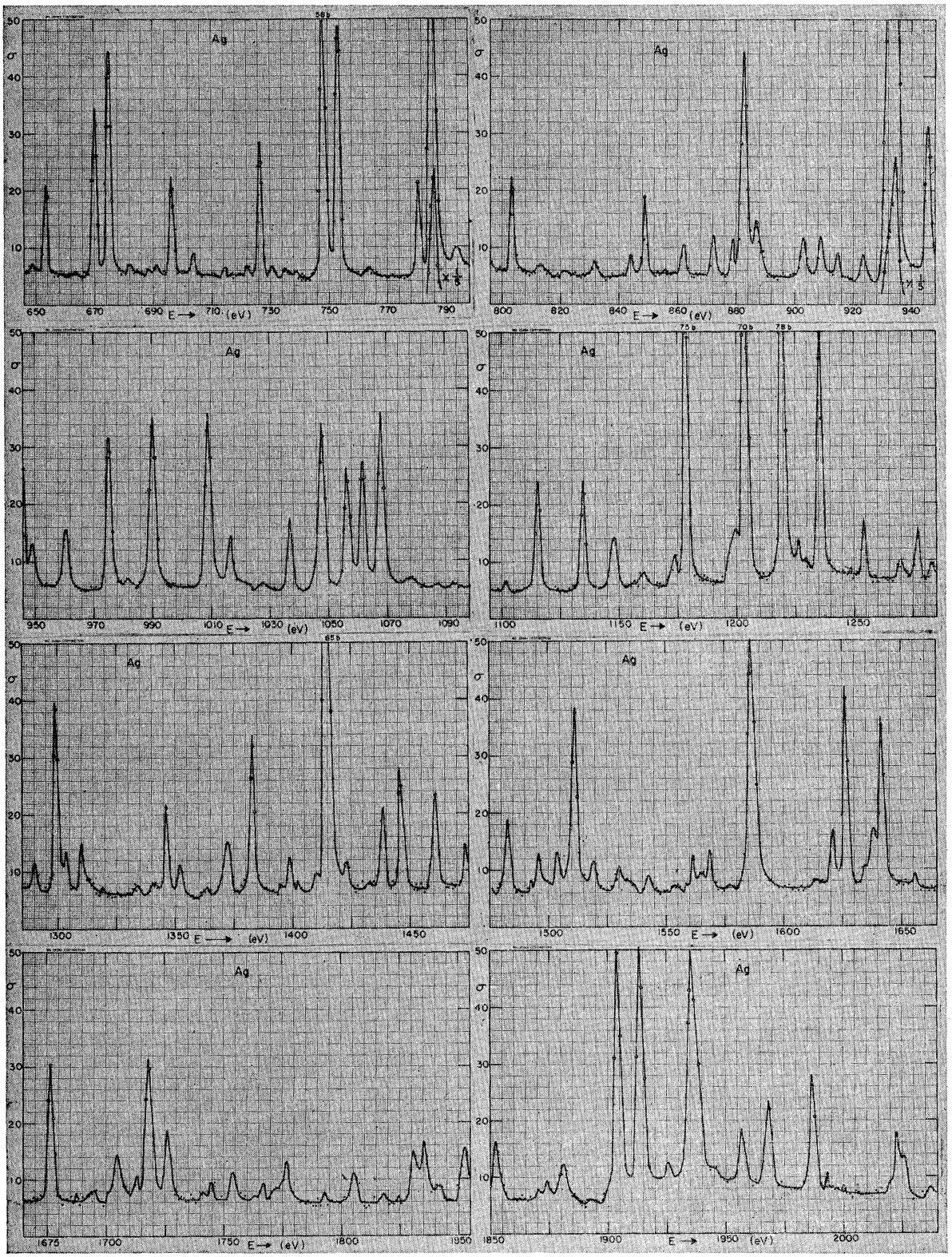


FIG. 2. *Continued.*

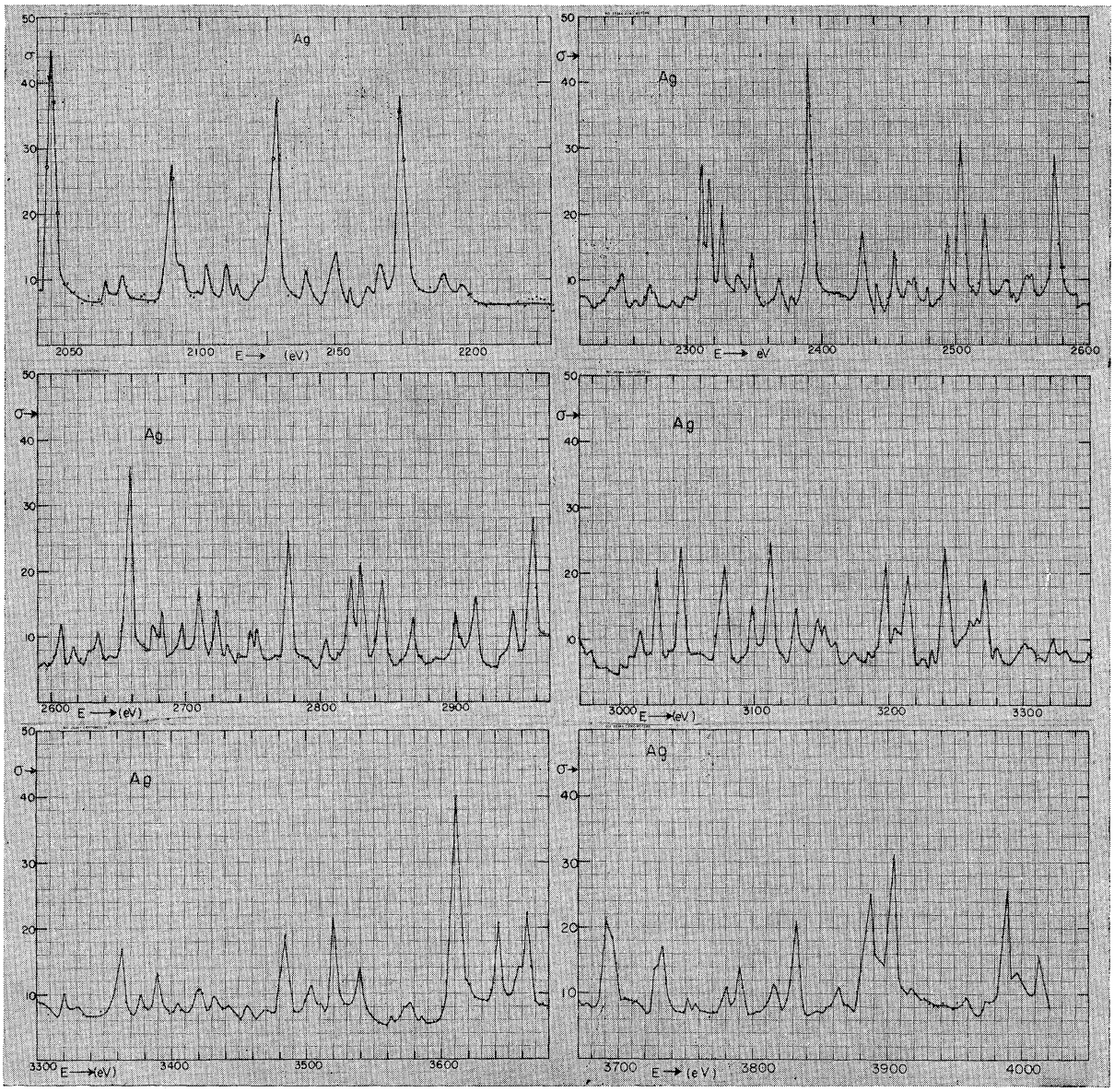


FIG. 2. *Continued.*

section versus energy. It should be noted that thickest sample used above 1200 eV was undesirably thin. It is likely, therefore, that more very weak levels in this energy range were missed than if the thicker sample had been used. Most of these weaker levels are probably due to $l=1$ interactions. The cross-section values are for the natural element which consists of nearly equal amounts of $Ag^{107}$ and $Ag^{109}$. The resonance cross sections should thus be doubled to give the isotopic cross section.

Table II lists the resonance energies and the measured values of $\langle 4ag\Gamma_n^0\rangle$ for the silver resonances. The isotopic abundance factor $a$, is approximately $\frac{1}{2}$ for both isotopes, so $4a=2$. Since $I=\frac{1}{2}$, the spin weight factor $(2g)$ for $s$-wave levels is $\frac{1}{2}$ or $\frac{3}{2}$ for $J=0$ or 1. The $l=1$ level could have $J=0$, 1, or 2, and $\langle 4ag\Gamma_n^1\rangle$ is shown for a few of the weaker levels on the assumption that they may be due to $l=1$ interactions.

The parameters for levels below 100 eV are from the earlier[2] self-indication measurements of Ag using a 35-m flight path. Those measurements revealed many weak levels which were interpreted as the detection of part of a $p$-wave level population. The present measurements, because of the greatly improved energy resolution, also show most of the weak "levels" previously reported. We believe that a few of the weak "levels" previously reported were due to spurious statistical fluctuation effects and we include in Table II a few weak levels which were not included in the earlier

TABLE II. Resonance parameters for the levels in natural silver. $g=\frac{3}{4}$ and $\frac{1}{4}$ for $J=1$ and 0, respectively. $a\simeq 0.5$ for both $Ag^{107}$ and $Ag^{109}$. The parameters for levels below 100 eV are from Ref. 2. The levels marked with asterisk are considered as $p$-wave levels.

| $E_0$ (eV) | $\Delta E_0$ (eV) | $\langle 4ag\Gamma_n^0\rangle$ (meV) | $\Delta\langle 4ag\Gamma_n^0\rangle$ (meV) | $\langle 4ag\Gamma_n^1\rangle$ (meV) |
|---|---|---|---|---|
| 5.20 | 0.01 | 8.16 | 0.06 | |
| 16.30 | 0.03 | 1.48 | 0.06 | |
| 30.50 | 0.06 | 2.00 | 0.18 | |
| 40.20 | 0.08 | 1.36 | 0.16 | |
| 41.50 | 0.08 | 1.32 | 0.16 | |
| 44.80 | 0.08 | 0.27 | 0.04 | |
| 51.40 | 0.10 | 4.48 | 0.40 | |
| 55.70 | 0.10 | 2.56 | 0.20 | |
| 70.80 | 0.11 | 4.76 | 0.44 | |
| 83.50 | 0.20 | 0.003 | 0.0007 | |
| 87.67 | 0.20 | 1.00 | 0.08 | |
| *91.50 | 0.20 | 0.005 | 0.001 | 27 |
| 106.29 | 0.06 | 0.012 | 0.004 | |
| 110.88 | 0.06 | 0.008 | 0.001 | |
| 128.04 | 0.08 | 0.008 | 0.004 | |
| 133.90 | 0.09 | 10.40 | 0.80 | |
| 139.70 | 0.09 | 0.18 | 0.02 | |
| 144.20 | 0.10 | 0.76 | 0.08 | |
| 162.40 | 0.11 | 0.02 | 0.01 | |
| *167.10 | 0.12 | 0.016 | 0.004 | 48 |
| 169.80 | 0.12 | 0.028 | 0.008 | |
| 173.10 | 0.13 | 5.00 | 0.40 | |
| *183.60 | 0.14 | 0.012 | 0.004 | 32 |
| 202.50 | 0.16 | 1.12 | 0.12 | |
| 209.60 | 0.17 | 2.48 | 0.20 | |
| 218.20 | 0.18 | 0.012 | 0.012 | |
| 251.29 | 0.22 | 2.20 | 0.16 | |
| 258.89 | 0.23 | 0.18 | 0.02 | |
| 264.47 | 0.24 | 0.24 | 0.02 | |
| 272.44 | 0.25 | 0.12 | 0.01 | |
| *274.90 | 0.25 | 0.02 | 0.008 | 36 |
| *283.90 | 0.27 | 0.016 | 0.008 | 28 |
| 290.86 | 0.28 | 0.76 | 0.08 | |
| 293.00 | 0.28 | 0.02 | 0.008 | 34 |
| 300.64 | 0.29 | 0.08 | 0.02 | |
| 310.92 | 0.15 | 10.00 | 2.00 | |
| 316.40 | 0.16 | 14.00 | 2.00 | |
| *322.10 | 0.16 | 0.02 | 0.008 | 31 |
| 327.80 | 0.16 | 0.40 | 0.06 | |
| 347.34 | 0.18 | 0.02 | 0.008 | |
| 356.20 | 0.19 | 0.02 | 0.008 | |
| 361.83 | 0.19 | 1.80 | 0.08 | |
| *382.10 | 0.21 | 0.02 | 0.008 | 26 |
| 387.00 | 0.21 | 3.32 | 0.12 | |
| 391.60 | 0.22 | 0.016 | 0.004 | |
| 398.00 | 0.22 | 1.52 | 0.08 | |
| *401.70 | 0.22 | 0.024 | 0.012 | 30 |
| 404.40 | 0.23 | 5.00 | 0.20 | |
| *410.01 | 0.23 | 0.016 | 0.008 | 20 |
| 428.40 | 0.25 | 0.88 | 0.08 | |
| 444.60 | 0.26 | 1.80 | 0.20 | |
| 461.40 | 0.28 | 1.08 | 0.12 | |
| 466.80 | 0.28 | 4.60 | 1.20 | |
| 469.61 | 0.28 | 2.00 | 0.80 | |
| 472.20 | 0.29 | 0.72 | 0.08 | |
| *476.10 | 0.29 | 0.16 | 0.02 | 168 |
| 479.54 | 0.29 | 0.12 | 0.02 | |
| 487.72 | 0.30 | 1.16 | 0.08 | |
| 495.20 | 0.31 | 0.04 | 0.02 | |
| 500.60 | 0.31 | 10.00 | 1.00 | |
| 512.27 | 0.32 | 0.68 | 0.08 | |
| 515.47 | 0.33 | 4.40 | 0.40 | |
| *524.90 | 0.33 | 0.02 | 0.008 | 19 |
| 526.60 | 0.34 | 0.04 | 0.02 | |
| 532.20 | 0.34 | 0.07 | 0.02 | |
| 554.51 | 0.36 | 10.00 | 1.00 | |
| 560.66 | 0.37 | 6.00 | 0.80 | |
| 565.43 | 0.37 | 8.00 | 0.80 | |
| 576.67 | 0.38 | 3.04 | 0.40 | |
| 587.47 | 0.40 | 6.40 | 0.60 | |
| 605.06 | 0.41 | 0.10 | 0.02 | |
| 607.93 | 0.42 | 2.60 | 0.20 | |
| 622.17 | 0.43 | 5.60 | 1.20 | |
| 625.59 | 0.43 | 0.64 | 0.08 | |
| *634.27 | 0.44 | 0.04 | 0.02 | 32 |
| 648.21 | 0.46 | 0.04 | 0.02 | |
| 653.50 | 0.46 | 1.00 | 0.08 | |
| 669.45 | 0.48 | 1.68 | 0.20 | |
| 674.50 | 0.49 | 3.00 | 0.28 | |
| 681.50 | 0.49 | 0.16 | 0.04 | |
| 687.40 | 0.50 | 0.08 | 0.02 | |
| 695.89 | 0.51 | 1.08 | 0.12 | |
| 703.51 | 0.52 | 0.26 | 0.02 | |
| 713.87 | 0.53 | 0.07 | 0.02 | |
| *721.26 | 0.54 | 0.04 | 0.01 | 33 |
| 726.08 | 0.54 | 1.04 | 0.12 | |
| 730.39 | 0.55 | 0.07 | 0.01 | |
| *734.70 | 0.55 | 0.04 | 0.01 | 52 |
| 747.49 | 0.57 | 5.20 | 0.40 | |
| 752.57 | 0.57 | 4.00 | 0.40 | |
| 764.00 | 0.59 | 0.13 | 0.04 | |
| 779.94 | 0.61 | 0.80 | 0.16 | |
| 784.74 | 0.61 | 11.60 | 1.20 | |
| 792.65 | 0.62 | 0.20 | 0.08 | |
| 803.80 | 0.63 | 1.80 | 0.40 | |
| 813.00 | 0.64 | 0.24 | 0.06 | |
| 822.00 | 0.65 | 0.16 | 0.06 | |
| 831.39 | 0.67 | 0.20 | 0.08 | |
| 844.04 | 0.68 | 0.24 | 0.06 | |
| 848.78 | 0.69 | 1.00 | 0.20 | |
| 861.83 | 0.70 | 0.52 | 0.08 | |
| 872.34 | 0.72 | 0.64 | 0.12 | |
| 878.75 | 0.72 | 0.52 | 0.12 | |
| 882.33 | 0.73 | 4.00 | 0.60 | |
| 886.67 | 0.73 | 0.40 | 0.12 | |
| 902.84 | 0.75 | 0.60 | 0.12 | |
| 908.82 | 0.76 | 0.52 | 0.12 | |
| 914.87 | 0.77 | 0.24 | 0.04 | |
| 923.29 | 0.78 | 0.32 | 0.04 | |
| 933.39 | 0.79 | 18.00 | 2.00 | |
| 945.24 | 0.81 | 2.00 | 0.20 | |
| 949.25 | 0.81 | 0.36 | 0.08 | |
| 960.59 | 0.83 | 0.72 | 0.12 | |
| 975.48 | 0.85 | 3.20 | 0.40 | |
| 981.40 | 0.85 | 0.02 | 0.02 | |
| 989.86 | 0.87 | 4.00 | 0.40 | |
| 1008.94 | 0.89 | 4.00 | 0.40 | |
| 1016.91 | 0.90 | 0.52 | 0.08 | |
| *1027.69 | 0.92 | 0.01 | 0.01 | |
| 1036.79 | 0.93 | 0.84 | 0.16 | |
| 1047.87 | 0.94 | 2.80 | 0.40 | |
| 1056.31 | 0.95 | 1.60 | 0.20 | |
| 1061.04 | 0.96 | 1.60 | 0.20 | |
| 1067.71 | 0.97 | 3.20 | 0.40 | |
| 1078.33 | 0.98 | 0.07 | 0.02 | |
| 1087.00 | 1.00 | 0.04 | 0.04 | |
| 1092.00 | 1.00 | 0.05 | 0.02 | |
| 1102.00 | 1.02 | 0.05 | 0.02 | |
| 1115.23 | 1.03 | 2.16 | 0.16 | |
| 1134.91 | 1.06 | 2.20 | 0.20 | |
| 1147.62 | 1.08 | 1.32 | 0.20 | |
| 1159.45 | 1.10 | 0.14 | 0.04 | |
| 1173.60 | 1.12 | 0.24 | 0.04 | |
| 1178.10 | 1.12 | 5.60 | 0.80 | |
| *1199.50 | 1.15 | 0.40 | 0.40 | |
| 1203.3 | 0.6 | 6.80 | 0.80 | |
| 1218.9 | 0.6 | 7.60 | 0.80 | |
| 1226.0 | 0.6 | 0.20 | 0.04 | |
| 1235.5 | 0.6 | 3.80 | 0.20 | |
| 1254.2 | 0.6 | 1.00 | 0.20 | |
| 1270.8 | 0.6 | 0.24 | 0.04 | |
| 1276.4 | 0.6 | 0.76 | 0.08 | |

TABLE II (*continued*)

| $E_0$ (eV) | $\Delta E_0$ (eV) | $\langle 4ag\Gamma_n^0\rangle$ (meV) | $\Delta\langle 4ag\Gamma_n^0\rangle$ (meV) | $\langle 4ag\Gamma_n^1\rangle$ (meV) |
|---|---|---|---|---|
| 1283.3 | 0.6 | 0.20 | 0.04 | |
| 1299.3 | 0.7 | 3.20 | 0.24 | |
| 1303.1 | 0.7 | 0.16 | 0.04 | |
| 1310.3 | 0.7 | 0.72 | 0.08 | |
| *1332.0 | 0.7 | 0.04 | 0.04 | |
| 1341.0 | 0.7 | 0.12 | 0.04 | |
| 1346.5 | 0.7 | 0.92 | 0.12 | |
| 1352.0 | 0.7 | 0.32 | 0.08 | |
| 1363.0 | 0.7 | 0.08 | 0.04 | |
| 1371.0 | 0.7 | 0.60 | 0.20 | |
| 1373.0 | 0.7 | 0.60 | 0.20 | |
| 1382.5 | 0.7 | 2.20 | 0.20 | |
| *1394.0 | 0.7 | 0.02 | 0.02 | |
| 1398.5 | 0.7 | 0.48 | 0.04 | |
| *1402.0 | 0.7 | 0.02 | 0.02 | |
| 1410.0 | 0.7 | 0.08 | 0.04 | |
| 1414.5 | 0.7 | 10.00 | 2.00 | |
| 1423.0 | 0.7 | 0.18 | 0.04 | |
| *1433.0 | 0.8 | 0.04 | 0.04 | |
| 1438.5 | 0.8 | 1.28 | 0.20 | |
| 1446.5 | 0.8 | 2.00 | 0.20 | |
| 1461.0 | 0.8 | 1.44 | 0.16 | |
| 1473.5 | 0.8 | 0.64 | 0.08 | |
| 1483.0 | 0.8 | 1.28 | 0.12 | |
| 1496.0 | 0.8 | 0.56 | 0.08 | |
| 1504.0 | 0.8 | 0.48 | 0.08 | |
| 1511.0 | 0.8 | 3.60 | 0.40 | |
| 1519.0 | 0.8 | 0.36 | 0.08 | |
| 1529.5 | 0.8 | 0.28 | 0.08 | |
| *1534.5 | 0.8 | 0.12 | 0.08 | |
| 1542.0 | 0.8 | 0.24 | 0.08 | |
| 1553.0 | 0.9 | 0.04 | 0.04 | |
| 1561.0 | 0.9 | 0.24 | 0.08 | |
| 1566.0 | 0.9 | 0.04 | 0.04 | |
| 1568.5 | 0.9 | 0.44 | 0.08 | |
| 1577.0 | 0.9 | 0.02 | 0.02 | |
| 1586.0 | 0.9 | 10.40 | 2.00 | |
| 1613.5 | 0.9 | 0.08 | 0.04 | |
| 1621.0 | 0.9 | 0.80 | 0.20 | |
| 1626.5 | 0.9 | 3.20 | 0.60 | |
| 1634.0 | 0.9 | 0.08 | 0.08 | |
| 1638.0 | 0.9 | 0.60 | 0.20 | |
| 1642.0 | 0.9 | 2.80 | 0.60 | |
| 1655.5 | 0.9 | 0.12 | 0.04 | |
| 1677.0 | 1.0 | 3.00 | 0.60 | |
| 1686.0 | 1.0 | 0.04 | 0.04 | |
| 1695.0 | 1.0 | 0.16 | 0.04 | |
| 1705.0 | 1.0 | 1.32 | 0.20 | |
| 1713.0 | 1.0 | 0.20 | 0.04 | |
| 1718.0 | 1.0 | 3.60 | 0.80 | |
| 1726.0 | 1.0 | 1.40 | 0.20 | |
| 1740.0 | 1.0 | 0.08 | 0.08 | |
| 1745.0 | 1.0 | 0.20 | 0.08 | |
| 1754.0 | 1.0 | 0.48 | 0.04 | |
| 1767.0 | 1.0 | 0.12 | 0.04 | |
| 1772.0 | 1.0 | 0.04 | 0.02 | |
| 1776.5 | 1.0 | 0.72 | 0.16 | |
| *1793.0 | 1.1 | 0.08 | 0.08 | |
| 1806.0 | 1.1 | 0.72 | 0.08 | |
| 1818.0 | 1.1 | 0.12 | 0.08 | |
| 1831.0 | 1.1 | 0.80 | 0.20 | |
| 1835.0 | 1.1 | 0.92 | 0.20 | |
| 1841.5 | 1.1 | 0.20 | 0.08 | |
| 1853.0 | 1.1 | 1.60 | 0.24 | |
| 1863.5 | 1.1 | 0.08 | 0.08 | |
| 1870.0 | 1.1 | 0.12 | 0.04 | |
| 1874.5 | 1.1 | 0.20 | 0.04 | |
| 1881.5 | 1.1 | 0.40 | 0.16 | |
| 1904.5 | 1.2 | 8.00 | 2.00 | |
| 1913.5 | 1.2 | 8.80 | 2.00 | |
| 1926.0 | 1.2 | 0.28 | 0.08 | |
| 1934.5 | 1.2 | 8.00 | 2.00 | |
| 1937.0 | 1.2 | 12.00 | 4.00 | |
| 1945.0 | 1.2 | 0.08 | 0.04 | |
| 1957.0 | 1.2 | 1.32 | 0.12 | |
| 1968.0 | 1.2 | 2.52 | 0.28 | |
| 1987.0 | 1.2 | 3.20 | 0.40 | |
| *1993.0 | 1.2 | 0.04 | 0.02 | |
| *2000.0 | 1.2 | 0.04 | 0.04 | |
| 2022.0 | 1.0 | 2.00 | 0.60 | |
| 2026.0 | 1.0 | 0.80 | 0.40 | |
| 2036.0 | 1.0 | 0.20 | 0.08 | |
| 2045.0 | 1.0 | 8.00 | 2.00 | |
| 2059.0 | 1.0 | 0.08 | 0.08 | |
| 2067.0 | 1.0 | 0.16 | 0.08 | |
| 2072.0 | 1.0 | 0.40 | 0.20 | |
| 2080.0 | 1.0 | 0.08 | 0.08 | |
| 2090.0 | 1.0 | 3.60 | 0.80 | |
| 2093.0 | 1.0 | 0.20 | 0.20 | |
| 2099.0 | 1.0 | 0.08 | 0.08 | |
| 2103.0 | 1.0 | 0.64 | 0.08 | |
| 2110.0 | 1.0 | 0.64 | 0.08 | |
| 2114.0 | 1.0 | 0.16 | 0.08 | |
| 2128.0 | 1.0 | 7.20 | 1.60 | |
| 2139.0 | 1.0 | 0.56 | 0.20 | |
| 2150.0 | 1.0 | 1.52 | 0.32 | |
| 2156.0 | 1.0 | 0.16 | 0.08 | |
| 2163.0 | 1.0 | 0.24 | 0.16 | |
| 2167.0 | 1.0 | 0.60 | 0.20 | |
| 2174.0 | 1.0 | 7.20 | 1.60 | |
| 2185.0 | 1.0 | 0.08 | 0.08 | |
| 2190.0 | 1.0 | 0.24 | 0.00 | |
| 2197.0 | 1.0 | 0.16 | 0.08 | |
| 2216.0 | 1.0 | 0.12 | 0.12 | |
| 2225.0 | 1.0 | 0.20 | 0.20 | |
| 2244.0 | 1.0 | 0.08 | 0.08 | |
| 2253.0 | 1.0 | 0.60 | 0.20 | |
| 2262.0 | 1.0 | 0.08 | 0.08 | |
| 2269.0 | 2.0 | 0.08 | 0.08 | |
| 2273.0 | 2.0 | 0.24 | 0.08 | |
| 2290.0 | 2.0 | 0.08 | 0.08 | |
| 2300.0 | 2.0 | 0.20 | 0.08 | |
| 2311.0 | 2.0 | 3.80 | 0.80 | |
| 2317.0 | 2.0 | 2.00 | 0.40 | |
| 2326.0 | 2.0 | 2.00 | 0.40 | |
| 2338.0 | 2.0 | 0.40 | 0.00 | |
| 2349.0 | 2.0 | 1.24 | 0.12 | |
| 2369.0 | 2.0 | 0.60 | 0.20 | |
| 2378.0 | 2.0 | 0.12 | 0.12 | |
| 2390.0 | 2.0 | 14.00 | 2.00 | |
| 2431.0 | 2.0 | 2.20 | 0.40 | |
| 2441.0 | 2.0 | 0.40 | 0.20 | |
| 2454.0 | 2.0 | 1.80 | 0.20 | |
| 2464.0 | 2.0 | 0.40 | 0.20 | |
| 2470.0 | 2.0 | 0.20 | 0.12 | |
| 2479.0 | 2.0 | 0.20 | 0.12 | |
| 2495.0 | 2.0 | 1.60 | 0.40 | |
| 2505.0 | 2.0 | 7.20 | 1.20 | |
| 2522.0 | 2.0 | 2.80 | 0.60 | |
| 2538.0 | 2.0 | 0.80 | 0.40 | |
| 2543.0 | 2.0 | 0.08 | 0.08 | |
| 2554.0 | 2.0 | 0.64 | 0.20 | |
| 2558.0 | 2.0 | 0.40 | 0.20 | |
| 2574.0 | 2.0 | 6.40 | 1.60 | |
| 2595.0 | 2.0 | 0.08 | 0.08 | |
| 2608.0 | 2.0 | 1.00 | 0.20 | |
| 2617.0 | 2.0 | 0.48 | 0.16 | |
| 2628.0 | 2.0 | 0.20 | 0.20 | |
| 2636.0 | 2.0 | 0.80 | 0.20 | |
| 2645.0 | 2.0 | 0.12 | 0.12 | |
| 2658.0 | 2.0 | 10.00 | 2.00 | |
| 2677.0 | 2.0 | 1.00 | 0.20 | |
| 2683.0 | 2.0 | 1.20 | 0.40 | |
| 2698.0 | 2.0 | 0.96 | 0.20 | |

TABLE II (*continued*)

| $E_0$ (eV) | $\Delta E_0$ (eV) | $\langle 4ag\Gamma_n^0\rangle$ (meV) | $\Delta\langle 4ag\Gamma_n^0\rangle$ (meV) | $\langle 4ag\Gamma_n^1\rangle$ (meV) |
|---|---|---|---|---|
| 2711.0 | 2.0 | 2.80 | 0.40 | |
| 2724.0 | 2.0 | 1.60 | 0.40 | |
| 2731.0 | 2.0 | 0.24 | 0.12 | |
| 2739.0 | 2.0 | 0.08 | 0.08 | |
| 2749.0 | 2.0 | 0.80 | 0.20 | |
| 2753.0 | 2.0 | 0.80 | 0.20 | |
| 2767.0 | 2.0 | 0.08 | 0.08 | |
| 2777.0 | 2.0 | 6.40 | 1.20 | |
| 2791.0 | 2.0 | 0.08 | 0.00 | |
| 2805.0 | 2.0 | 0.60 | 0.20 | |
| 2813.0 | 2.0 | 0.20 | 0.20 | |
| 2824.0 | 2.0 | 2.80 | 0.60 | |
| 2831.0 | 2.0 | 2.80 | 0.60 | |
| 2846.0 | 2.0 | 4.40 | 0.80 | |
| 2860.0 | 2.0 | 0.08 | 0.08 | |
| 2869.0 | 2.0 | 1.60 | 0.40 | |
| 2875.0 | 2.0 | 0.08 | 0.08 | |
| 2887.0 | 2.0 | 0.08 | 0.08 | |
| 2901.0 | 2.0 | 1.20 | 0.20 | |
| 2915.0 | 2.0 | 2.80 | 0.40 | |
| 2937.0 | 2.0 | 0.20 | 0.20 | |
| 2944.0 | 2.0 | 2.00 | 0.40 | |
| 2958.0 | 2.0 | 8.00 | 2.00 | |
| 2978.0 | 2.0 | 0.08 | 0.08 | |
| 2989.0 | 2.0 | 0.08 | 0.08 | |
| 3000.0 | 2.0 | 0.08 | 0.08 | |
| 3016.0 | 2.0 | 1.00 | 0.40 | |
| 3028.0 | 2.0 | 4.80 | 0.92 | |
| 3039.0 | 2.0 | 0.08 | 0.08 | |
| 3046.0 | 2.0 | 6.80 | 1.40 | |
| 3058.0 | 2.0 | 0.20 | 0.20 | |
| 3079.0 | 2.0 | 6.00 | 1.20 | |
| 3100.0 | 2.0 | 2.00 | 0.40 | |
| 3112.0 | 2.0 | 4.80 | 1.20 | |
| 3120.0 | 2.0 | 0.08 | 0.08 | |
| 3131.0 | 2.0 | 2.40 | 0.60 | |
| 3148.0 | 2.0 | 1.20 | 0.40 | |
| 3153.0 | 2.0 | 0.60 | 0.20 | |
| 3160.0 | 2.0 | 0.40 | 0.20 | |
| 3175.0 | 2.0 | 0.60 | 0.20 | |
| 3185.0 | 2.0 | 0.20 | 0.20 | |
| 3192.0 | 3.0 | 4.40 | 1.20 | |
| 3207.0 | 3.0 | 0.40 | 0.20 | |
| 3214.0 | 3.0 | 5.20 | 1.20 | |
| 3224.0 | 3.0 | 0.20 | 0.20 | |
| 3234.0 | 3.0 | 0.40 | 0.20 | |
| 3242.0 | 3.0 | 9.20 | 2.00 | |
| 3260.0 | 3.0 | 0.08 | 0.08 | |
| 3265.0 | 3.0 | 0.08 | 0.08 | |
| 3273.0 | 3.0 | 2.80 | 0.80 | |
| 3280.0 | 3.0 | 0.40 | 0.20 | |
| 3301.0 | 3.0 | 0.80 | 0.40 | |
| 3306.0 | 3.0 | 0.40 | 0.40 | |
| 3311.0 | 3.0 | 0.08 | 0.08 | |
| 3324.0 | 3.0 | 0.60 | 0.20 | |
| 3332.0 | 3.0 | 0.20 | 0.20 | |
| 3349.0 | 3.0 | 0.08 | 0.08 | |
| 3365.0 | 3.0 | 5.20 | 1.20 | |
| 3378.0 | 3.0 | 0.60 | 0.20 | |
| 3391.0 | 3.0 | 2.00 | 0.40 | |
| 3405.0 | 3.0 | 0.40 | 0.20 | |
| 3423.0 | 3.0 | 1.20 | 0.40 | |
| 3432.0 | 3.0 | 0.60 | 0.20 | |
| 3444.0 | 3.0 | 0.08 | 0.08 | |
| 3457.0 | 3.0 | 0.40 | 0.20 | |
| 3471.0 | 3.0 | 0.20 | 0.20 | |
| 3485.0 | 3.0 | 4.40 | 0.80 | |
| 3505.0 | 3.0 | 2.20 | 0.40 | |
| 3511.0 | 3.0 | 0.08 | 0.08 | |
| 3522.0 | 3.0 | 6.00 | 1.20 | |
| 3540.0 | 3.0 | 2.40 | 0.80 | |
| 3562.0 | 3.0 | 0.20 | 0.20 | |
| 3578.0 | 3.0 | 0.80 | 0.40 | |
| 3586.0 | 3.0 | 0.80 | 0.08 | |
| 3610.0 | 3.0 | 20.00 | 4.00 | |
| 3620.0 | 3.0 | 0.08 | 0.08 | |
| 3643.0 | 3.0 | 5.20 | 1.20 | |
| 3658.0 | 3.0 | 0.40 | 0.40 | |
| 3664.0 | 3.0 | 6.40 | 1.60 | |
| 3676.0 | 3.0 | 0.08 | 0.08 | |
| 3692.0 | 3.0 | 12.00 | 2.80 | |
| 3714.0 | 3.0 | 0.20 | 0.20 | |
| 3726.0 | 3.0 | 2.00 | 2.00 | |
| 3733.0 | 3.0 | 6.00 | 2.00 | |
| 3751.0 | 3.0 | 0.40 | 0.20 | |
| 3757.0 | 3.0 | 0.20 | 0.20 | |
| 3780.0 | 3.0 | 1.00 | 0.40 | |
| 3790.0 | 3.0 | 2.80 | 1.20 | |
| 3815.0 | 3.0 | 2.40 | 0.80 | |
| 3832.0 | 3.0 | 6.40 | 2.00 | |
| 3848.0 | 3.0 | 0.20 | 0.20 | |
| 3855.0 | 3.0 | 0.08 | 0.08 | |
| 3864.0 | 3.0 | 0.80 | 0.20 | |
| 3870.0 | 3.0 | 0.08 | 0.08 | |
| 3887.0 | 3.0 | 14.00 | 4.00 | |
| 3904.0 | 3.0 | 17.20 | 4.00 | |
| 3917.0 | 3.0 | 0.20 | 0.20 | |
| 3942.0 | 3.0 | 0.08 | 0.08 | |
| 3958.0 | 3.0 | 0.40 | 0.20 | |
| 3972.0 | 3.0 | 0.20 | 0.20 | |
| 3989.0 | 3.0 | 14.00 | 4.00 | |
| 3996.0 | 4.0 | 0.40 | 0.40 | |

listing[2] even though they are in the energy region previously studied. The parameters in Table II for levels below 100 eV are from the 35-m flight-path studies.[2]

### C. Iodine ($Z=53$, $A=127$, $I=\frac{5}{2}$)

The total-cross-section measurements for iodine were performed in the energy intervals 100–300 eV, 300–1200 eV, and 1200–4000 eV using detection channel widths of 0.4, 0.2, and 0.1 $\mu$sec, respectively.

Transmission samples of solid elemental iodine having $1/n=10.76$, 50, and 283 b/atom were used. The container faces consisted of 0.00025-in.-thick Mylar and 0.018-in. thickness of 2$S$ aluminum.

Figure 3 presents curves of the "measured" cross section versus energy. Table III lists the resonance energies and the measured values of $\langle 2g\Gamma_n^0\rangle$. The results for the resonances below 150 eV are from our earlier 35-m flight path self-indication measurements.[2] The value of $2g$ is 5/6 or 7/6 for $J=2$ and 3, respectively ($l=0$).

### D. Cesium ($Z=55$, $A=133$, $I=\frac{7}{2}$)

Total-cross-section measurements for Cs were made in the energy intervals 100–300 eV, 300–1200 eV, and 1200–4000 eV, using detection interval widths of 0.4, 0.2, and 0.1 $\mu$sec respectively. The samples were in the form of $Cs_2SO_4$ in containers having thin Al windows.

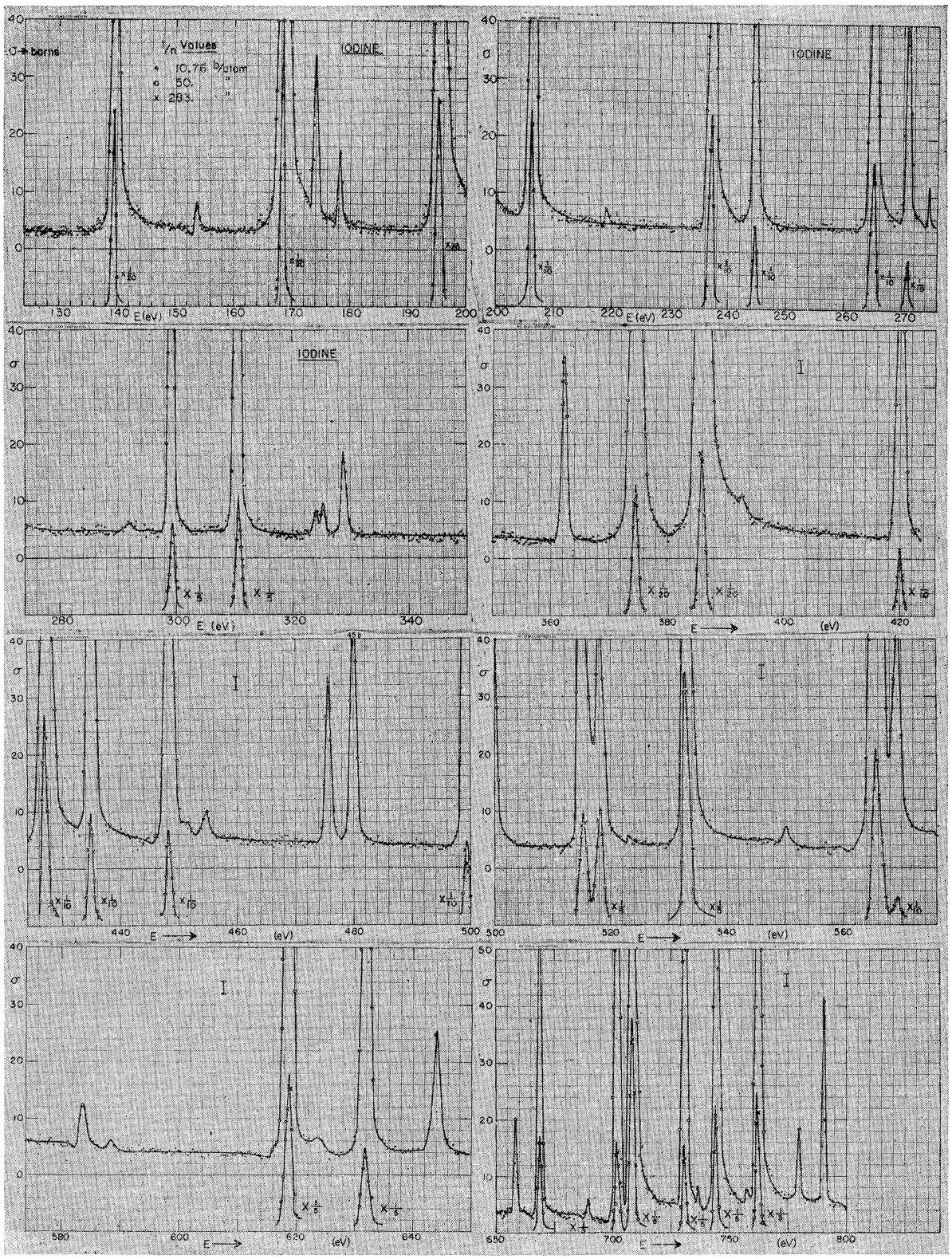


FIG. 3. The "measured" total neutron cross section for iodine versus energy from 124 to 4000 eV. The considerations are similar to those discussed in the caption of Fig. 1.

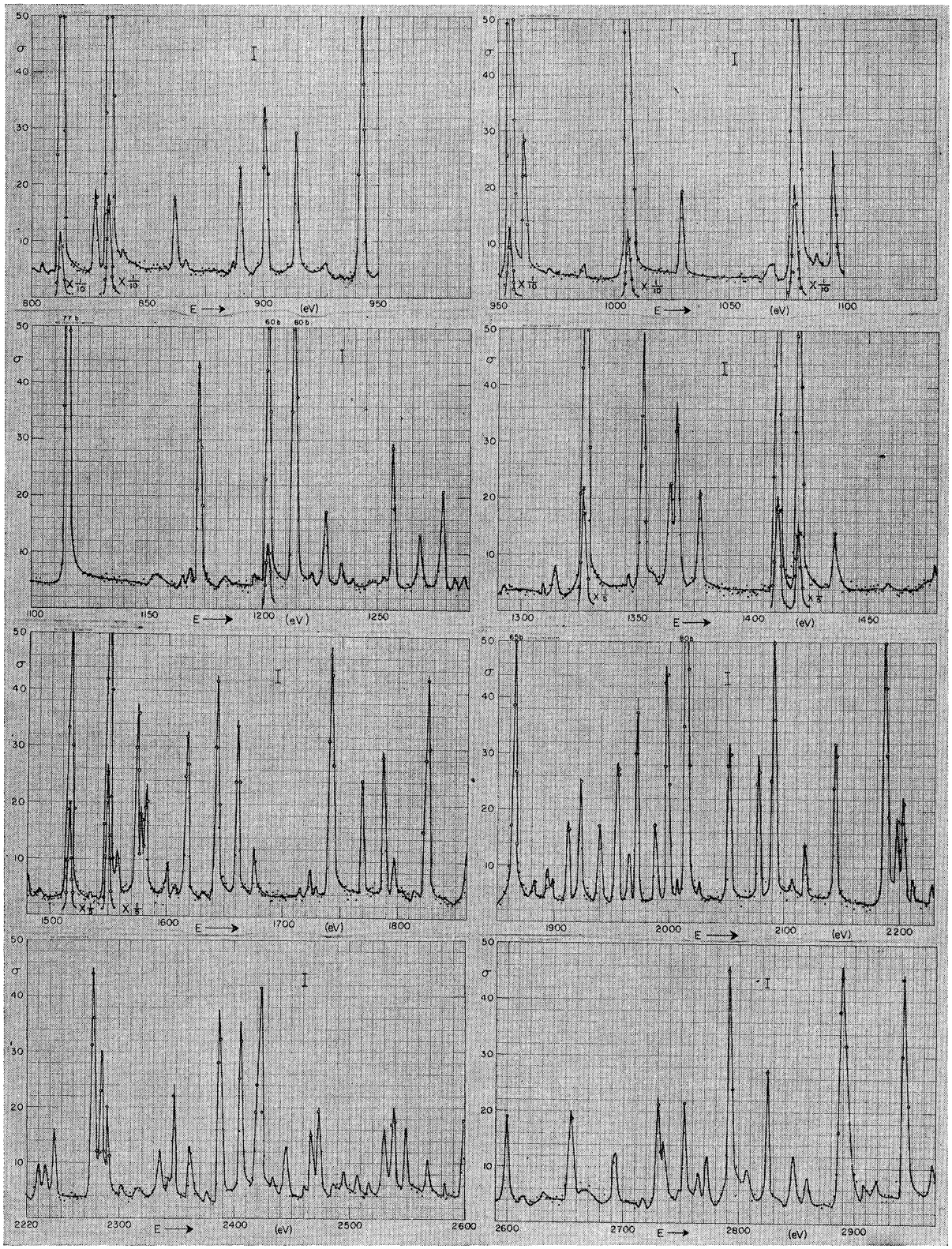


FIG. 3. *Continued.*

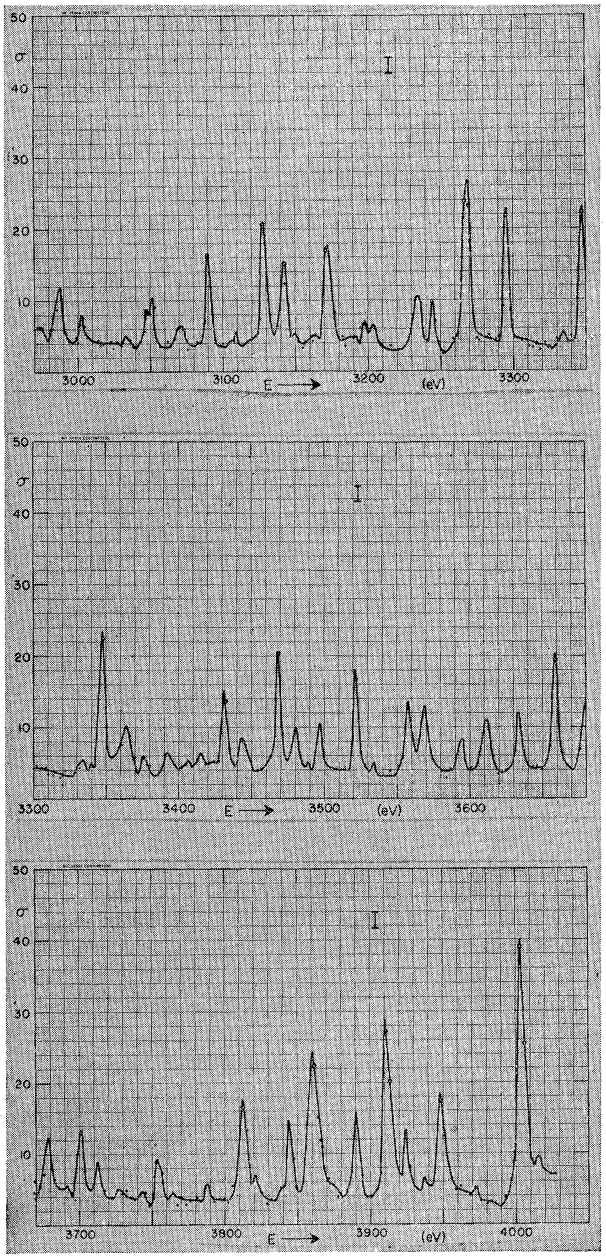


FIG. 3. *Continued.*

Two different thicknesses corresponding to $(1/n)=50$ and 400 b/atom of Cs were used for each energy interval. Corrections were made for the transmission effects of the sulfur and oxygen components of the samples so the curves in Fig. 4 present the "measured" cross section of Cs as a function of energy.

The measured values of the resonance energies and values of $\langle 2g\Gamma_n^0\rangle$ are presented in Table IV. The thickest transmission sample $(1/n=50$ b/atom) was much thinner than desirable to obtain precise values for the cross section between resonances and to observe very weak resonances. Further measurements on this nucleus will be made when a thicker sample is available. The values of $\langle 2g\Gamma_n^0\rangle$ for the first five levels are from Ref. 6.

## III. DISCUSSION OF THE RESULTS

### A. Mean Level Spacings, Distribution of $g\Gamma_n^0$ Values, and the $l=0$ Strength Functions

Figures 6–9 show the number of observed levels $N(E)$ versus the neutron energy $E$ for Nb, Ag, I, and Cs, respectively. The straight lines through the origin which give best fits to the initial parts of the curve fit relatively up to $E\approx 6$ keV for Nb, 2 keV for Ag, 3 keV for I, and 3 keV for Cs. The corresponding mean level spacings (including all observed levels) are

$$\bar{D}=(32.5\pm 1.5)\text{ eV for } \mathrm{Nb}^{93},$$
$$\bar{D}=(8.75\pm 0.4)\text{ eV for Ag},$$
$$\bar{D}=(13.0\pm 0.5)\text{ eV for } \mathrm{I}^{127},$$
$$\bar{D}=(20\pm 1)\text{ eV for } \mathrm{Cs}^{133}.$$

Figures 10–13 show histograms of the reduced neutron widths for the four elements for equal intervals of $y=\langle g\Gamma_n^0\rangle^{1/2}$ except $y=\langle ag\Gamma_n^0\rangle^{1/2}$ for natural silver. The Porter-Thomas single-channel $(\nu=1)$ theoretical distribution corresponds to a Gaussian with its maximum at $y=0$ while a two-channel $(\nu=2)$ distribution is of the form of $y$ times a Gaussian and is zero at $y=0$. The plots are highest in the first interval, which corresponds to the region of the weakest levels. The greatest effect of this kind occurs for Nb where the first four intervals contain 120, 14, 9, and 7 levels, respectively, for intervals of width $y=0.8$ $(\text{meV})^{1/2}$. When a choice $y=0.2$ $(\text{meV})^{1/2}$ is made, the first eight intervals have 27, 53, 25, 15, 5, 2, 4, and 3 levels, respectively. Since Nb is known to be near the peak of the $p$-wave strength function, most of these weak levels are probably due to $l=1$. The excess of weak levels is less pronounced for Ag, I, and Cs, but the first one or two intervals of the histograms are still well above the values (near 27 to 31 for silver, 32 to 36 for iodine, or 21 to 24 for cesium) that one would select as the reasonable extrapolation for the $\nu=1$ (Gaussian) curves which give best fit to all but the first one or two intervals.

Before attempting to draw detailed conclusions from Figs. 10–13, it is well to review briefly the experimental shortcomings of the data which are apt to cause the observed distributions to differ from the true ones. These include:

(a) The "observation" of a weak level involves noting a small dip in the thick-sample transmission curve relative to the values for the adjacent time-of-flight channels. A "threshold" is always set which hopefully, but not certainly, prevents the false identification as levels of those dips which are due merely to statistical fluctuations in the data. It is unlikely that we

TABLE III. Resonance parameters for the levels in iodine. $g=7/12$ and $5/12$ for $J=3$ and 2, respectively. The levels marked with asterisk are most probably $p$ wave or spurious. Resonance parameters for levels below 150 eV are from Ref. 2.

| $E_0$ (eV) | $\Delta E_0$ (eV) | $\langle 2g\Gamma_n^0\rangle$ (meV) | $\Delta\langle 2g\Gamma_n^0\rangle$ (meV) | $E_0$ (eV) | $\Delta E_0$ (eV) | $\langle 2g\Gamma_n^0\rangle$ (meV) | $\Delta\langle 2g\Gamma_n^0\rangle$ (meV) |
|---|---|---|---|---|---|---|---|
| 20.40 | 0.00 | 0.31 | 0.02 | 901.35 | 0.75 | 0.75 | 0.10 |
| 31.20 | 0.06 | 3.40 | 0.36 | 914.87 | 0.77 | 0.74 | 0.06 |
| 37.70 | 0.08 | 7.20 | 0.81 | 927.15 | 0.78 | 0.04 | 0.01 |
| 45.40 | 0.08 | 3.70 | 0.74 | 942.86 | 0.80 | 1.40 | 0.10 |
| 66.00 | 0.10 | 0.27 | 0.03 | 954.89 | 0.82 | 4.50 | 0.40 |
| 78.50 | 0.20 | 3.90 | 0.34 | 960.59 | 0.83 | 0.86 | 0.10 |
| 90.25 | 0.20 | 2.90 | 0.31 | 987.30 | 0.86 | 0.04 | 0.01 |
| 139.50 | 0.09 | 5.70 | 0.51 | 1006.30 | 0.89 | 4.80 | 0.60 |
| 145.70 | 0.10 | 0.012 | 0.0017 | 1029.50 | 0.92 | 0.50 | 0.08 |
| *153.61 | 0.11 | 0.015 | 0.002 | 1067.00 | 0.97 | 0.06 | 0.03 |
| 168.40 | 0.12 | 8.00 | 1.00 | 1069.50 | 0.97 | 0.09 | 0.04 |
| 173.80 | 0.13 | 0.20 | 0.02 | 1078.30 | 0.98 | 9.00 | 1.00 |
| *178.03 | 0.13 | 0.07 | 0.01 | 1088.10 | 1.00 | 0.04 | 0.01 |
| 195.23 | 0.15 | 7.40 | 0.20 | 1095.10 | 1.01 | 0.80 | 0.10 |
| 206.10 | 0.16 | 2.40 | 0.20 | 1115.20 | 1.03 | 4.40 | 0.60 |
| 237.05 | 0.20 | 2.60 | 0.20 | 1156.20 | 1.09 | 0.10 | 0.03 |
| 244.64 | 0.21 | 0.70 | 0.10 | *1165.30 | 1.10 | 0.02 | 0.02 |
| 264.95 | 0.24 | 2.20 | 0.20 | *1169.00 | 1.11 | 0.02 | 0.02 |
| 270.97 | 0.25 | 0.40 | 0.10 | 1172.50 | 1.12 | 1.20 | 0.10 |
| 274.50 | 0.25 | 0.02 | 0.01 | 1183.50 | 1.13 | 0.04 | 0.02 |
| 291.96 | 0.28 | 0.03 | 0.01 | 1195.90 | 1.15 | 0.02 | 0.02 |
| 299.21 | 0.29 | 0.70 | 0.10 | 1202.1 | 1.2 | 2.20 | 0.20 |
| 310.60 | 0.15 | 1.00 | 0.10 | 1213.7 | 1.2 | 2.90 | 0.40 |
| 324.37 | 0.16 | 0.02 | 0.005 | 1221.9 | 1.2 | 0.02 | 0.02 |
| 325.34 | 0.16 | 0.028 | 0.005 | 1227.1 | 1.2 | 0.40 | 0.05 |
| 328.70 | 0.17 | 0.14 | 0.02 | 1234.2 | 1.2 | 0.10 | 0.02 |
| 362.20 | 0.19 | 0.30 | 0.02 | *1239.6 | 1.2 | 0.02 | 0.02 |
| 374.50 | 0.20 | 6.40 | 0.20 | 1248.0 | 1.2 | 0.06 | 0.02 |
| 385.83 | 0.21 | 10.70 | 0.70 | *1252.9 | 1.2 | 0.02 | 0.02 |
| 392.70 | 0.22 | 0.02 | 0.02 | 1256.6 | 1.2 | 0.62 | 0.10 |
| 420.00 | 0.24 | 1.14 | 0.10 | *1262.7 | 1.2 | 0.02 | 0.02 |
| 426.93 | 0.25 | 5.10 | 0.40 | 1268.2 | 1.3 | 0.28 | 0.04 |
| 434.78 | 0.25 | 2.10 | 0.20 | 1278.2 | 1.3 | 0.52 | 0.08 |
| *439.81 | 0.26 | 0.02 | 0.02 | 1283.3 | 1.3 | 0.04 | 0.02 |
| 448.29 | 0.26 | 2.20 | 0.20 | 1287.7 | 1.3 | 0.06 | 0.02 |
| 454.61 | 0.27 | 0.05 | 0.01 | 1309.6 | 1.3 | 0.02 | 0.02 |
| 475.82 | 0.29 | 0.40 | 0.04 | 1314.8 | 1.3 | 0.16 | 0.05 |
| 480.12 | 0.29 | 0.56 | 0.04 | 1326.6 | 1.3 | 3.40 | 0.60 |
| 499.16 | 0.31 | 1.70 | 0.30 | 1346.1 | 1.4 | 0.05 | 0.02 |
| 515.47 | 0.33 | 1.70 | 0.20 | 1352.2 | 1.4 | 2.30 | 0.20 |
| 518.25 | 0.33 | 1.60 | 0.20 | 1364.6 | 1.4 | 0.65 | 0.10 |
| 532.93 | 0.34 | 3.30 | 0.20 | 1367.4 | 1.4 | 1.05 | 0.15 |
| 550.24 | 0.36 | 0.05 | 0.02 | 1377.1 | 1.4 | 0.56 | 0.15 |
| 565.80 | 0.37 | 5.60 | 0.60 | 1404.2 | 1.5 | 0.03 | 0.03 |
| 569.14 | 0.38 | 0.80 | 0.15 | 1410.7 | 1.5 | 3.50 | 0.50 |
| 583.96 | 0.39 | 0.10 | 0.02 | 1420.2 | 1.5 | 3.20 | 0.40 |
| 588.64 | 0.40 | 0.02 | 0.01 | 1435.8 | 1.5 | 0.44 | 0.05 |
| 619.20 | 0.43 | 2.30 | 0.10 | 1479.3 | 1.6 | 0.08 | 0.04 |
| 623.88 | 0.43 | 0.02 | 0.01 | 1490.3 | 1.6 | 0.03 | 0.02 |
| 632.00 | 0.44 | 1.36 | 0.04 | 1515.1 | 1.6 | 4.80 | 0.40 |
| 644.48 | 0.45 | 0.36 | 0.08 | 1535.6 | 1.7 | 0.02 | 0.02 |
| 658.64 | 0.47 | 0.20 | 0.04 | 1548.9 | 1.7 | 6.60 | 1.00 |
| 668.97 | 0.48 | 1.68 | 0.08 | 1558.1 | 1.7 | 0.18 | 0.08 |
| 689.38 | 0.50 | 0.04 | 0.02 | 1574.3 | 1.7 | 1.80 | 0.40 |
| 701.98 | 0.52 | 3.70 | 0.20 | 1578.6 | 1.7 | 0.30 | 0.20 |
| 708.50 | 0.52 | 11.00 | 2.00 | 1582.0 | 1.7 | 0.82 | 0.15 |
| 730.93 | 0.55 | 3.60 | 0.20 | 1600.3 | 1.8 | 0.28 | 0.05 |
| 736.39 | 0.56 | 0.02 | 0.02 | 1605.6 | 1.8 | 0.08 | 0.04 |
| 744.13 | 0.56 | 5.80 | 0.40 | 1617.2 | 1.8 | 1.60 | 0.20 |
| 757.69 | 0.58 | 0.03 | 0.01 | 1630.6 | 1.8 | 0.04 | 0.02 |
| 762.30 | 0.58 | 6.40 | 0.40 | 1642.5 | 1.8 | 2.50 | 0.30 |
| 779.34 | 0.60 | 0.26 | 0.06 | 1660.9 | 1.9 | 1.90 | 0.10 |
| 790.20 | 0.62 | 0.64 | 0.10 | 1675.9 | 1.9 | 0.40 | 0.05 |
| 805.00 | 0.63 | 0.02 | 0.02 | 1714.2 | 2.0 | 0.03 | 0.03 |
| 813.00 | 0.64 | 2.40 | 0.50 | 1723.0 | 2.0 | 0.15 | 0.05 |
| 828.11 | 0.66 | 0.36 | 0.06 | *1728.9 | 2.0 | 0.03 | 0.03 |
| 833.37 | 0.67 | 5.20 | 0.40 | 1741.8 | 2.0 | 4.20 | 0.60 |
| *839.35 | 0.68 | 0.02 | 0.02 | 1768.0 | 2.1 | 1.30 | 0.16 |
| 861.83 | 0.70 | 0.34 | 0.04 | 1787.6 | 2.1 | 1.36 | 0.20 |
| 866.71 | 0.71 | 0.04 | 0.01 | 1795.9 | 2.1 | 0.38 | 0.08 |
| 889.58 | 0.74 | 0.50 | 0.10 | 1813.8 | 2.1 | 0.04 | 0.02 |

TABLE III (*continued*)

| $E_0$ (eV) | $\Delta E_0$ (eV) | $\langle 2g\Gamma_n^0\rangle$ (meV) | $\Delta\langle 2g\Gamma_n^0\rangle$ (meV) | $E_0$ (eV) | $\Delta E_0$ (eV) | $\langle 2g\Gamma_n^0\rangle$ (meV) | $\Delta\langle 2g\Gamma_n^0\rangle$ (meV) |
|---|---|---|---|---|---|---|---|
| 1825.6 | 2.2 | 3.40 | 0.60 | 2806.0 | 2.0 | 0.16 | 0.06 |
| 1860.0 | 2.2 | 0.20 | 0.10 | *2813.0 | 2.0 | 0.02 | 0.02 |
| 1865.0 | 2.2 | 5.60 | 0.60 | 2825.0 | 2.0 | 2.20 | 0.40 |
| 1882.0 | 2.3 | 0.20 | 0.05 | 2846.0 | 2.0 | 1.00 | 0.20 |
| 1895.0 | 2.3 | 0.34 | 0.10 | 2859.0 | 2.0 | 0.38 | 0.10 |
| 1899.0 | 2.3 | 0.20 | 0.05 | 2869.0 | 2.0 | 0.03 | 0.03 |
| 1912.0 | 2.3 | 0.85 | 0.10 | 2893.0 | 2.0 | 15.00 | 5.00 |
| 1923.0 | 2.3 | 1.36 | 0.20 | 2908.0 | 2.0 | 0.30 | 0.10 |
| 1940.0 | 2.4 | 0.88 | 0.06 | 2919.0 | 2.0 | 0.30 | 0.10 |
| 1954.0 | 2.4 | 1.40 | 0.20 | 2925.0 | 2.0 | 0.05 | 0.05 |
| 1965.0 | 2.4 | 0.46 | 0.10 | 2930.0 | 2.0 | 0.05 | 0.05 |
| 1972.0 | 2.4 | 2.20 | 0.30 | 2943.0 | 2.0 | 6.40 | 0.60 |
| 1988.5 | 2.5 | 0.92 | 0.06 | 2967.0 | 2.0 | 0.60 | 0.10 |
| 1997.0 | 2.5 | 4.50 | 0.50 | 2988.0 | 2.0 | 0.65 | 0.15 |
| 2007.0 | 1.0 | 0.12 | 0.04 | 3002.0 | 2.0 | 0.70 | 0.05 |
| 2015.0 | 1.0 | 7.00 | 0.50 | 3035.0 | 2.0 | 0.15 | 0.05 |
| 2027.0 | 1.0 | 0.04 | 0.02 | 3048.0 | 2.0 | 0.35 | 0.10 |
| 2042.0 | 1.0 | 0.02 | 0.02 | 3053.0 | 2.0 | 0.65 | 0.20 |
| 2053.0 | 1.0 | 2.00 | 0.20 | 3071.0 | 2.0 | 0.35 | 0.10 |
| 2068.0 | 1.0 | 0.04 | 0.02 | 3090.0 | 2.0 | 2.00 | 0.40 |
| 2079.0 | 1.0 | 1.80 | 0.20 | 3109.0 | 2.0 | 0.15 | 0.05 |
| 2092.0 | 1.0 | 4.20 | 0.40 | 3128.0 | 2.0 | 2.50 | 0.50 |
| 2109.0 | 1.0 | 0.30 | 0.10 | 3143.0 | 2.0 | 1.50 | 0.40 |
| 2121.0 | 1.0 | 0.58 | 0.12 | 3162.0 | 2.0 | 0.06 | 0.06 |
| *2133.0 | 1.0 | 0.02 | 0.02 | 3172.0 | 2.0 | 3.00 | 0.50 |
| 2145.0 | 1.0 | 2.10 | 0.10 | 3190.0 | 3.0 | 0.15 | 0.05 |
| 2188.0 | 1.0 | 7.00 | 0.50 | 3197.0 | 3.0 | 0.20 | 0.10 |
| 2199.0 | 1.0 | 0.80 | 0.20 | 3204.0 | 3.0 | 0.20 | 0.10 |
| 2204.0 | 1.0 | 0.80 | 0.20 | 3234.0 | 3.0 | 1.00 | 0.20 |
| 2212.0 | 1.0 | 0.40 | 0.10 | 3244.0 | 3.0 | 0.75 | 0.20 |
| 2231.0 | 1.0 | 0.42 | 0.10 | 3267.0 | 3.0 | 7.00 | 1.50 |
| 2237.0 | 1.0 | 0.36 | 0.10 | 3296.0 | 3.0 | 2.50 | 0.50 |
| 2245.0 | 1.0 | 0.70 | 0.10 | 3335.0 | 3.0 | 0.15 | 0.05 |
| 2278.0 | 2.0 | 4.60 | 0.60 | 3348.0 | 3.0 | 4.00 | 0.80 |
| 2285.0 | 2.0 | 1.30 | 0.50 | 3364.0 | 3.0 | 1.00 | 0.30 |
| 2290.0 | 2.0 | 1.00 | 0.20 | 3375.0 | 3.0 | 0.40 | 0.10 |
| 2303.0 | 2.0 | 0.12 | 0.05 | 3391.0 | 3.0 | 0.40 | 0.10 |
| 2317.0 | 2.0 | 0.10 | 0.05 | 3405.0 | 3.0 | 0.10 | 0.05 |
| 2336.0 | 2.0 | 0.70 | 0.10 | 3416.0 | 3.0 | 0.14 | 0.05 |
| 2349.0 | 2.0 | 1.50 | 0.20 | 3432.0 | 3.0 | 2.00 | 0.40 |
| 2363.0 | 2.0 | 0.70 | 0.10 | 3443.0 | 3.0 | 1.00 | 0.30 |
| 2377.0 | 2.0 | 0.08 | 0.02 | 3468.0 | 3.0 | 3.00 | 0.50 |
| 2389.0 | 2.0 | 3.20 | 0.20 | 3480.0 | 3.0 | 0.90 | 0.20 |
| 2407.0 | 2.0 | 2.90 | 0.20 | 3497.0 | 3.0 | 1.00 | 0.30 |
| 2423.0 | 2.0 | 5.00 | 0.40 | 3522.0 | 3.0 | 2.60 | 0.60 |
| 2434.0 | 2.0 | 0.08 | 0.02 | 3534.0 | 3.0 | 0.08 | 0.05 |
| 2446.0 | 2.0 | 0.70 | 0.10 | 3557.0 | 3.0 | 2.00 | 0.40 |
| 2468.0 | 2.0 | 1.00 | 0.22 | 3569.0 | 3.0 | 1.60 | 0.40 |
| 2475.0 | 2.0 | 1.50 | 0.50 | 3595.0 | 3.0 | 0.60 | 0.20 |
| 2486.0 | 2.0 | 0.10 | 0.05 | 3613.0 | 3.0 | 1.70 | 0.40 |
| 2495.0 | 2.0 | 0.20 | 0.05 | 3634.0 | 3.0 | 1.60 | 0.40 |
| 2508.0 | 2.0 | 0.20 | 0.05 | 3658.0 | 3.0 | 5.00 | 1.00 |
| 2517.0 | 2.0 | 0.10 | 0.05 | 3680.0 | 3.0 | 2.00 | 0.40 |
| 2530.0 | 2.0 | 1.40 | 0.40 | 3701.0 | 3.0 | 2.00 | 0.40 |
| 2538.0 | 2.0 | 1.40 | 0.40 | 3713.0 | 3.0 | 0.70 | 0.15 |
| 2549.0 | 2.0 | 1.40 | 0.40 | 3726.0 | 3.0 | 0.10 | 0.05 |
| 2566.0 | 2.0 | 0.56 | 0.15 | 3732.0 | 3.0 | 0.05 | 0.05 |
| 2583.0 | 2.0 | 0.08 | 0.02 | 3742.0 | 3.0 | 0.10 | 0.05 |
| 2600.0 | 2.0 | 1.50 | 0.40 | 3754.0 | 3.0 | 0.80 | 0.30 |
| 2614.0 | 2.0 | 0.05 | 0.02 | 3764.0 | 3.0 | 0.05 | 0.05 |
| 2632.0 | 2.0 | 0.07 | 0.02 | 3786.0 | 3.0 | 0.20 | 0.10 |
| *2643.0 | 2.0 | 0.03 | 0.03 | 3812.0 | 3.0 | 5.00 | 1.00 |
| 2655.0 | 2.0 | 1.50 | 0.40 | 3821.0 | 3.0 | 0.15 | 0.05 |
| 2664.0 | 2.0 | 0.10 | 0.10 | 3838.0 | 3.0 | 0.10 | 0.10 |
| 2671.0 | 2.0 | 0.18 | 0.10 | 3844.0 | 3.0 | 2.50 | 0.50 |
| 2685.0 | 2.0 | 0.02 | 0.02 | 3861.0 | 3.0 | 13.00 | 4.00 |
| 2693.0 | 2.0 | 1.04 | 0.08 | 3874.0 | 3.0 | 0.05 | 0.05 |
| 2717.0 | 2.0 | 0.04 | 0.02 | 3890.0 | 3.0 | 3.00 | 0.50 |
| 2730.0 | 2.0 | 1.50 | 0.50 | 3914.0 | 3.0 | 11.00 | 3.00 |
| 2734.0 | 2.0 | 0.80 | 0.20 | 3924.0 | 3.0 | 1.50 | 0.50 |
| 2753.0 | 2.0 | 1.50 | 0.20 | 3937.0 | 3.0 | 0.15 | 0.05 |
| 2765.0 | 2.0 | 0.40 | 0.10 | 3948.0 | 3.0 | 4.00 | 1.00 |
| 2773.0 | 2.0 | 0.80 | 0.20 | 3972.0 | 3.0 | 0.04 | 0.04 |
| 2791.0 | 2.0 | 6.20 | 0.60 | 4003.0 | 4.0 | 18.00 | 5.00 |

have entirely excluded such "false levels" from Tables I–IV, but we believe that relatively few are included. Since the peak in the $l=0$ Porter-Thomas distribution for $y=\langle g\Gamma_n^0\rangle^{1/2}$ occurs for $y=0$, we are probably missing a small, but unknown number of weak $s$-wave levels. This latter effect should cause the experimental histogram to be below the $\nu=1$ theoretical curve if the $\langle g\Gamma_n^0\rangle$ values are not too different for the levels associated with compound nuclear levels corresponding to $J=I-\frac{1}{2}$ and $J=I+\frac{1}{2}$. For Ag there is the additional

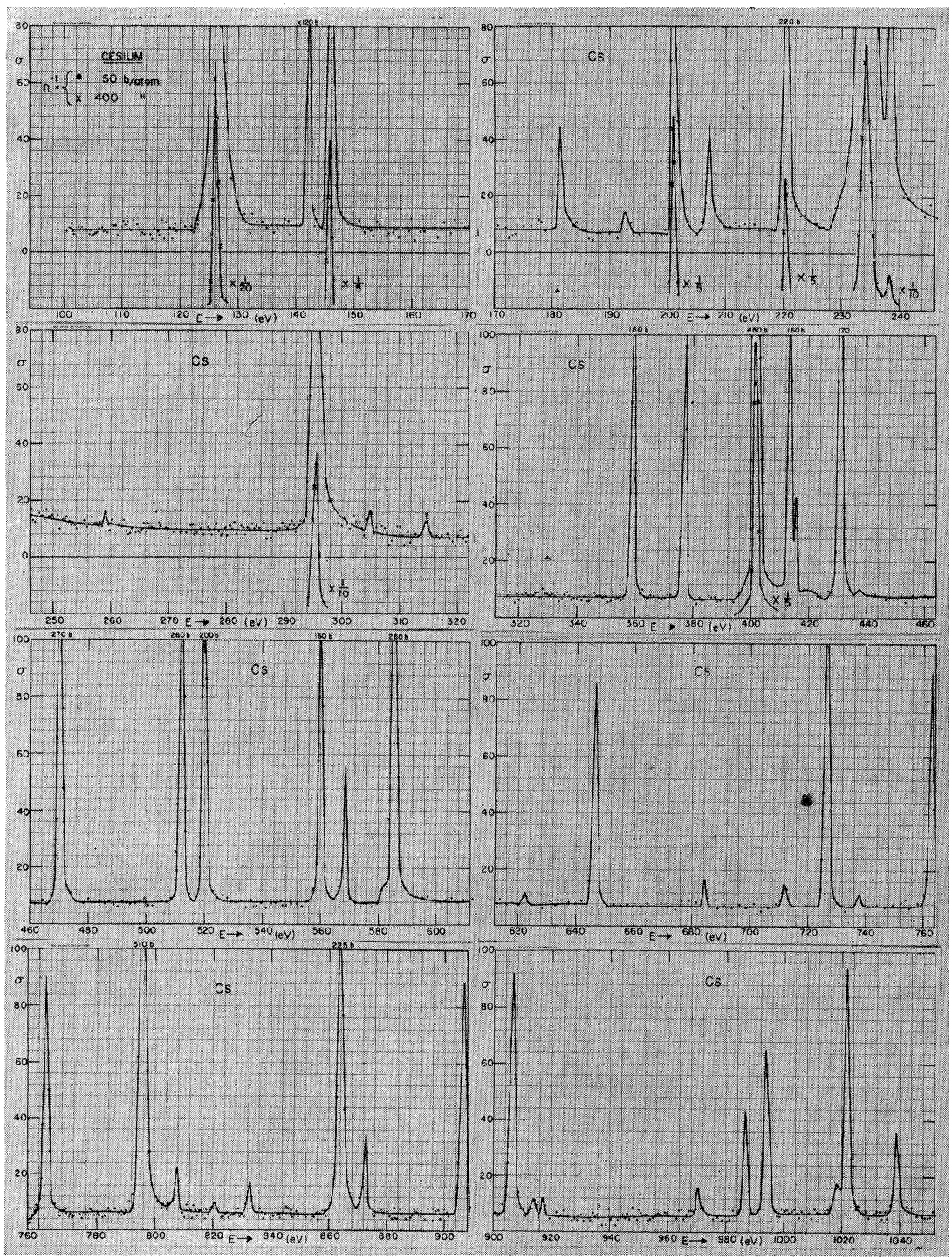


FIG. 4. The "measured" total neutron cross section for cesium versus energy from 100 to 3460 eV. The accuracy of the cross section between resonances is much poorer than usual since the thickest $Cs_2SO_4$ sample was too thin for best results. Otherwise the considerations are similar to those described in the caption of Fig. 1.

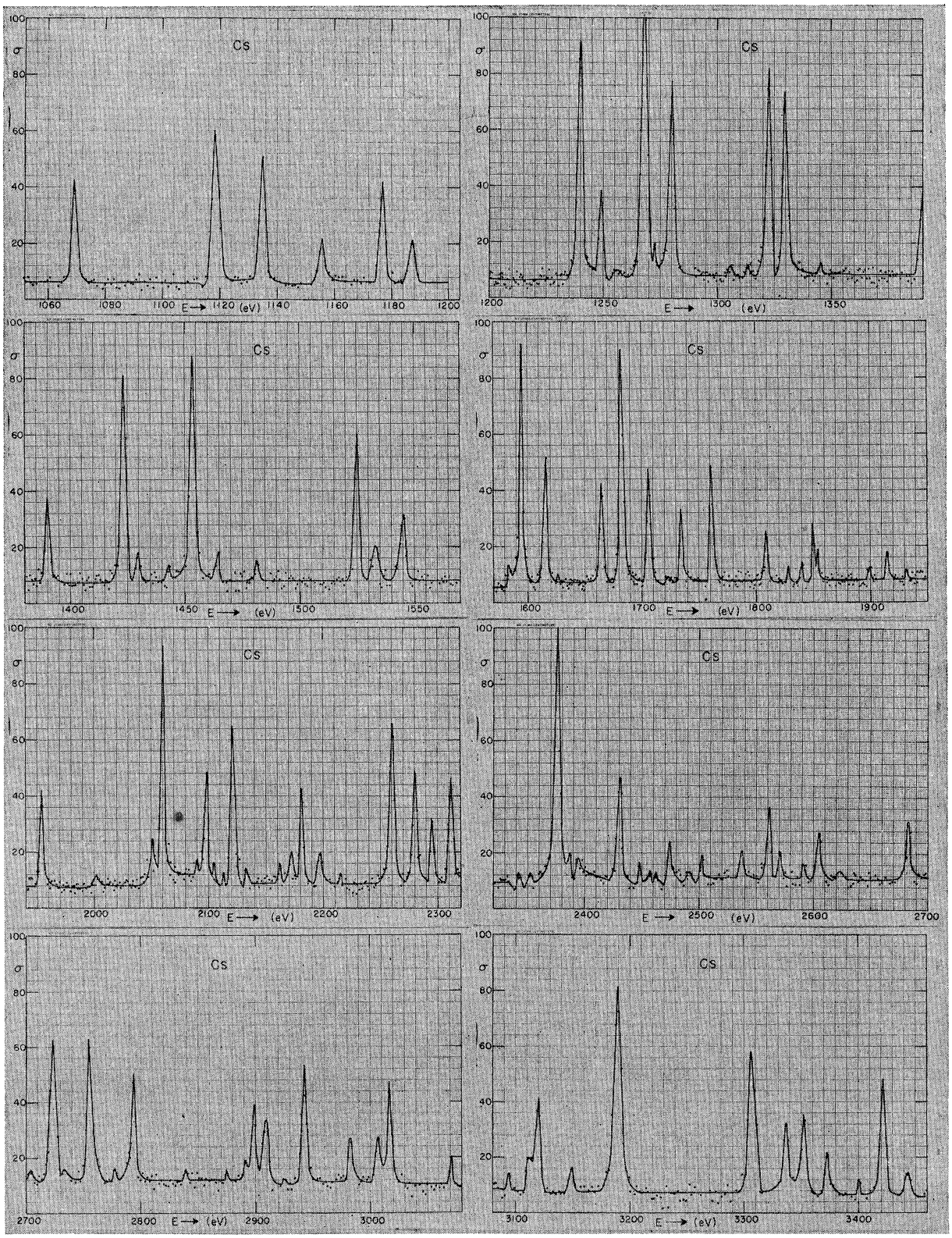


FIG. 4. *Continued.*

TABLE IV. Resonance parameters for the levels in cesium. $g=9/16$ and $7/16$ for $J=4$ and 3, respectively. The levels marked with asterisk are most probably spurious. The resonance parameters for levels below 100 eV have been taken from BNL 325, Suppl. 1 (unpublished).

| $E_0$ (eV) | $\Delta E_0$ (eV) | $\Delta$ (eV) | $\langle 2g\Gamma_n^0\rangle$ (meV) | $\Delta\langle 2g\Gamma_n^0\rangle$ (meV) | $E_0$ (eV) | $\Delta E_0$ (eV) | $\Delta$ (eV) | $\langle 2g\Gamma_n^0\rangle$ (meV) | $\Delta\langle 2g\Gamma_n^0\rangle$ (meV) |
|---|---|---|---|---|---|---|---|---|---|
| 5.90 | 0.04 | 0.07 | 2.10 | 0.30 | 1423.2 | 0.7 | 1.1 | 3.80 | 0.60 |
| 22.60 | 0.30 | 0.13 | 1.40 | 0.20 | 1429.1 | 0.8 | 1.1 | 0.32 | 0.10 |
| 47.80 | 0.60 | 0.19 | 2.80 | 0.40 | 1443.3 | 0.8 | 1.1 | 0.10 | 0.08 |
| 83.10 | 1.50 | 0.25 | 1.00 | 0.30 | 1453.1 | 0.8 | 1.1 | 5.40 | 1.00 |
| 94.80 | 1.80 | 0.27 | 2.00 | 0.60 | 1464.6 | 0.8 | 1.1 | 0.32 | 0.10 |
| 126.07 | 0.08 | 0.31 | 9.80 | 1.00 | 1480.9 | 0.8 | 1.1 | 0.14 | 0.08 |
| 142.16 | 0.09 | 0.33 | 0.50 | 0.10 | 1524.9 | 0.8 | 1.1 | 2.20 | 0.20 |
| 145.86 | 0.10 | 0.34 | 2.30 | 0.20 | 1533.1 | 0.8 | 1.1 | 0.44 | 0.10 |
| 181.47 | 0.14 | 0.38 | 0.16 | 0.04 | 1545.5 | 0.8 | 1.1 | 1.00 | 0.10 |
| 192.50 | 0.15 | 0.39 | 0.02 | 0.01 | 1583.8 | 0.9 | 1.1 | 0.10 | 0.10 |
| 200.90 | 0.16 | 0.39 | 2.00 | 0.40 | 1594.2 | 0.9 | 1.1 | 10.00 | 2.00 |
| 207.30 | 0.17 | 0.40 | 0.20 | 0.04 | 1616.3 | 0.9 | 1.1 | 3.00 | 0.60 |
| 220.35 | 0.18 | 0.41 | 1.50 | 0.10 | 1627.0 | 0.9 | 1.1 | 0.08 | 0.08 |
| 234.40 | 0.20 | 0.43 | 26.00 | 4.00 | 1664.6 | 0.9 | 1.1 | 2.20 | 0.20 |
| 238.40 | 0.20 | 0.43 | 0.90 | 0.10 | 1682.5 | 1.0 | 1.1 | 10.00 | 2.00 |
| 259.00 | 0.23 | 0.45 | 0.02 | 0.02 | 1705.5 | 1.0 | 1.2 | 3.00 | 0.40 |
| 295.60 | 0.28 | 0.48 | 5.30 | 0.50 | 1726.0 | 1.0 | 1.2 | 0.04 | 0.04 |
| 304.90 | 0.15 | 0.49 | 0.02 | 0.02 | 1734.8 | 1.0 | 1.2 | 1.20 | 0.12 |
| *315.88 | 0.16 | 0.50 | 0.02 | 0.02 | 1760.9 | 1.0 | 1.2 | 3.00 | 0.40 |
| 359.01 | 0.19 | 0.53 | 2.00 | 0.10 | 1809.6 | 1.1 | 1.2 | 0.80 | 0.20 |
| 377.43 | 0.20 | 0.54 | 0.96 | 0.10 | 1828.6 | 1.1 | 1.2 | 0.10 | 0.06 |
| 401.16 | 0.22 | 0.56 | 12.00 | 2.00 | 1843.0 | 1.1 | 1.2 | 0.12 | 0.06 |
| 413.50 | 0.23 | 0.57 | 2.90 | 0.50 | 1849.3 | 1.1 | 1.2 | 0.70 | 0.20 |
| 415.53 | 0.24 | 0.57 | 0.20 | 0.10 | 1853.7 | 1.1 | 1.2 | 0.30 | 0.20 |
| 430.83 | 0.25 | 0.58 | 3.10 | 0.20 | 1899.5 | 1.1 | 1.2 | 0.10 | 0.12 |
| 437.50 | 0.25 | 0.58 | 0.02 | 0.02 | 1915.5 | 1.2 | 1.2 | 0.30 | 0.20 |
| 469.89 | 0.28 | 0.60 | 4.70 | 0.60 | 1934.4 | 1.2 | 1.2 | 0.08 | 0.10 |
| 511.63 | 0.32 | 0.63 | 5.50 | 0.60 | 1954.0 | 1.2 | 1.2 | 2.00 | 0.20 |
| 519.67 | 0.33 | 0.64 | 4.70 | 0.30 | 2000.0 | 1.2 | 1.2 | 0.06 | 0.06 |
| 560.30 | 0.37 | 0.66 | 3.30 | 0.20 | 2051.0 | 1.0 | 1.0 | 0.70 | 0.20 |
| 568.39 | 0.38 | 0.66 | 0.80 | 0.04 | 2060.0 | 1.0 | 1.0 | 11.00 | 2.00 |
| 585.52 | 0.39 | 0.67 | 7.00 | 1.00 | 2090.0 | 1.0 | 1.0 | 0.10 | 0.10 |
| 622.59 | 0.43 | 0.70 | 0.04 | 0.04 | 2099.0 | 1.0 | 1.0 | 2.60 | 0.60 |
| 646.28 | 0.46 | 0.71 | 2.00 | 0.10 | 2114.0 | 1.0 | 1.0 | 0.04 | 0.04 |
| 684.44 | 0.50 | 0.73 | 0.10 | 0.04 | 2122.0 | 1.0 | 1.0 | 6.60 | 1.40 |
| 712.31 | 0.53 | 0.74 | 0.12 | 0.04 | 2133.0 | 1.0 | 1.0 | 0.10 | 0.10 |
| 726.61 | 0.54 | 0.75 | 4.40 | 0.40 | 2161.0 | 1.0 | 1.0 | 0.20 | 0.10 |
| 738.00 | 0.56 | 0.76 | 0.04 | 0.04 | 2172.0 | 1.0 | 1.0 | 0.50 | 0.10 |
| 762.87 | 0.59 | 0.77 | 2.80 | 0.20 | 2182.0 | 1.0 | 1.0 | 2.80 | 0.60 |
| 795.72 | 0.62 | 0.79 | 10.80 | 1.00 | 2197.0 | 1.0 | 1.0 | 1.00 | 0.20 |
| 807.56 | 0.64 | 0.79 | 0.40 | 0.08 | 2261.0 | 1.0 | 1.0 | 7.00 | 1.40 |
| 821.00 | 0.65 | 0.80 | 0.06 | 0.06 | 2280.0 | 2.0 | 1.0 | 4.80 | 1.00 |
| 832.71 | 0.67 | 0.80 | 0.20 | 0.06 | 2295.0 | 2.0 | 1.0 | 1.40 | 0.40 |
| 863.92 | 0.71 | 0.82 | 6.20 | 0.40 | 2312.0 | 2.0 | 1.0 | 4.60 | 1.00 |
| 872.34 | 0.72 | 0.82 | 0.66 | 0.06 | 2343.0 | 2.0 | 1.0 | 0.04 | 0.04 |
| 906.57 | 0.76 | 0.84 | 3.50 | 0.20 | 2352.0 | 2.0 | 1.0 | 0.04 | 0.04 |
| 914.11 | 0.77 | 0.84 | 0.08 | 0.04 | 2376.0 | 2.0 | 1.0 | 22.00 | 6.00 |
| *917.16 | 0.77 | 0.84 | 0.08 | 0.06 | 2387.0 | 2.0 | 1.0 | 0.20 | 0.20 |
| 970.48 | 0.84 | 0.87 | 0.20 | 0.10 | 2392.0 | 2.0 | 1.0 | 0.30 | 0.20 |
| 986.44 | 0.86 | 0.87 | 1.20 | 0.40 | 2429.0 | 2.0 | 1.0 | 4.00 | 0.80 |
| 994.15 | 0.87 | 0.88 | 2.50 | 0.60 | 2447.0 | 2.0 | 1.0 | 0.10 | 0.10 |
| 1018.69 | 0.90 | 0.89 | 0.20 | 0.20 | 2458.0 | 2.0 | 1.0 | 0.04 | 0.04 |
| 1021.38 | 0.91 | 0.89 | 5.30 | 1.00 | 2474.0 | 2.0 | 1.0 | 1.08 | 0.30 |
| 1038.62 | 0.93 | 0.90 | 1.20 | 0.20 | 2492.0 | 2.0 | 1.0 | 0.10 | 0.10 |
| 1069.63 | 0.97 | 0.91 | 1.60 | 0.24 | 2503.0 | 2.0 | 1.0 | 0.60 | 0.20 |
| 1118.30 | 1.04 | 0.93 | 6.00 | 1.20 | 2524.0 | 2.0 | 1.0 | 0.04 | 0.04 |
| 1134.91 | 1.06 | 0.94 | 3.40 | 0.70 | 2537.0 | 2.0 | 1.0 | 0.70 | 0.20 |
| 1156.21 | 1.09 | 0.95 | 0.70 | 0.08 | 2561.0 | 2.0 | 1.0 | 2.40 | 0.60 |
| 1176.99 | 1.12 | 0.96 | 2.00 | 0.30 | 2570.0 | 2.0 | 1.0 | 0.70 | 0.20 |
| 1187.04 | 1.14 | 0.96 | 0.60 | 0.06 | 2591.0 | 2.0 | 1.0 | 0.30 | 0.10 |
| 1239.7 | 0.6 | 1.0 | 6.60 | 1.20 | 2604.0 | 2.0 | 1.0 | 1.40 | 0.30 |
| 1249.3 | 0.6 | 1.0 | 1.20 | 0.20 | 2623.0 | 2.0 | 1.0 | 0.10 | 0.10 |
| 1267.6 | 0.6 | 1.0 | 10.00 | 2.00 | 2683.0 | 2.0 | 1.0 | 2.40 | 0.60 |
| 1272.6 | 0.6 | 1.0 | 0.08 | 0.08 | 2705.0 | 2.0 | 1.0 | 0.04 | 0.04 |
| 1280.1 | 0.6 | 1.0 | 5.00 | 1.00 | 2723.0 | 2.0 | 1.0 | 11.00 | 2.00 |
| 1306.3 | 0.7 | 1.0 | 0.06 | 0.04 | 2733.0 | 2.0 | 1.0 | 0.04 | 0.04 |
| 1312.8 | 0.7 | 1.0 | 0.06 | 0.04 | 2755.0 | 2.0 | 1.0 | 12.00 | 2.00 |
| 1322.0 | 0.7 | 1.0 | 4.40 | 0.80 | 2777.0 | 2.0 | 1.0 | 0.10 | 0.10 |
| 1329.3 | 0.7 | 1.0 | 4.00 | 0.80 | 2794.0 | 2.0 | 1.0 | 5.20 | 1.00 |
| 1345.4 | 0.7 | 1.0 | 0.04 | 0.04 | 2838.0 | 2.0 | 1.0 | 0.10 | 0.10 |
| 1389.8 | 0.7 | 1.0 | 1.00 | 0.10 | 2876.0 | 2.0 | 1.0 | 0.04 | 0.04 |

TABLE IV (*continued*)

| $E_0$ (eV) | $\Delta E_0$ (eV) | $\Delta$ (eV) | $\langle 2g\Gamma_n^0\rangle$ (meV) | $\Delta\langle 2g\Gamma_n^0\rangle$ (meV) | $E_0$ (eV) | $\Delta E_0$ (eV) | $\Delta$ (eV) | $\langle 2g\Gamma_n^0\rangle$ (meV) | $\Delta\langle 2g\Gamma_n^0\rangle$ (meV) |
|---|---|---|---|---|---|---|---|---|---|
| 2892.0 | 2.0 | 1.0 | 0.04 | 0.04 | 3150.0 | 2.0 | 2.0 | 0.60 | 0.20 |
| 2898.0 | 2.0 | 1.0 | 3.60 | 1.00 | 3190.0 | 3.0 | 2.0 | 20.00 | 4.00 |
| 2910.0 | 2.0 | 2.0 | 2.70 | 0.60 | 3306.0 | 3.0 | 2.0 | 13.00 | 3.00 |
| 2925.0 | 2.0 | 2.0 | 0.04 | 0.04 | 3335.0 | 3.0 | 2.0 | 3.70 | 0.80 |
| 2943.0 | 2.0 | 2.0 | 5.60 | 1.00 | 3354.0 | 3.0 | 2.0 | 4.60 | 1.00 |
| 2982.0 | 2.0 | 2.0 | 1.80 | 0.40 | 3373.0 | 3.0 | 2.0 | 1.80 | 0.40 |
| 3007.0 | 2.0 | 2.0 | 1.60 | 0.40 | 3402.0 | 3.0 | 2.0 | 0.40 | 0.20 |
| 3016.0 | 2.0 | 2.0 | 4.80 | 1.00 | 3422.0 | 3.0 | 2.0 | 6.00 | 1.00 |
| 3071.0 | 2.0 | 2.0 | 0.70 | 0.20 | 3444.0 | 3.0 | 2.0 | 1.00 | 0.20 |
| 3095.0 | 2.0 | 2.0 | 0.30 | 0.10 | 3480.0 | 3.0 | 2.0 | 26.00 | 6.00 |
| 3114.0 | 2.0 | 2.0 | 0.40 | 0.10 | 3500.0 | 3.0 | 2.0 | 2.00 | 1.00 |
| 3120.0 | 2.0 | 2.0 | 6.00 | 2.00 | | | | | |

requirement that $\langle g\Gamma_n^0\rangle$ be not too different for the two isotopes.

(b) At higher neutron energy the experimental resolution width eventually increases approximately as $E^{3/2}$, so one is less certain of resolving closely spaced levels or of observing weak levels. This effect explains

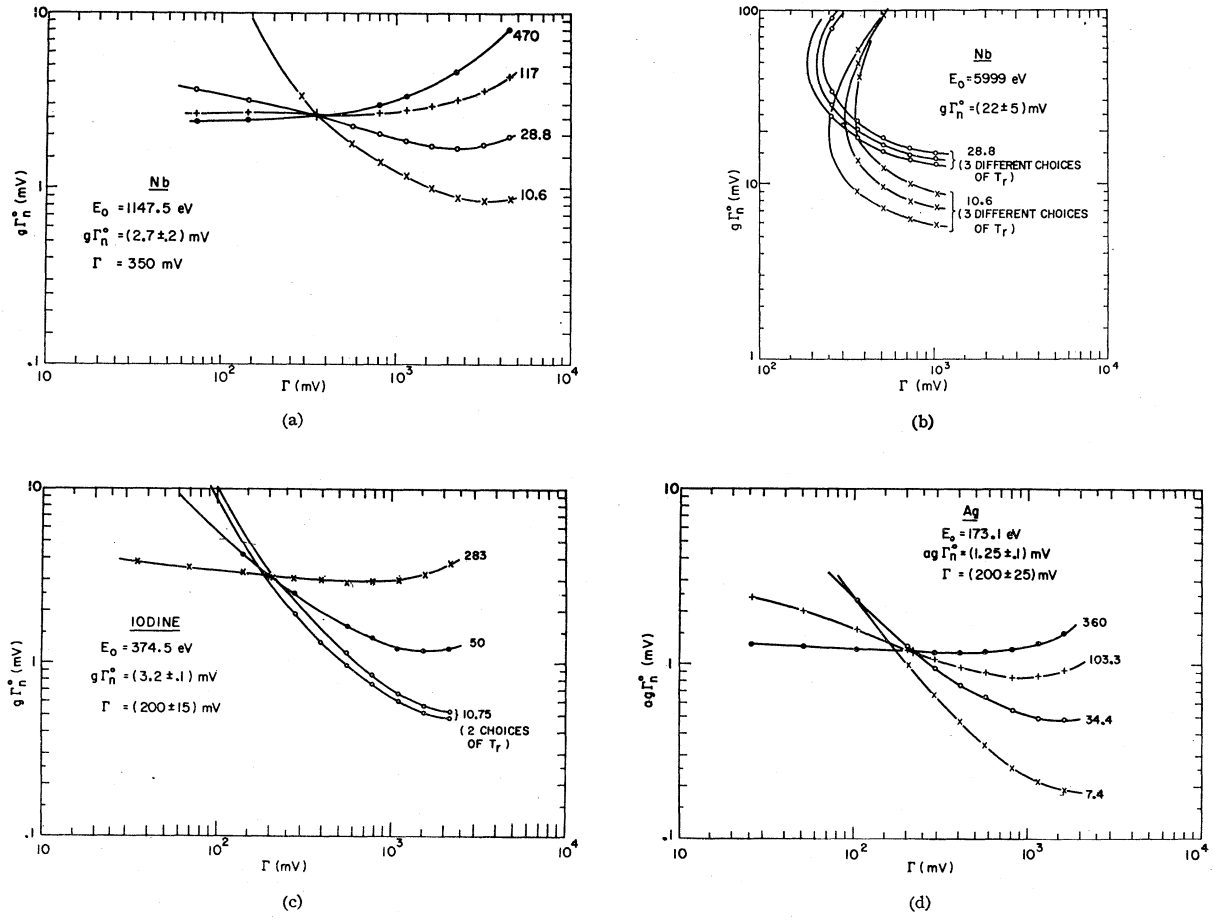


FIG. 5. Some examples of area analysis for obtaining the resonance level parameters. The numbers on the right of each curve represent the thickness of the sample in b/atom.

the decreased slopes of the experimental $N(E)$ versus $E$ curves at the upper ends of Figs. 6–9. Since Figs. 10–13 are based on the levels observed up to the energy regions where Figs. 6–9 were reasonably linear, they should correspond to fairly uniform high-quality data regions. The cesium results, and the silver results above 1200 eV,

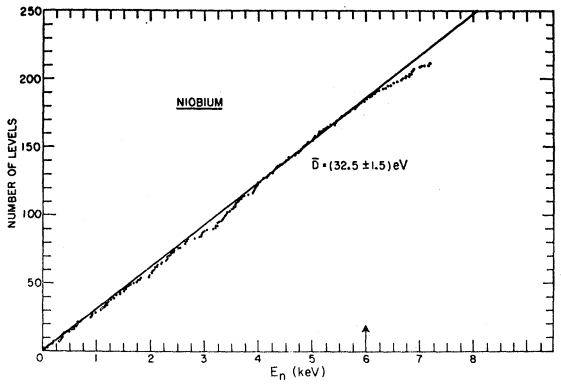


FIG. 6. A plot of the cumulative number of levels observed versus energy for niobium. The value of $\bar{D}=(32.5\pm1.5)$ eV is for all of the observed levels belonging to different spins and parities.

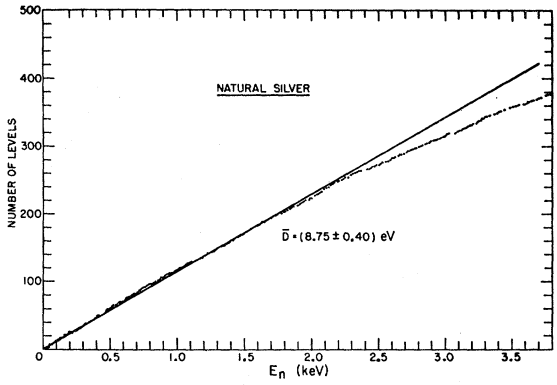


FIG. 7. A plot of the cumulative number of levels observed versus energy for natural silver. $\bar{D}=(8.75\pm0.40)$ eV is for all levels belonging to two isotopes and different spins.

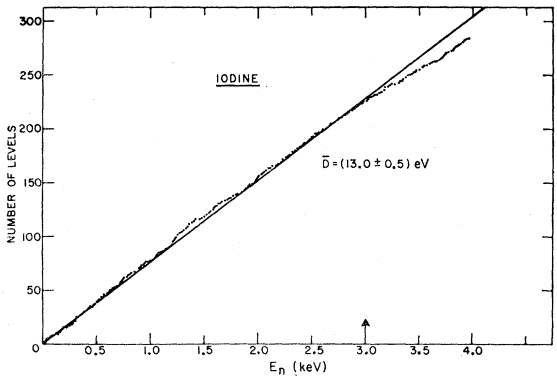


FIG. 8. A plot of the cumulative number of levels observed versus energy for iodine. $\bar{D}=(13.0\pm0.5)$ eV is for all levels.

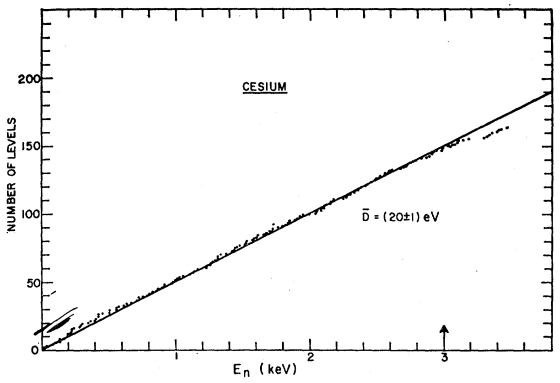


FIG. 9. A plot of the cumulative number of levels observed versus energy for Cs. $\bar{D}=(20\pm1)$ eV is for all levels.

are of poorer quality because an optimum sample thickness was not used for the "thick sample."

(c) If, as is probably the case, we are observing many of the stronger $l=1$ levels (in spite of the extra centrifugal force barrier effect which tends to drastically reduce the $\Gamma_n$ values for these resonances), it is highly unlikely that we are including *all* $l=1$ levels. Measurements with better resolution or better statistical accuracy would probably reveal many more still-weaker $l=1$ levels. Eventually of course, one would expect to observe levels belonging to still higher angular momen-

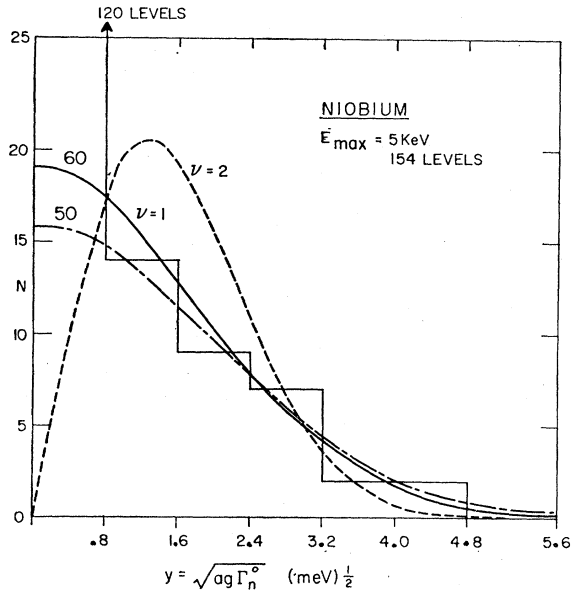


FIG. 10. A histogram of the observed experimental distribution of $y=\langle g\Gamma_n^0\rangle^{1/2}$ values for niobium. The theoretical distributions of $\nu=1$ and $\nu=2$ normalized to the number of levels within brackets are shown for a comparison. In this case the vertical scale is chosen in such a way that the large number of cases for $y<0.8$ $(\text{meV})^{1/2}$ are not plotted directly but indicated with the number of such levels widths observed. The Porter-Thomas distribution ($\nu=1$) normalized for 50 and for 60 widths seem to bracket the region of best agreement with the experimental data for $\langle\Gamma_n^0\rangle^{1/2}>0.8$. This predicts an excess of about 100 small observed widths in the experimental data. The $\nu=2$ curve gives a poor fit.

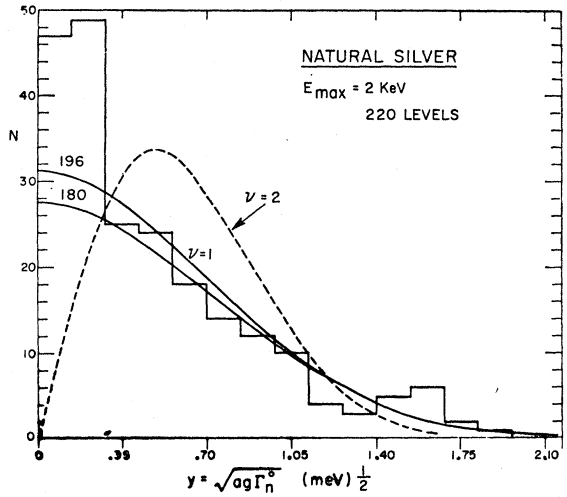


FIG. 11. A histogram of the observed distribution of $y=\langle ag\Gamma_n^0\rangle^{1/2}$ for natural silver. The theoretical distributions of $\nu=1$ and $\nu=2$ normalized to number of levels within brackets are shown for a comparison. Best agreement for $y>0.35$ is for a $\nu=1$ curve with $N=190$.

tum ($l=2$, $l=3$, etc.) as the experimental ability to observe weak levels is increased indefinitely. Thus one must be somewhat careful in deciding what one means by "the true situation" when examining Figs. 6–13. For example, in the case of Nb (Fig. 10) the distribution 27, 53, 25, 15, 2, 4, 3 for the first eight intervals of $y=0.2$ (meV)$^{1/2}$ shows a decrease for the first channel relative to the second while the opposite effect would be expected to occur if all widths and spacings were equally likely to be detected. This suggests that at least 40 levels have been missed for Nb, or their strength has been added to that of other levels when two or more unresolved levels are treated as one.

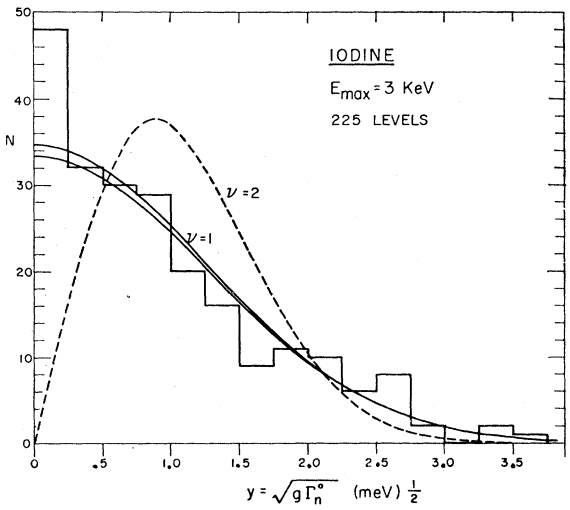


FIG. 12. A histogram of the observed distribution of $N$ versus $y$ for iodine. The theoretical distributions of $\nu=1$ and $\nu=2$ normalized for 216 levels are also shown for a comparison. An additional $\nu=1$, $N=210$ curve is also shown.

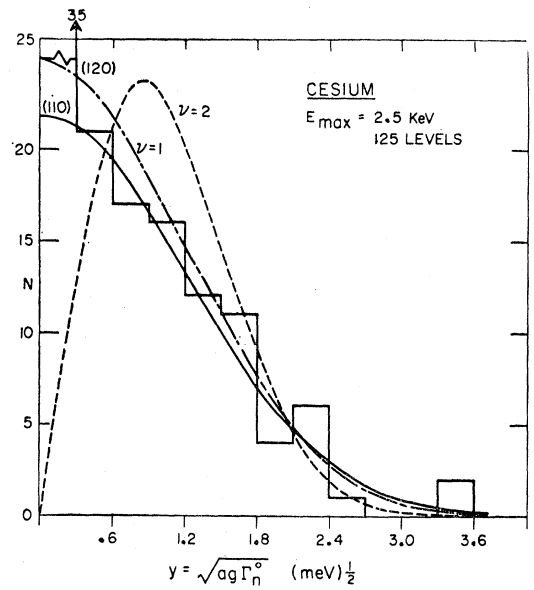


FIG. 13. A histogram of the observed distribution of $N$ versus $y$ for cesium. The theoretical distributions of $\nu=1$ and $\nu=2$ normalized for 120 levels are shown for a comparison. A bracketing $\nu=1$, $N=110$ curve is shown to test the sensitivity of the fit for $y>0.30$.

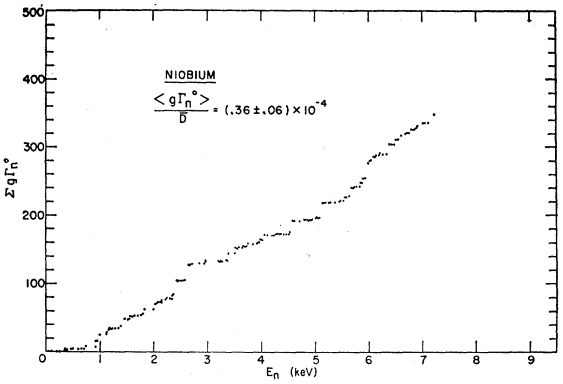


FIG. 14. A plot of $\Sigma g\Gamma_n^0$ versus $E$ for niobium. The slope of the curve determines the strength function.

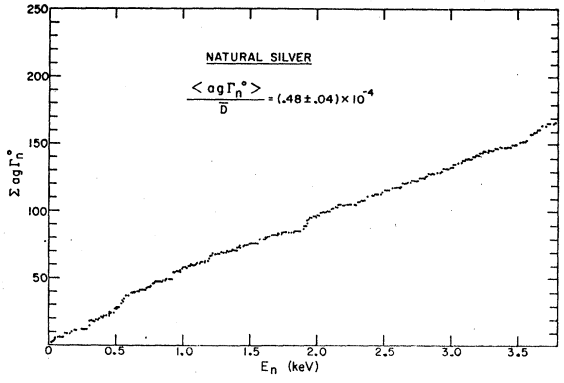


FIG. 15. A plot of $\Sigma ag\Gamma_n^0$ versus $E$ for natural silver.

TABLE V. $S$-wave strength functions for Nb, natural Ag, I, and Cs. The weighted mean value for Nb has a 10% estimated deduction for the contribution of $p$-wave levels, and all weighted mean values give slightly greater weighting to the first half of the energy region.

| Energy interval (eV) | $Nb^{93}$ $S_0\times10^4$ | Ag $S_0\times10^4$ | $I^{127}$ $S_0\times10^4$ | $Cs^{133}$ $S_0\times10^4$ |
|---|---|---|---|---|
| 0–1000 | 0.17±0.08 | 0.57±0.10 | 0.76±0.13 | 0.70±0.15 |
| 0–2000 | 0.32±0.12 | 0.48±0.16 | 0.64±0.08 | 0.61±0.09 |
| 0–3500 | 0.42±0.10 | 0.43±0.04 | 0.58±0.06 | 0.66±0.07 |
| 0–4000 | 0.41±0.10 | 0.45±0.04 | 0.61±0.06 | |
| 0–7500 | 0.46±0.08 | | | |
| Weighted mean | 0.40±0.09 | 0.45±0.05 | 0.62±0.09 | 0.68±0.09 |

In view of the above considerations, the most reasonable interpretation seems to be that the experimental excess of weak levels (i.e., in the first one or two boxes in the histograms) in Figs. 10–13 represents the excess of observed $p$-wave plus spurious "levels" over the missed weak $l=0$ levels.

The plots in Figs. 14–17 show the experimental values of $\sum_j(g\Gamma_n^0)_j$ for all levels having $E_j<E$. In the case of silver the ordinate is $\sum_j(ag\Gamma_n^0)_j$. The mean slopes of these plots give the $l=0$ strength functions $S_0$ averaged over compound nuclear spin states. The silver results also include an average over isotopes for $A=107$ and 109. If the contributions are assumed to be essentially all due to $l=0$ levels, the corresponding averaged $l=0$ strength functions are as indicated on the figures. Slightly different values from those indicated on the figures are the selected "best values" as discussed below.

One expects to find considerable fluctuation in the slope of the curves of $\sum_j(g\Gamma_n^0)_j$ versus $E$ due to statistical effects. An inspection of Table I and Fig. 14 shows that Nb has only relatively weak levels below 900 eV, so measurements limited to that region would give a value for $S_0$ which is several times smaller than that obtained using the full 8-keV region. A best straight line through the data would have its zero at $E_n\approx700$ eV. The silver, iodine, and cesium curves, Figs. 15, 16, and 17, have the opposite shapes with a slightly greater than average slope in the first 800 eV. It is thus expected that a value of $S_0$ averaged over our entire energy regions will differ significantly from values based only on the parameters for a few levels observed in a small energy interval.

Table V shows the dependence of the strength functions $S_0$ on the size of the energy region starting at $E=0$. The weighted mean values, $S_0=(0.40\pm0.09)\times10^{-4}$ for Nb, $(0.46\pm0.05)\times10^{-4}$ for Ag, $(0.62\pm0.09)\times10^{-4}$ for I, and $(0.68\pm0.09)\times10^{-4}$ for Cs, represent our "best judgment" values based on the data. The results give greater weighting to the first part of the energy region, and the indicated uncertainties are a little greater than those due to statistical considerations alone and correspond to standard deviations. The Nb value has been decreased by 10% to take account of the estimated fractional contributlon to the apparent $S_0$ value due to $p$-wave levels. Figure 10 shows an excess of about 102 weak Nb levels in the first interval which is probably due to $l=1$ levels. This means that, of the 154 total levels, an estimated 52 are due to $l=0$ interactions. Note that the statistical uncertainty in $S_0$ is based on the estimated number of $l=0$ levels rather than the total number of levels.

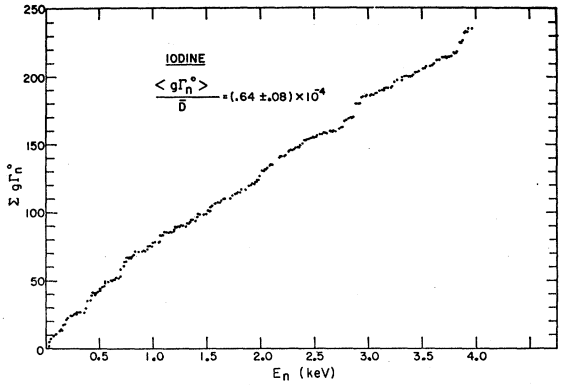


FIG. 16. A plot of $\Sigma g\Gamma_n^0$ versus $E$ for iodine.

An examination of Figs. 10–13 suggests that the number of excess weak levels, relative to a best Porter-Thomas fit to the upper parts of the curves, is about 102 out of 154 for Nb, about 40 out of 220 for Ag, about 14 out of 225 for I, and about 11 out of 125 for Cs. This does not, however, yield a best value of $D$ for $l=0$ levels due to missed small level spacings.

Figures 18–21 show the distribution of nearest-neighbor level spacings for niobium to 5 keV, natural silver to 2 keV, iodine to 3 keV, and cesium to 2.5 keV. For Figs. 19–21, the starred levels in Tables II–IV were not included. This represents an attempt to exclude many of the levels which are most apt to be $p$-wave levels for those elements. The theory was discussed in the preceding papers.[3,4] For a single population orthogonal (Wigner) distribution, denoted $P_0^0(1)$ on the theoretical curves in the figures, the level

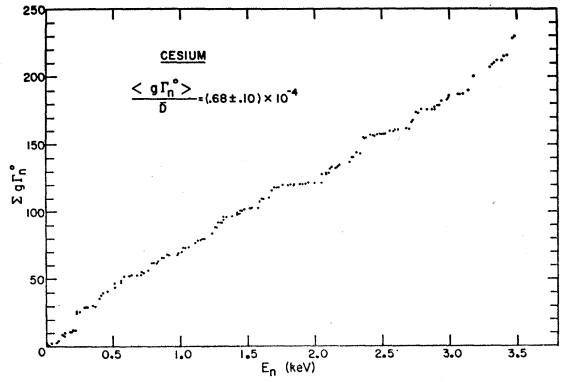


FIG. 17. A plot of $\Sigma g\Gamma_n^0$ versus $E$ for cesium.

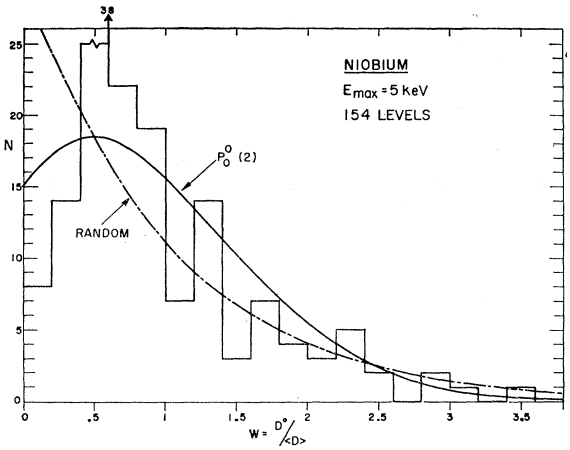


FIG. 18. Histogram of the observed distribution of nearest-neighbor level spacings for niobium. The theoretical distributions of random, Wigner (orthogonal ensemble) single and two equal-level populations are also shown.

repulsion effect predicts an absence of very small spacings. For a large enough mixture of independent populations one eventually expects to obtain a best fit to the "random" curve. In the case of the Nb, there are two $s$-wave populations and four $p$-wave populations corresponding to the various $J$ and parity states accessible to the incoming neutron. It is thus not surprising that a best fit in Fig. 18 is to the "random" curve. The $P_0^0(2)$ curve is for the case of two equal independent merged orthogonal distributions.

In examining Fig. 18 one notices the relatively small numbers (8 and 14) of spacings for the first two intervals in the histogram. The value 38 for the third interval is extra large. If, in fact, many small spacings are missed, the effect is to count the sum of two (or more) adjacent level spacings as a single spacing equal to their sums. According to this reasoning perhaps $\approx 18$ to 22 of the spacings in the third interval of the histogram of Fig. 18 should *each* be split into two smaller intervals. The same effect may apply to a lesser extent for the fourth and fifth intervals. The missed levels do not significantly alter the $s$-wave strength functions since the $\langle g\Gamma_n^0\rangle$ values for the "two levels counted as one" cases are about equal to the sums of the two separate $\langle g\Gamma_n^0\rangle$ values in each case. We estimate that about five $l=0$ Nb levels were missed relative to the estimate based on Fig. 10. (Many more $l=1$ levels are missed.) We choose $\langle D\rangle = (96\pm 8)$ eV and $\langle g\Gamma_n^0\rangle = (3.8\pm 1.0)$ meV as our best estimated values for the $l=0$ levels of $Nb^{93}$.

For natural silver Fig. 19 shows a best fit to the $P_0^0(1)$ single population curve for small spacings, but to the $P_0^0(2)$ two equal population curves for the larger spacings. Since silver has approximately equal abundances of the $Ag^{107}$ and $Ag^{109}$ isotopes, both with $I=\frac{1}{2}$, there are four $l=0$ level populations plus a number of observed $p$-wave levels. For $l=0$ one has $J=0$ or 1 for the spin of the compound nucleus. There may be many times more $J=1$ than $J=0$ levels[4] in which case a distribution near that for two equal merged populations might be expected to give a fair fit. The behavior of the histogram in Fig. 19 for the first few intervals suggests that $\approx 15$ to 30 $l=0$ silver levels were missed to 2 keV. We choose $\langle D\rangle = (9.4\pm 0.8)$ eV and $\langle 2ag\Gamma_n^0\rangle = (0.86\pm 0.12)$ meV as our best estimates for the parameters for the $l=0$-level distributions for natural silver. The value $\langle D\rangle = (18.8\pm 1.6)$ eV is the average $l=0$ spacing per isotope of silver.

For iodine (Fig. 20) one would expect a best fit for $l=0$ levels for the theoretical case of two approximately equal independent merged orthogonal populations since the compound nuclear states of $J=2$ and $J=3$ are expected to have comparable level densities. In Fig. 20 the best fit is for the $P_0^0(1)$ single population case. We have, however, made plots of the number of observed level spacings having $D \leqslant 2$, 4, 6, 8, 10, and 12 eV versus the total number of level spacings. These curves all show a pronounced decrease in slope at higher energies suggesting that 15–30 small level spacings have been missed. A somewhat similar result is obtained if one assumes that a $P_0^0(2)$ curve should apply in Fig. 20 and notes the implied number of missed small spacings in the first three intervals of the histogram. When this is done a value of 15–30 is also obtained as an estimate of the number of missed small level spacings. On the basis of these considerations, together with those discussed earlier, we select as the final results for the $l=0$ iodine levels $\langle D\rangle = (13.5\pm 0.8)$ eV and $\langle g\Gamma_n^0\rangle = (0.84\pm 0.15)$ meV.

$Cs^{133}$ has $I=\frac{7}{2}$ so $l=0$ interactions produce states of $J=3$ and $J=4$ which should have comparable level densities. One expects a best fit for the $P_0^0(2)$ two-population curve rather than for the $P_0^0(1)$ curve. The first part of Fig. 21 gives a better fit for the $P_0^0(1)$ shape, but it cannot explain the high end of the histogram. If one uses the first three histogram intervals in Fig. 21

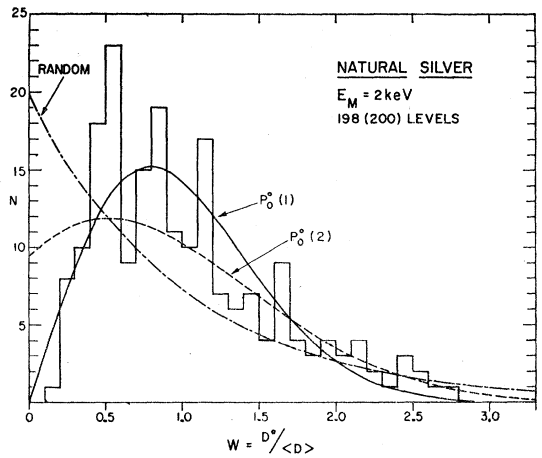


FIG. 19. Histogram of the observed distribution of nearest-neighbor spacing for natural silver. The curves are the theoretical distributions as indicated.

and assumes that the $P_0^0(2)$ curve should apply, then $\approx 12$ small spacings seem to be missing. Some of these will combine in pairs to give spurious larger spacings such as those in the fifth and sixth intervals of the histogram. A net loss of $\approx 8$ $s$-wave levels is estimated as due to missing small level spacings. On the basis of all of the above considerations we give $\langle D\rangle = (20.5\pm 1.2)$ eV and $\langle g\Gamma_n^0\rangle = (1.4\pm 0.2)$ meV for the $l=0$ levels of $Cs^{133}$.

The preceding values for $\langle D\rangle$ have been averaged over spin states for the compound nucleus. Without implying that $\langle D\rangle$ is equal to the two spin states of each isotope, or for the $Ag^{107}$ and $Ag^{109}$ isotopes, the average $\langle D\rangle$ per spin state (and per isotope for silver) are $(188\pm 16)$ eV for $Nb^{93}$, $(37.6\pm 3.2)$ eV for Ag, $(27\pm 1.6)$ eV for $I^{127}$, and $(41\pm 2.4)$ eV for $Cs^{133}$ for $l=0$ neutron interactions.

The above results are in reasonable agreement with the results of earlier measurements for these elements if one considers the greater resolution of the present measurements and restricts comparison to the corresponding energy region of our present data.

Saplakoglu *et al.*[9] obtained $S_0 = 0.10\times 10^{-4}$ for Nb for an energy region to about 800 eV. We find many weak levels in this region which were missed in their measurements with $\approx 40$ nsec/m resolution, but we obtain $S_0 = 0.11\times 10^{-4}$ for the same energy region.

Hughes *et al.*[7,8] obtained $S_0 = 0.98\times 10^{-4}$ for iodine to 100 eV and $S_0 = (1.0\pm 0.2)\times 10^{-4}$ for Cs to 250 eV. Their iodine results were based on 7 levels, and the Cs results were based on 12 levels. On statistical grounds alone[3] their results should be stated as $S_0 = (0.98\pm 0.6)\times 10^{-4}$ for iodine and $S_0 = (1.0\pm 0.4)\times 10^{-4}$ for Cs. (It should be noted that the uncertainties in $S_0$ values tended to be grossly understimated during the period before about 1959.) These results compare with our values of $S_0 = (0.85\pm 0.25)\times 10^{-24}$ for Cs to 500 eV, and $S_0 = (0.68\pm 0.09)\times 10^{-4}$ for Cs using all of our data.

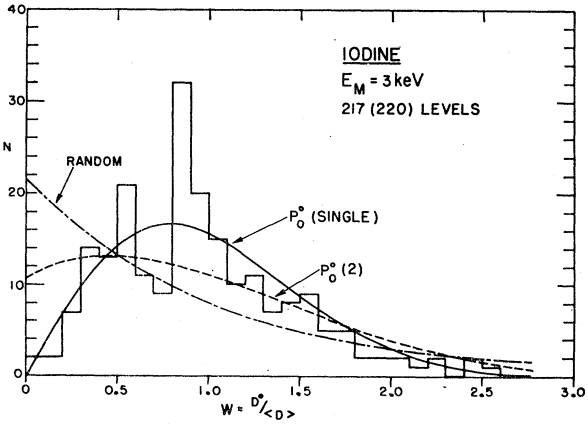


FIG. 20. Histogram of the observed nearest-neighbor level spacing distributions for iodine. The curves are the theoretical distributions as indicated.

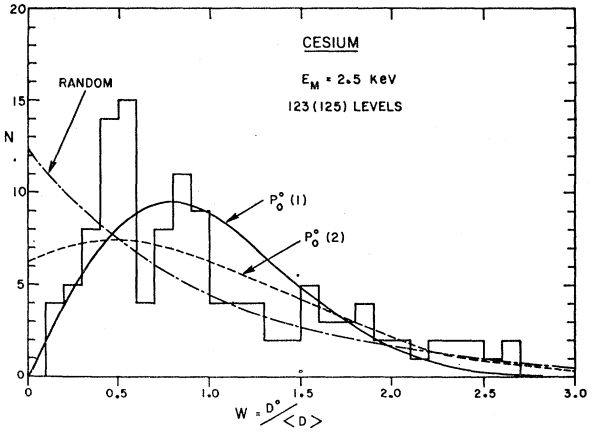


FIG. 21. Histogram of the observed nearest-neighbor level spacing distributions for cesium. The curves are the theoretical distributions as indicated.

### B. The $l=1$ Strength Function

The earlier self-indication studies[2] of silver using a 35-m flight path showed an excess of weak levels which were interpreted as due to $l=1$. An analysis gave $S_1 = (1.7\pm 0.8)\times 10^{-4}$. If a level is due to $l=1$ one defines a $\Gamma_n^1$ for the level as

$$\Gamma_n^1 \equiv \Gamma_n^0(1+K^2R^2)/(K^2R^2) \approx \Gamma_n^0(515 \text{ keV}+E)/E \quad \text{for Nb},$$

where $\Gamma_n^0 = \Gamma_n(1 \text{ eV}/E)^{1/2}$ as usual, $K$ = neutron momentum (relative motion), and $R$ = effective nuclear radius where the centrifugal force barrier terminates near the nuclear surface owing to the greater attractive effect of nuclear forces. The extra factor for $\Gamma^1$ relative to $\Gamma_n^0$ is the inverse of the centrifugal barrier penetration factor. Similarly,

$$3S_1 \equiv \frac{1}{\Delta E}\sum_i (g\Gamma_n^1)_i \quad \left(\text{or } \frac{1}{\Delta E}\sum_i (ag\Gamma_n^1)_i\right)$$

defines the $l=1$ strength function. Here $\Delta E$ is the energy interval of the summation, and $(2l+1)=3$ for $l=1$ is the coefficient multiplying $S_1$.

Saplakoglu *et al.*[9] obtained a value $S_1 = (5.5\pm 2.8)\times 10^{-4}$ for Nb on the basis of seven low-lying weak levels which were somewhat arbitrarily taken to be $p$ wave because of the excess of weak levels in this region. The indicated uncertainty is based only on the number (7) of assumed levels and does not take into account the possibility of error in identification. On the basis of a similar arbitrary classification of certain weak Nb levels as due to $l=1$, Desjardins *et al.*[2] obtained $S_1 = (6\pm 2)\times 10^{-4}$ for Nb using our 35-m path for self-indication studies over a larger energy range.

Values of $S_1 = (5.0\pm 0.5)\times 10^{-4}$ for Nb, $S_1 = (2.5\pm 0.5)\times 10^{-4}$ for Ag, and $S_1 = (1.3\pm 0.25)\times 10^{-4}$ for I were

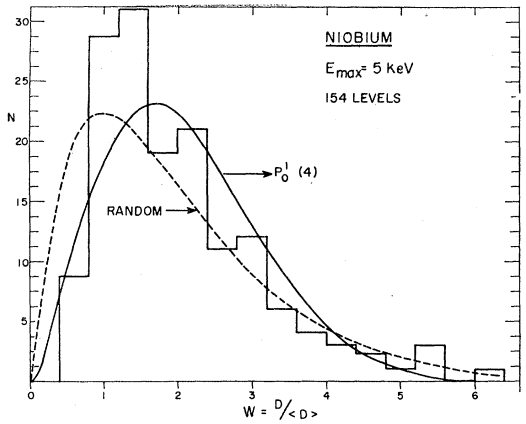


FIG. 22. Histogram of the experimental distribution of next-nearest-neighbor level spacings for niobium. The curves are the theoretical distributions for the cases of a random distribution of energy levels and the predictions of the random-matrix model for four equal-level populations as calculated by Leff.

reported by Seth *et al.*[10] based on the behavior of the average total cross sections in the 3–650-keV energy region. It is difficult for us to assess what systematic effects may be present in such measurements. They also obtained $S_0=(0.80\pm0.05)\times10^{-4}$ for Nb, $(0.40\pm0.05)\times10^{-4}$ for Ag, and $(0.55\pm0.2)\times10^{-4}$ for I. The silver and iodine $S_0$ values agree with our results, but the Nb value is about double our value for $S_0$.

In attempting to evaluate $S_1$ for Nb from the present data, we are confronted with the problem that we know that about 100 of our weak Nb levels to 5 keV are probably due to $l=1$, but we do not know which of these observed levels are $p$ wave. Furthermore, there are probably $\approx50$ missed $l=1$ levels. If a cut-off method is used that excludes the stronger $p$-wave levels one is apt to greatly underestimate the value of $S_1$. Figure 1 lists values of $2g\Gamma_n^1$ for all Nb levels for which a computed value of $2g\Gamma_n^1$ is $<300$ meV. A certain number of these are $s$-wave or "spurious" levels. The fraction of the levels which are $s$-wave should increase for the region of largest $g\Gamma_n^1$ values which contribute most strongly to the calculation of $S_1$. After trying several methods of attempting to estimate the value of $S_1$ we have finally chosen the value $S_1=(3.0\pm1.5)\times10^{-4}$.

It should be pointed out that the values of $S_0$ and $S_1$ in the optical model *are* energy-dependent and can, in principle, change appreciably in going from the energy region 1–5 keV to the energy region 100–500 keV. The model does not, however, predict gross changes for a few keV change in neutron energy.

TABLE VI. Results of the modified $\chi^2$ analysis for the agreement of the experimental data for nearest-neighbor spacing distributions of Nb, Ag, I, and Cs with the various theoretical distribution functions.

| Element | Energy interval (eV) | No. of levels assumed | $\langle D\rangle$ (eV) | $\chi^2$ values Random | $P_0^0(1)$ | $P_0^0(2)$ | $P_u^0(1)$ |
|---|---|---|---|---|---|---|---|
| Nb | 0–5000 | 154 | 32.0 | 53.3 | 47.5 | 42.9 | 86.5 |
| Ag | 0–2000 | 200 | 10.0 | 101 | 32.0 | 52.5 | 101 |
| I | 0–3000 | 220 | 13.6 | 131 | 32.8 | 68.5 | 40 |
| Cs | 0–2500 | 125 | 20.0 | 48.2 | 30.8 | 32.3 | 68 |

TABLE VII. The observed values of the correlation coefficients between adjacent spacings for Nb, Ag, I, and Cs excluding starred levels for Ag, I, and Cs.

| Energy interval | Nb (all levels) | Ag | I | Cs |
|---|---|---|---|---|
| 0–1000 | $-0.13\pm0.20$ | $-0.19\pm0.10$ | $-0.43\pm0.10$ | $-0.23\pm0.14$ |
| 0–2000 | $-0.20\pm0.11$ | $-0.11\pm0.07$ | $-0.22\pm0.08$ | $-0.15\pm0.10$ |
| 0–3000 | $-0.06\pm0.10$ | | $-0.20\pm0.07$ | |
| 0–5000 | $-0.02\pm0.08$ | | | |

## C. Further Analysis of Level-Spacing Distributions

We have already discussed above the nearest-neighbor spacing distributions for Nb, Ag, I, and Cs from the point of view of estimating the number of missed small level spacings on the assumption that the currently favored theories on level-spacing distributions should apply. The preceding discussions were relative to the facts that (a) we are probably detecting varying numbers of $p$-wave levels relative to $s$-wave levels for the different nuclei, and (b) we are probably missing some weak levels and some small level spacings. We now consider the results of various statistical tests for the level-spacing distributions. The results of these analyses should be examined with a full consideration of the previously discussed shortcomings of the data.

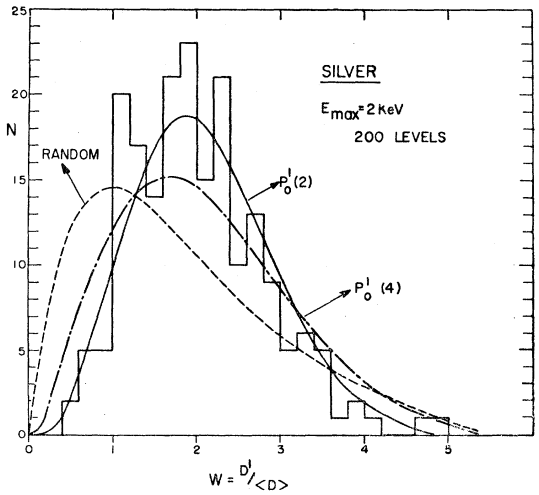


FIG. 23. The histogram of the observed next-nearest-neighbor level spacing distribution for natural silver. The curves are the theoretical distributions as indicated.

[10] K. K. Seth, R. H. Tabany, E. G. Bilpuch, and H. W. Newson, Bull. Am. Phys. Soc. **9**, 167 (1964). More detailed results are tabulated in the Proceedings of the Gatlinburg Conference on Compound Nuclear States, 1963 (unpublished).

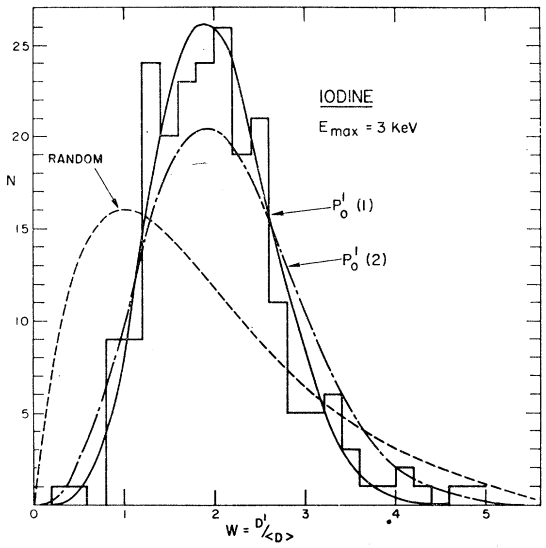


FIG. 24. The histogram of the observed next-nearest-neighbor level spacing distribution for iodine. The theoretical distributions are also shown for comparison.

Table VI lists the results of $\chi^2$ tests of "goodness of fit" of the various theoretical curves of Figs. 18–21 to the experimental histograms. The results of Table VI show that the curve $P_{\leftarrow 0}{}^{0\rightarrow}(2)$ for two equal merged orthogonal[3] populations agrees best with the experimental results for Nb, but the single orthogonal $P_0{}^0(1)$ distribution agrees best with the experimental results for the remaining elements. The $P_u{}^0(1)$ theoretical curve is for a single unitary population.

Table VII shows the correlation coefficient between adjacent spacings for various energy intervals starting from $E=0$. The theory and the expected effect of the limitations of the experimental data were discussed in earlier papers.[3,4] For a single orthogonal ensemble Porter obtained the value $-0.253$ using a Monte Carlo method involving random $N\times N$ matrices. Leff[11] investigated the expected value for two independent merged orthogonal populations having a ratio $R$ of level densities. The predicted values are $-0.24$, $-0.19$, $-0.20$, $-0.24$, $-0.26$, and $-0.29$ for $R=0$, $\frac{1}{9}$, $\frac{1}{3}$, $\frac{1}{2}$, $\frac{3}{5}$, and 1, respectively.

Figures 22–25 show the next-nearest-neighbor spacing distributions for the four elements, again omitting the starred levels for Ag, I, and Cs. The notation $P_0{}^n(m)$ for a theoretical curve means that $m$ independent orthogonal populations with same average spacing have been merged, and one examines the distribution for the spacings between levels having $n$ intermediate levels. There are $(n+1)$ dependent spacing series for a given $n$ depending on whether one starts with the first level, the second level, etc., up to the $(n+1)$st level. This should be considered when noting the ordinate values on the histogram. The $P_u{}^0(1)$ shape is for the nearest-neighbor spacing distribution for a single unitary population. It has been shown[3] by Gunson that $P_u{}^0(1)$ is the same as $P_0{}^1(2)$ except for the absissa scale. It should be noted in comparing the theoretical curves with the experimental histograms that the effect of missed levels is to cause some of our "observed" next-nearest-neighbor spacings to be actual next-next-nearest neighbor spacings, etc. Thus a few extra observed spacings at the high end of the distribution which appear to be incompatible with the *a priori* favored theoretical curves should not be given too much weight.

[11] H. S. Leff, State University of Iowa Report, 1963 (unpublished).

TABLE VIII. Results of the $\chi^2$ analysis for the agreement of the experimental data for the next-nearest-neighbor spacing distribution of Nb, Ag, I, and Cs with the various theoretical distribution functions. The least value of $\chi^2$ corresponds to the best agreement.

| Element | Energy interval (eV) | No. of levels assumed | $\langle D\rangle$ eV | $\chi^2$ values Random | Porter Kahn | Leff (2 seq) | Leff (4 seq) | $P^1{}_{\text{Unitary}}$ |
|---|---|---|---|---|---|---|---|---|
| Nb | 0–5000 | 154 | 32.0 | 27.1 | 75.3 | 36.5 | 24.6 | 201 |
| Ag | 0–2000 | 200 | 10.0 | 74.5 | 21.4 | 16.4 | 30.5 | 77.3 |
| I | 0–3000 | 220 | 13.6 | 116.5 | 16.0 | 28.0 | 55.3 | 40.0 |
| Cs | 0–2500 | 125 | 20.0 | 39.5 | 36.3 | 18.9 | 18.9 | 90.0 |

Table VIII shows the modified[3] $\chi^2$ test results for the fit of the experimental histograms of Figs. 22–25 with various theoretical curves appropriate to the next-nearest-neighbor spacing distributions. The Porter-Kahn[12] distribution is for the case of a single orthogonal ensemble. Leff[13] has extended the results of Monte Carlo calculations for two and four merged independent populations.

In the case of iodine we have also prepared plots of the histograms for $D^2$, $D^3$, $\cdots$, $D^7$ corresponding to the

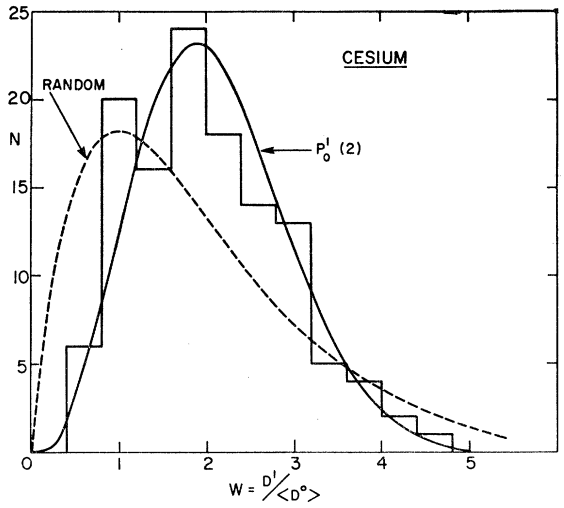


FIG. 25. The histogram of the observed next-nearest-neighbor level spacing distribution for cesium. The theoretical curves are also shown for comparison.

[12] P. B. Kahn and C. E. Porter, Nucl. Phys. 48, 385 (1963).

[13] H. S. Leff (private communication). We wish to thank Dr. Leff for communicating these results prior to publication.

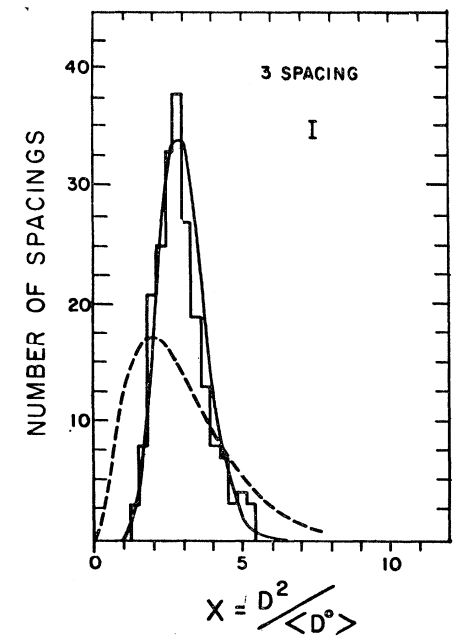


(a)

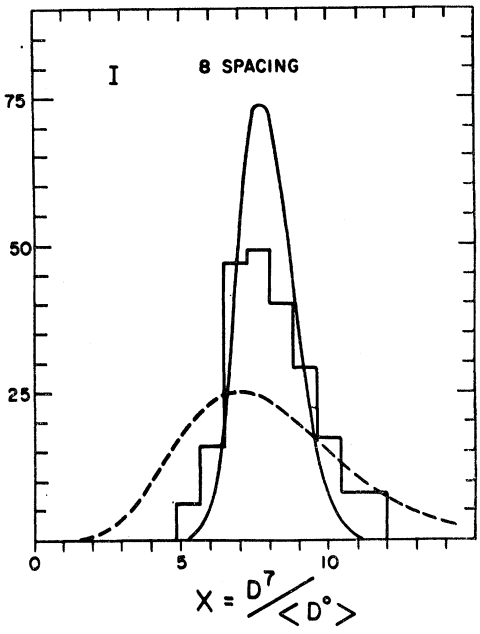


(b)

FIG. 26. The experimental histograms of the higher order of spacings of iodine. The theoretical distributions of random occurrence of energy levels (broken curves) and the random matrix model as calculated by Porter (solid curves) are also shown for comparison.

spacing distribution for levels having 2, 3, $\cdots$, 7 levels between a given pair. The $D^2$ and $D^7$ distributions are shown in Fig. 26(a) and 26(b) along with the appropriate theoretical curves for the cases of a random level spacing distribution and a single-population orthogonal distribution. The theoretical functions for the orthogonal distribution were obtained by Porter[14] on the basis of Monte Carlo calculations using 10 000, 10×10 matrices. The experimental cases should correspond to two or more merged orthogonal populations and thus be intermediate between the two theoretical distributions. The histogram for $D^2$ is matched surprisingly closely by the theoretical single population orthogonal distribution curve.

TABLE IX. The experimental results of the correlation coefficient between adjacent neutron reduced widths of Nb, Ag, I, and Cs.

| Energy interval (eV) | Nb | Ag | I | Cs |
|---|---|---|---|---|
| 0–1000 | −0.18±0.23 | 0.02±0.10 | 0.01±0.12 | −0.11±0.14 |
| 0–2000 | −0.09±0.15 | 0.08±0.07 | −0.04±0.08 | −0.11±0.10 |
| 0–3000 | −0.13±0.12 | 0.04±0.06 | −0.08±0.07 | −0.16±0.08 |
| 0–4000 | −0.08±0.10 | | −0.07±0.07 | |
| 0–5000 | −0.06±0.09 | | | |

In conclusion one can say that the experimental results are in reasonable agreement with the favored theoretical curves when one takes account of the shortcomings of the experimental data.

### D. Other Correlation Coefficients

In the interests of completeness we have also investigated the correlation coefficients between adjacent-level $(g\Gamma_n^0)$ values and between a given $(g\Gamma_n^0)$ value for a level and the average of its spacing from its adjacent levels on either side. The results are shown in Tables IX and X. As far as we know, the theoretically expected values are zero. Experimental values are near zero and are probably consistent with the value zero.

## CONCLUSION

Total neutron cross-section measurements have been made on Nb, Ag, I, and Cs with a much higher energy resolution than previously available. Much more precise values of average level spacings and $s$-wave strength functions have been obtained. The statistical properties of levels, for example, the level-spacing and neutron reduced-width distributions, have been tested much more stringently. The results on the level-spacing dis-

TABLE X. Correlation between the neutron reduced widths $(g\Gamma_n^0)$ of a level and the average of the spacing of its nearest-neighbor levels as a function of the energy interval.

| Energy interval (eV) | Nb | Ag | I | Cs |
|---|---|---|---|---|
| 0–1000 | −0.60±0.16 | −0.05±0.10 | −0.02±0.12 | −0.05±0.14 |
| 0–2000 | 0.03±0.15 | 0.02±0.07 | −0.01±0.08 | −0.05±0.10 |
| 0–3000 | 0.02±0.11 | 0.14±0.06 | 0.10±0.07 | −0.03±0.08 |
| 0–4000 | 0.08±0.10 | | 0.12±0.06 | |
| 0–5000 | 0.04±0.09 | | | |

[14] C. E. Porter, Brookhaven National Laboratory Report No. BNL 6763 (unpublished).

tributions seem to be compatible with the predictions of the random-matrix model and the width distributions favor a Porter-Thomas distribution as opposed to the exponential distribution in $\Gamma_n^0$. An excess of weak levels over that predicted by the Porter-Thomas distribution has been observed in all nuclei studied. These are most probably $p$-wave levels.

## ACKNOWLEDGMENTS

The authors take pleasure in acknowledging the assistance of J. S. Petersen and the velocity-selector technicians A. Blake, S. Marshall, J. Spiteri, and D. Ryan in the various phases of these measurements. Bum-Nai Ham and Young-He-Ham were very helpful in the final analysis of the data. Dr. J. L. Rosen and Dr. J. S. Desjardins made major contributions to the 1959–60 self-indication measurements for Nb and I using the 35-m flight path. Our special thanks go to Ann McDowell and James Cleary for the careful preparation of the figures. Finally, we wish to express our appreciation for the assistance rendered by the technical staff of the Nevis Synchrocyclotron.

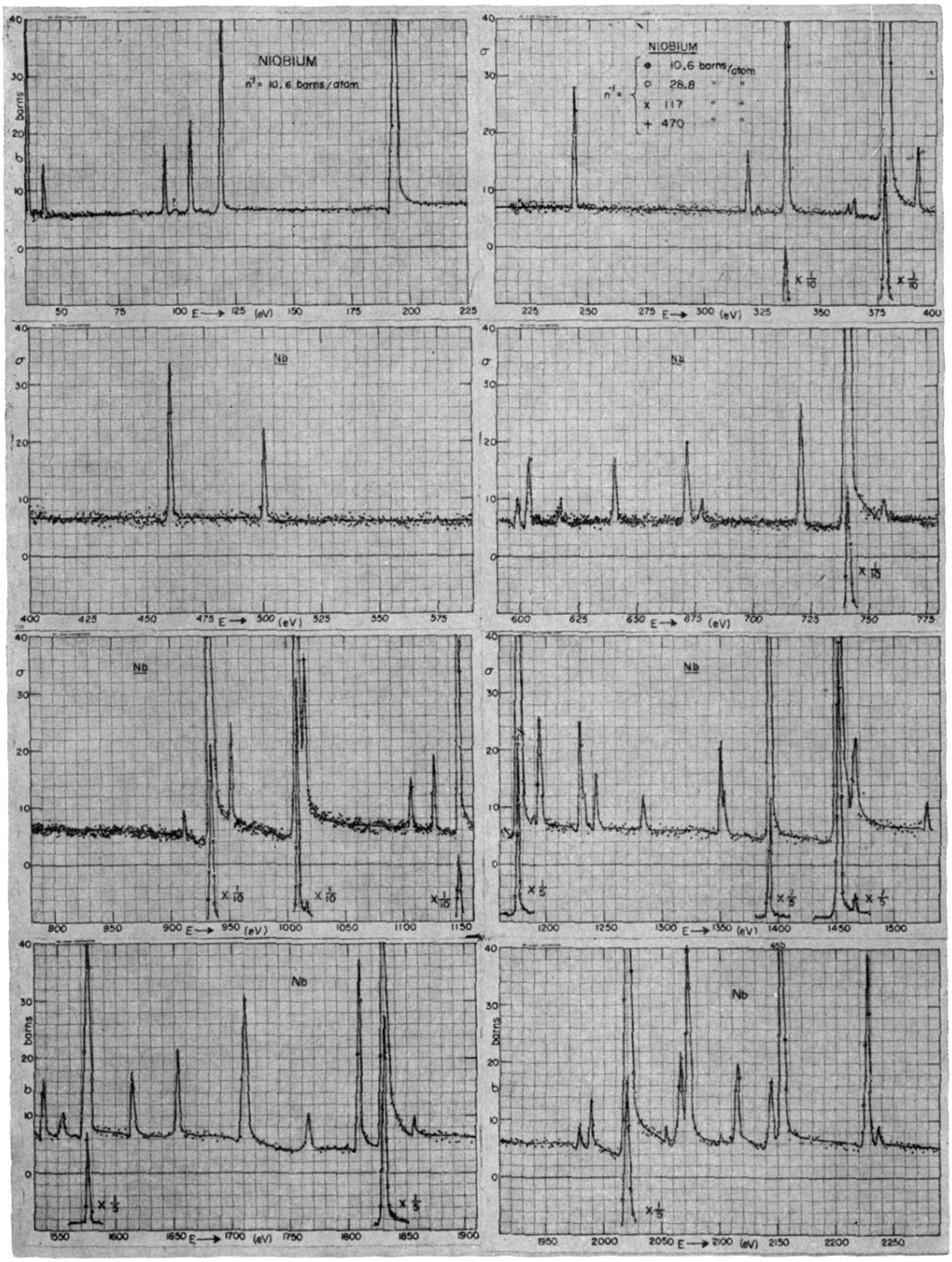


FIG. 1. The "measured" total neutron cross section of $Nb^{93}$ versus energy from 35 to 7250 eV. The measurements used four sample thicknesses as indicated, with the cross section between resonances mainly determined from the thick-sample data. At resonance the data for progressively thinner samples was used. When the resonance cross section exceeds full-scale value an insert scale is shown having its zero start at the bottom of the page with a factor of 5, 10, or 20, as indicated reduction in the height of the curve. In the region of resonance the peak cross-section values are distorted by Doppler level broadening, the instrumental energy resolution, and by the $(1/n)$ value for the thinnest sample. The cross-section values are in barns.

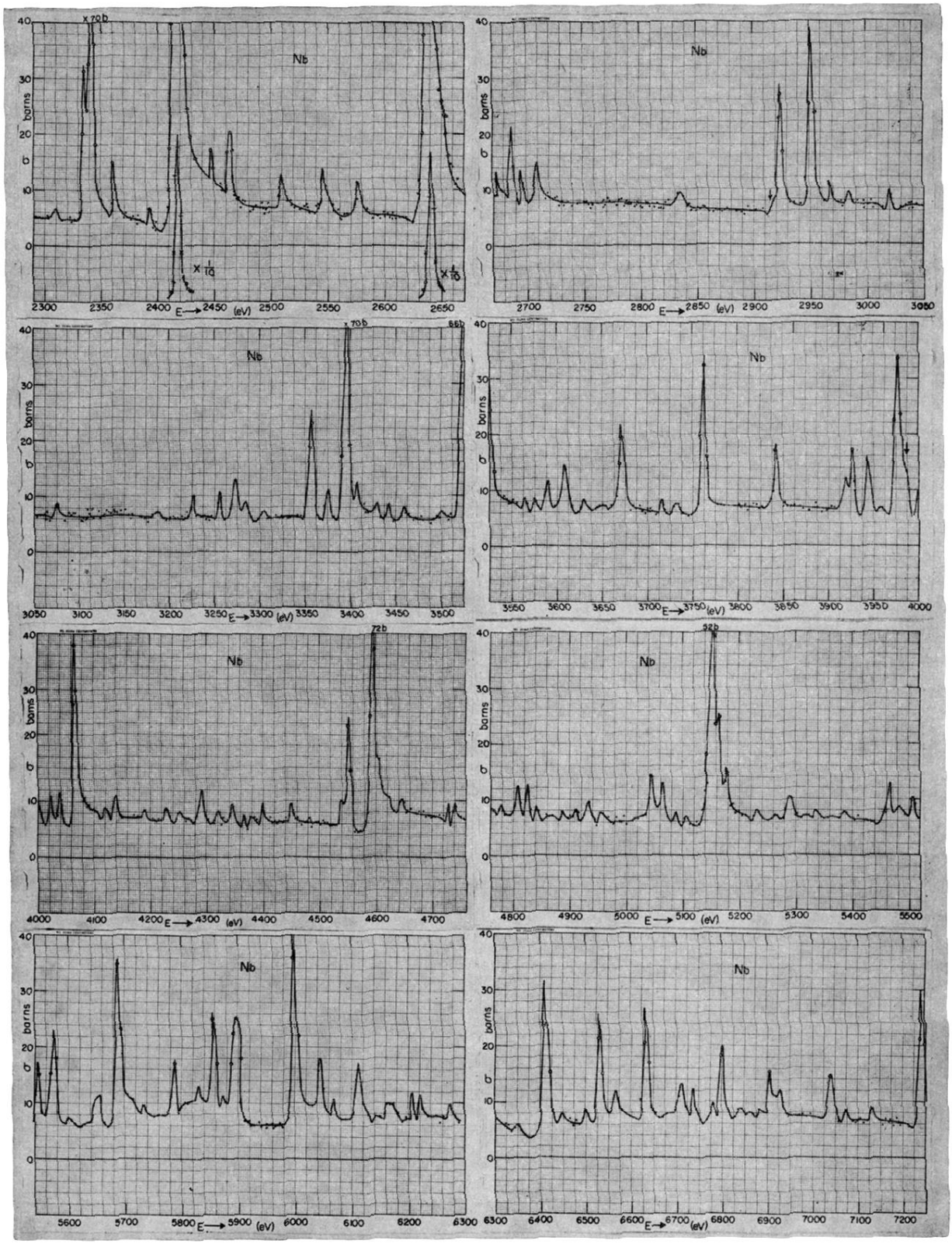


FIG. 1. *Continued.*

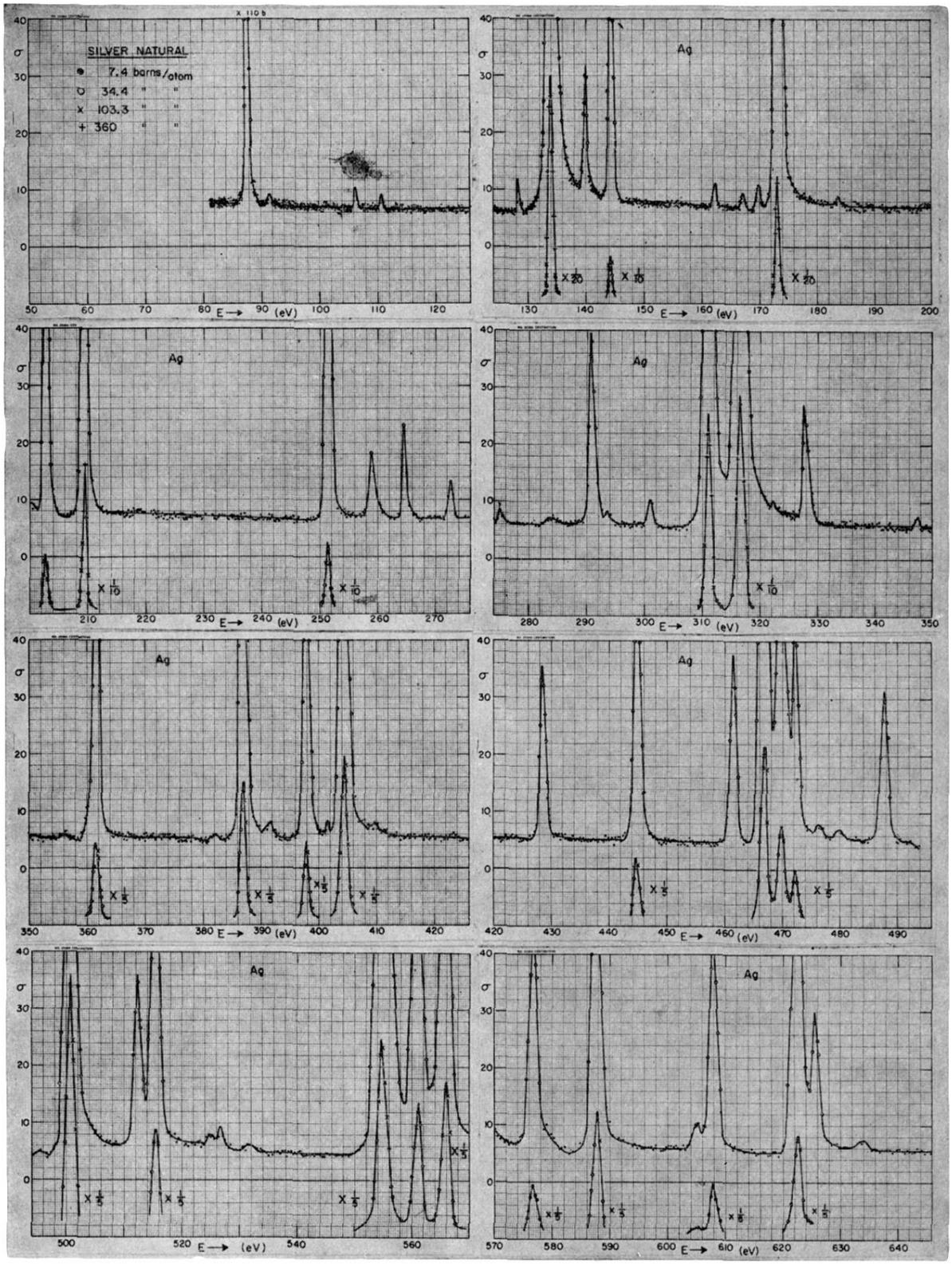


FIG. 2. The "measured" total neutron cross section for natural silver versus energy from 80 to 4000 eV. The considerations for the curves are similar to those described in the caption of Fig. 1.

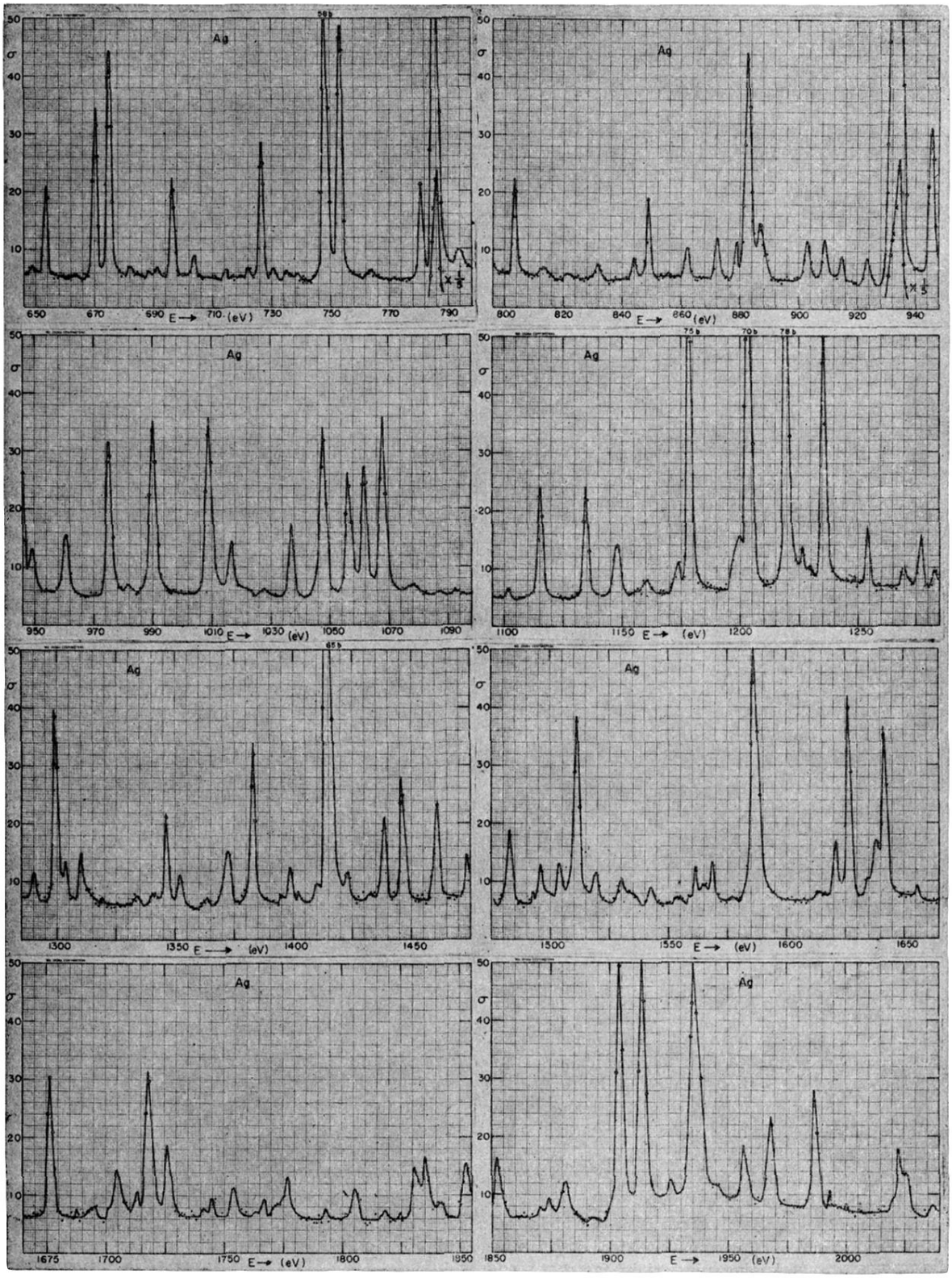


FIG. 2. *Continued.*

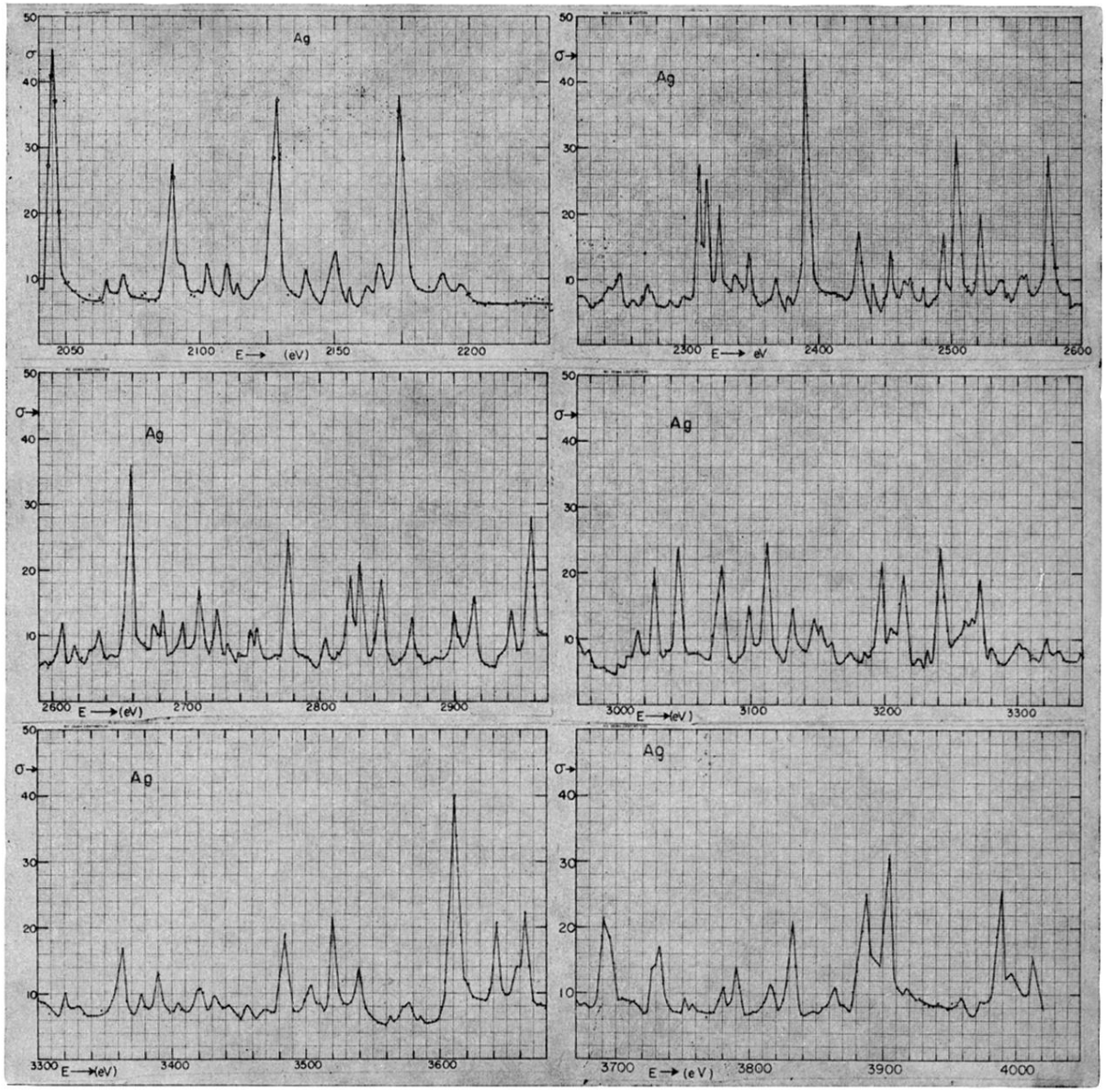


FIG. 2. *Continued.*

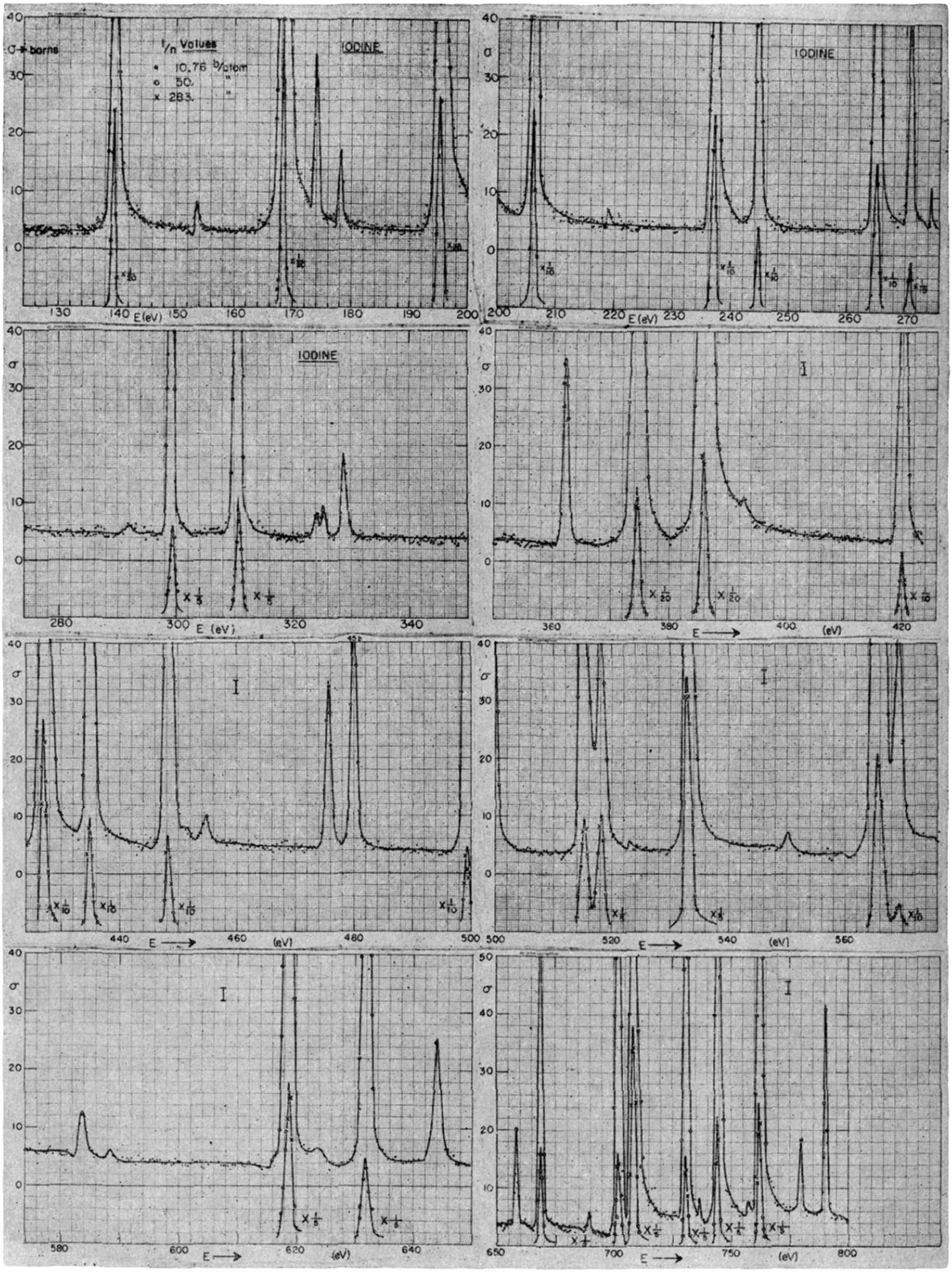


FIG. 3. The "measured" total neutron cross section for iodine versus energy from 124 to 4000 eV. The considerations are similar to those discussed in the caption of Fig. 1.

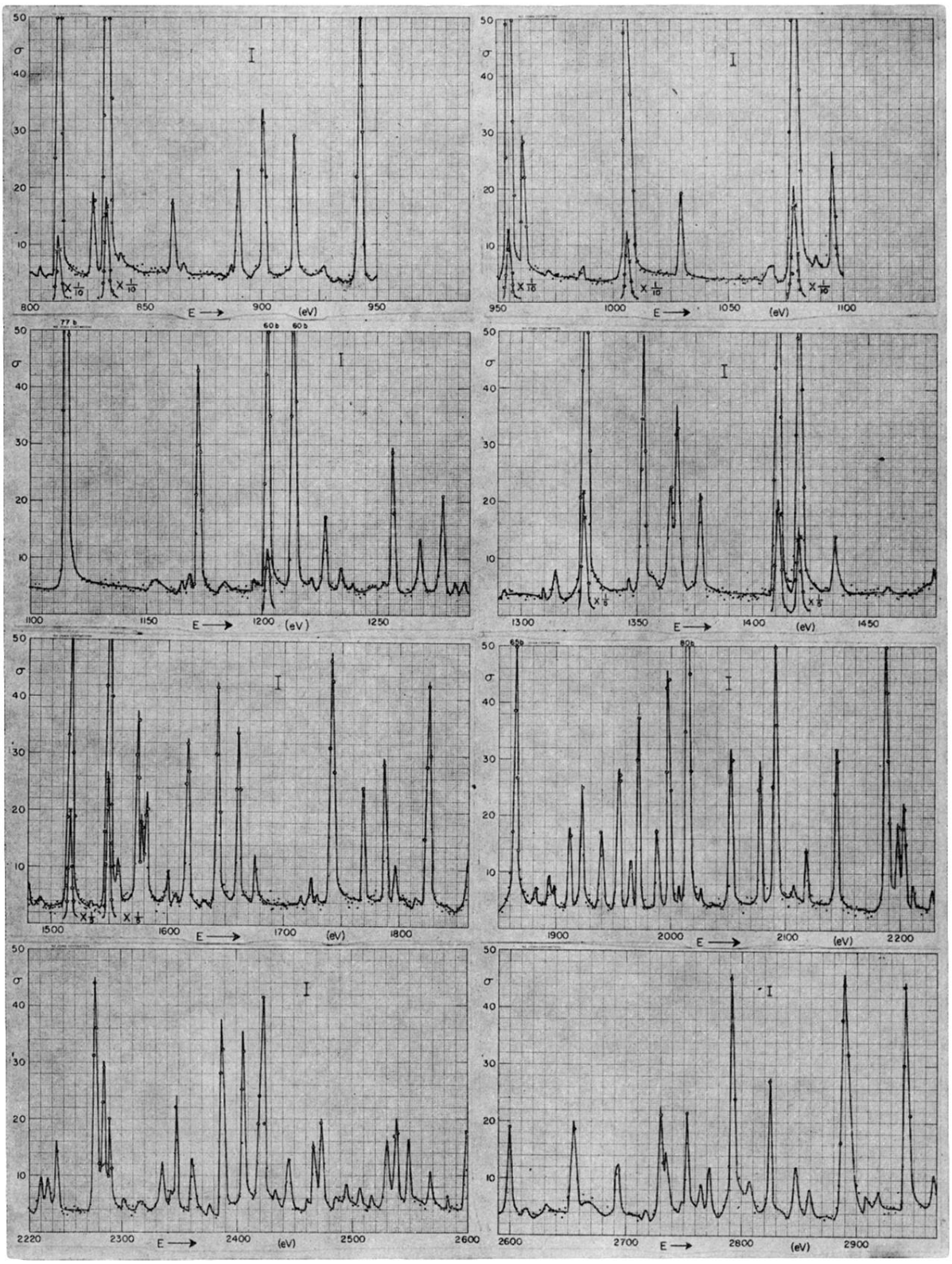


FIG. 3. *Continued.*

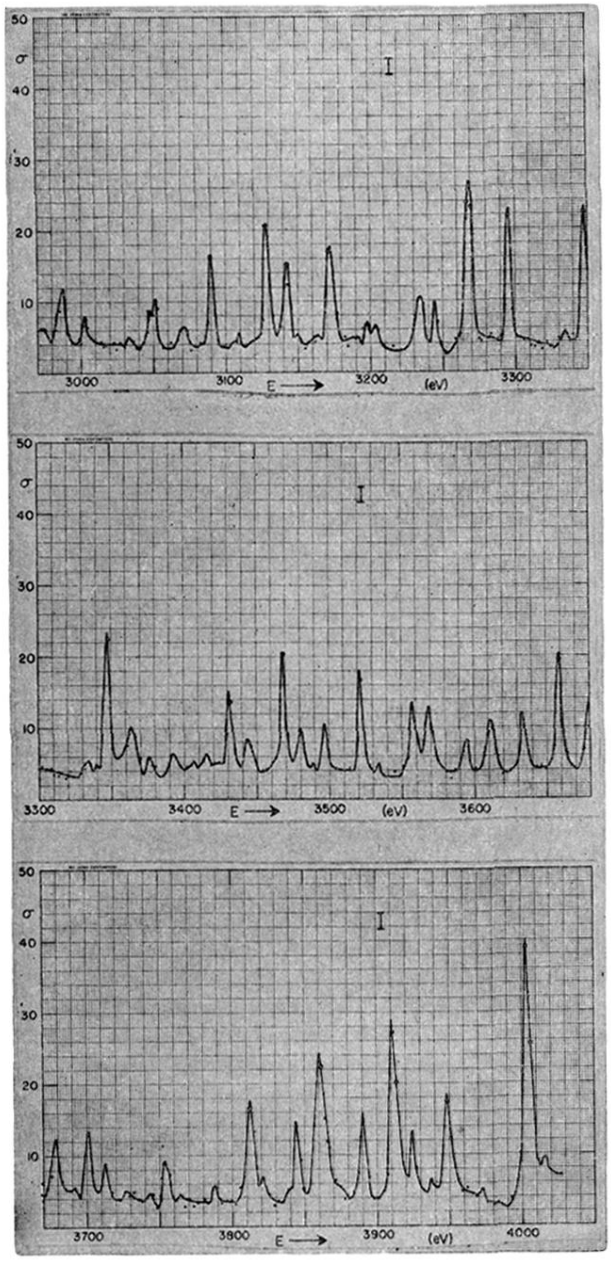


FIG. 3. *Continued.*

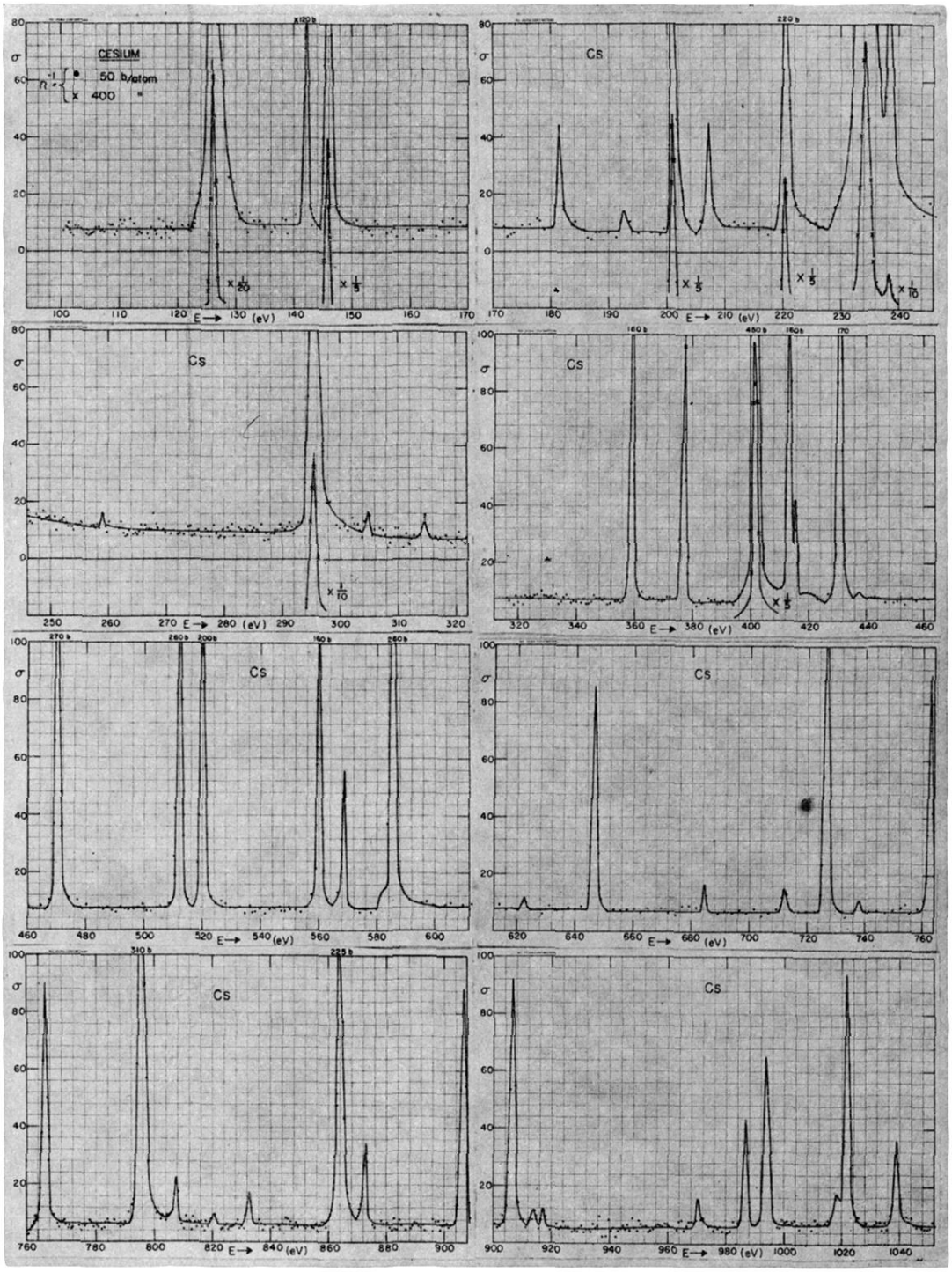


FIG. 4. The "measured" total neutron cross section for cesium versus energy from 100 to 3460 eV. The accuracy of the cross section between resonances is much poorer than usual since the thickest $Cs_2SO_4$ sample was too thin for best results. Otherwise the considerations are similar to those described in the caption of Fig. 1.

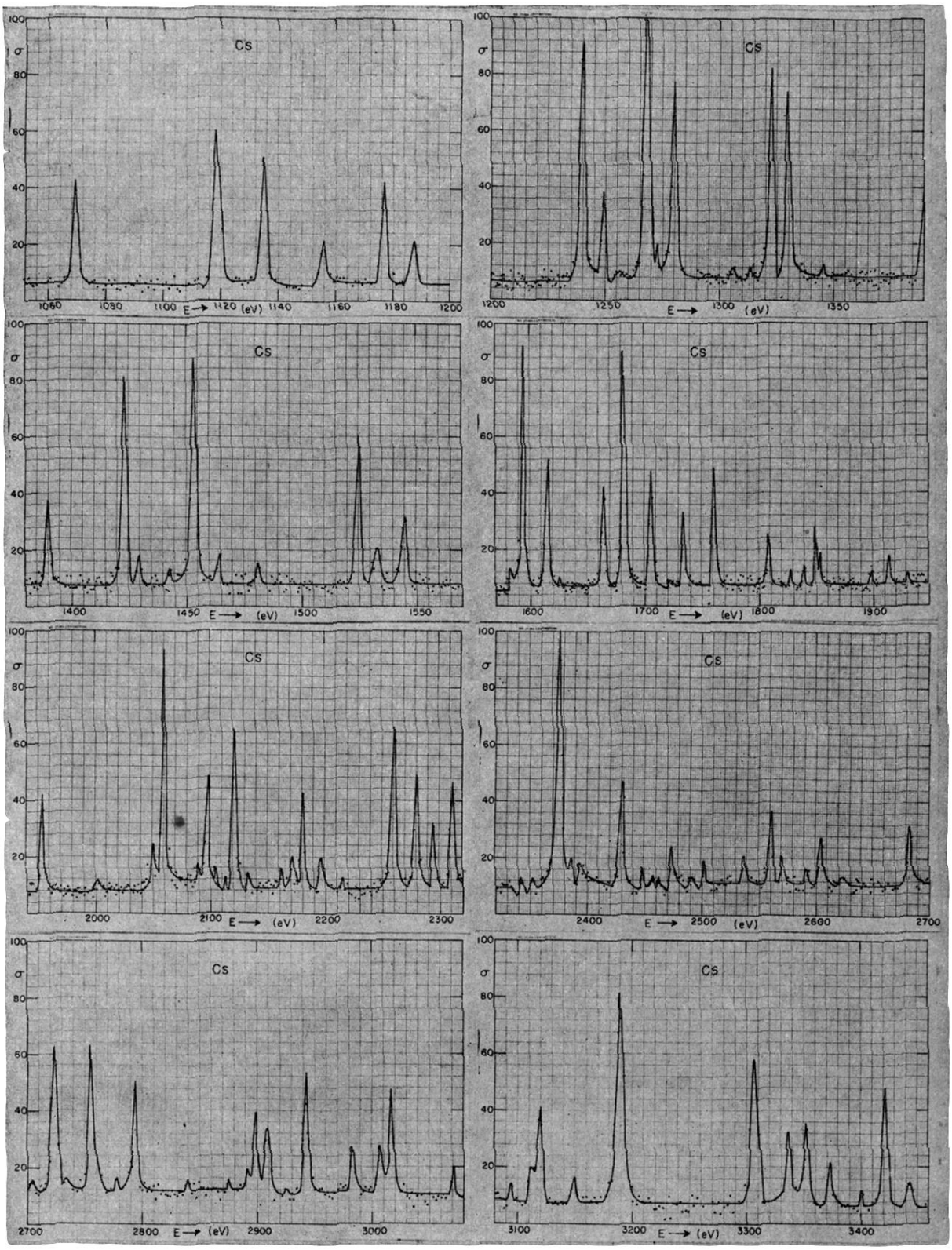


FIG. 4. *Continued.*